Calhoun
Institutional Archive of the Naval Postgraduate School



Calhoun: The NPS Institutional Archive

DSpace Repository

Theses and Dissertations | 1. Thesis and Dissertation Collection, all items

1968-06

Calibration of turbine test rig with impulse turbine at high pressure ratios

Lenzini, Martin Joseph

Monterey, California. U.S. Naval Postgraduate School

http://hdl.handle.net/10945/11753

This publication is a work of the U.S. Government as defined in Title 17, United States Code, Section 101. Copyright protection is not available for this work in the United States.

Downloaded from NPS Archive: Calhoun



http://www.nps.edu/library

Calhoun is the Naval Postgraduate School's public access digital repository for research materials and institutional publications created by the NPS community. Calhoun is named for Professor of Mathematics Guy K. Calhoun, NPS's first appointed -- and published -- scholarly author.

Dudley Knox Library / Naval Postgraduate School
411 Dyer Road / 1 University Circle
Monterey, California USA 93943

NPS ARCHIVE
1968
LENZINI, M.

CALIBRATION OF TURBINE TEST RIG WITH IMPULSE TURBINE AT HIGH PRESSURE RATIOS

by

Martin Joseph Lenzini

DUDLEY KNOX LIBRARY
NAVAL POSTGRADUATE SCHOOL
MONTEREY, CA 93943-5101

Gaylord
SHELF BINDER
Syracuse, N. Y.
Stockton, Calif.

UNITED STATES
NAVAL POSTGRADUATE SCHOOL

THESIS

CALIBRATION OF TURBINE TEST RIG WITH
IMPULSE TURBINE AT HIGH PRESSURE RATIOS

by

Martin Joseph Lenzini

June 1968

This document is subject to special export controls and each transmittal to foreign government or foreign nationals may be made only with prior approval of the U. S. Naval Postgraduate School.

CALIBRATION OF TURBINE TEST RIG WITH IMPULSE TURBINE AT HIGH PRESSURE RATIOS

by

Martin Joseph Lenzini
Captain, United States Marine Corps
B.S., University of New Mexico, 1961

Submitted in partial fulfillment of the

requirements for the degree of

AERONAUTICAL ENGINEER

from the

NAVAL POSTGRADUATE SCHOOL
June 1968

NPS ARCHIVE
1968
LENZINI, M
~~Thesis L527 c.1~~

ABSTRACT

The Transonic Turbine Test Rig of the Turbo-Propulsion Laboratory, Department of Aeronautics, of the Naval Post-graduate School was designed to investigate the performance of turbines with transonic or supersonic rotor inlet velocities. The test rig has provisions for testing single stage axial turbines at high pressure ratios and at variable axial and radial clearances. The present study describes the calibration of the turbine test rig with an impulse turbine at high pressure ratios. The turbine stage consists of a double circular-arc rotor with sharp leading edges and a stator with converging nozzle type blading. The results of the flow rate calibration and labyrinth seal leakage tests are described. The instrumentation necessary to separate rotor and stator losses is also discussed.

DUDLEY KNOX LIBRARY
NAVAL POSTGRADUATE SCHOOL
MONTEREY, CA 93943-5101

TABLE OF CONTENTS

SECTION		PAGE
1.	INTRODUCTION	13
2.	TURBINE DESCRIPTION	15
3.	TEST INSTALLATION	17
4.	FLOW NOZZLE CALIBRATION	22
5.	PLENUM LABYRINTH SEAL LEAK RATE	25
6.	ANALYSIS AND DATA REDUCTION	29
	6.1 General	29
	6.2 Flow Rate Determination	29
	6.3 Stator Entrance Properties	31
	6.4 Stator Discharge Properties	31
	6.5 Rotor Discharge Properties	37
	6.6 Performance Parameters	41
7.	DESCRIPTION OF TURBINE TESTS	44
8.	RESULTS AND DISCUSSION OF TURBINE TESTS	47
9.	RECOMMENDATIONS	55
REFERENCES		88
APPENDIX I:	COMPUTER PROGRAMS FOR FLOW RATE DETERMINATION AND TURBINE TEST DATA REDUCTION	89
APPENDIX II:	EVALUATION OF THE FORCE ACTING ON THE STATOR ASSEMBLY BY THE STATOR DISCHARGE PRESSURE.	140

DUDLEY KNOX LIBRARY
NAVAL POSTGRADUATE SCHOOL
MONTEREY, CA 93943-5101

LIST OF ILLUSTRATIONS

FIGURE		PAGE
1.	Blade Profiles Circular-Arc Rotor Converging Stator	57
2.	Converging Stator (View showing stator entrance)	58
3.	Circular-Arc Rotor (View showing rotor entrance)	59
4.	Mean Radius Blade Profile Converging Stator	60
5.	Mean Radius Blade Profile Circular-Arc Rotor with Sharp Leading Edges	61
6.	Blade Profile Circular-Arc Rotor with Blunt Leading Edges	62
7.	Blade Profile Contoured Rotor	63
8.	Blade Profile Converging-Diverging Stator.	64
9.	Piping Installation, Transonic Turbine Test Rig	65
10.	Transonic Turbine Test Rig.	66
11.	Turbine Blading Arrangement	67
12.	Closure Plate Assembly Transonic Turbine Test Rig.	68
13.	Closure Plate Calibration Rig (View showing closure plate assembly setup for calibration run)	69

14. Closure Plate Assembly Installation
Transonic Turbine Test Rig 70
15. Turbine and Shroud Details 71
16. Circular-Arc Rotor and Bearing Assembly
Mounted in Rotor Bearing Stand 72
17. Floating Stator Assembly 73
18. Flow Nozzle Discharge Coefficient
Transonic Turbine Test Rig 74
19. Referred Labyrinth Seal Leak Rate
Transonic Turbine Test Rig 75
20. Referred Labyrinth Seal Leak Rate
Transonic Turbine Test Rig 76
21. Modified Referred Labyrinth Seal Leak
Rate Transonic Turbine Test Rig 77
22. Pressure Survey at Stator Entrance
Pressure Ratio = 2.0 78
23. Velocity Diagram of Turbine Stage 79
24. Thermodynamic Process of Fluid
in an Axial Turbine Stage 80
25. Total-Static Efficiency at Various
Axial Clearances 81
26. Referred Moment versus Referred RPM
Pressure Ratio = 2.0 82
27. Efficiency Total-Static Initial
Turbine Tests 83
28. Referred Moment versus Referred RPM
Initial Turbine Tests 84

29. Stator Torque Capsule Variation with RPM Transonic Turbine Test Rig 85
30. Stator Torque Capsule Variation with Temperature Transonic Turbine Test Rig 86
31. Stator and Rotor Loss Coefficient versus Hood Temperature at 13080 RPM and Pressure Ratio of 2.5 87

TABLE OF SYMBOLS

Latin

A	Cross-sectional area (in^2)
a	Flow channel throat diameter (in)
a	Speed of sound (ft/sec)
b	Blade width (in)
C	Conversion factor, $2gJc_p$ ($ft^2/sec^2 - {}^oR$)
c_p	Specific heat at constant pressure ($BTU/lb_m - {}^oR$)
D	Diameter (in)
F	Force (lb_f)
g	Gravitational constant ($32.174\ lb_m - ft/lb_f - sec^2$)
h	Blade height (in)
HP	Horsepower
h_w	Differential pressure across turbine flow nozzle ($in\ H_2O$)
J	Conversion factor ($778.16\ ft - lb_f/BTU$)
K	Work coefficient (dimensionless)
K_{is}	Head coefficient (dimensionless)
K_n	Flow nozzle discharge coefficient (dimensionless)
M	Moment ($ft - lb_f$)
M	Absolute Mach number (dimensionless)
M_R	Relative Mach number (dimensionless)
N	Rotational speed (rpm)
P_t	Total pressure (psia)
P	Static pressure (psia)
R	Gas constant ($ft - lb_f/lb_m - {}^oR$)
R_e	Reynolds number (dimensionless)

R_m	Mean radius (in)
r	Radius (in)
r	Labyrinth pressure ratio (dimensionless)
r*	Theoretical degree of reaction (dimensionless)
s	Distance between blades (in)
s	Entropy ($BTU/lb_m - {}^\circ R$)
T	Static temperature ($^\circ R$)
T_t	Total temperature ($^\circ R$)
t	Blade thickness at trailing edge (in)
t	Static temperature ($^\circ F$)
t_t	Total temperature ($^\circ F$)
U	Peripheral velocity (ft/sec)
V	Absolute velocity (ft/sec)
W	Relative velocity (ft/sec)
$\dot{W}$	Flow rate (lb_m/sec)
Y_1	Expansion factor (dimensionless)
Z	Number of blades in a row

Greek

α	Absolute flow discharge angle (degrees)
α_n	Coefficient of thermal expansion of flow nozzle (dimensionless)
β	Relative flow discharge angle (degree)
γ	Ratio of specific heats (dimensionless)
δ	Referred pressure (dimensionless)
ζ	Loss coefficient (dimensionless)
η	Efficiency (dimensionless)
θ	Referred temperature (dimensionless)
ξ	Area restriction factor (dimensionless)

Φ Flow function (dimensionless)

Φ_L Referred labyrinth seal leak rate (in^2)

Φ_{LM} Modified referred labyrinth seal leak rate (in^2)

Angular velocity (radians/sec)

Subscripts

a Axial direction

ax Area normal to the axial direction

Cl Closure plate

D Dynamometer

E Equivalent thermodynamic property

h Blade hub

h Hood

is Isentropic

L Labyrinth seals

m Mean streamline

n Flow nozzle properties

o Stator entrance properties

P Labyrinth plenum properties

R Rotor

REF Referred value

S Stator

t Blade tip

th Theoretical value

u Peripheral direction

1 Stator discharge properties

2 Rotor discharge properties

SECTION 1

INTRODUCTION

Turbines for modern gas turbine plants and jet propulsion units must operate at high pressure ratios. It is advantageous to use stages with supersonic or transonic flows in the rotating rows thereby limiting the number of stages and increasing the specific work output. Although the efficiency of such stages may prove to be somewhat lower than that of rotating rows with subsonic flows, they are desirable for use in low-weight power plants. An application presently under consideration by NASA is the use of a single-stage supersonic turbine in a hydrogen-fueled open-cycle auxiliary space power plant [1].

Very little quantitative information on supersonic and transonic turbine performance is available in the literature. Therefore, a Transonic Turbine Test Rig was built at the Naval Postgraduate School, Monterey, California. The test rig was designed by Dr. M. H. Vavra of the Department of Aeronautics to determine the effect of different blading arrangements on turbine efficiency and to separate the total losses of the turbine into those of the rotating and the stationary rows of blades. With the Transonic Turbine Test Rig, investigation of turbine performance for transonic and supersonic rotor inlet velocities is possible.

The present study is concerned with the installation modifications and calibration tests necessary to obtain meaningful data for transonic or supersonic turbine performance analysis at high pressure ratios. Initial calibration

tests using an impulse turbine with a stator, consisting of converging nozzle type blading, and a rotor with circular-arc profiles with sharp leading edges are described. Several instrumentation difficulties were experienced during the initial tests which required a number of modifications to the test installation. Tests are described which were carried out with the turbine after the different modifications of the Turbine Test Rig.

The author wishes to express his deep appreciation to Dr. M. H. Vavra for his guidance during the experimental work and for his help in the reporting of the study. Thanks are also given to Mr. J. E. Hammer for his generous assistance during the project.

SECTION 2

TURBINE DESCRIPTION

The turbine investigated is a single stage axial flow turbine of the impulse type which was designed for transonic rotor inlet velocities. The rotor has double circular-arc blade profiles with sharp leading edges and is one of three rotors presently available for the Transonic Turbine Test Rig, which hereafter is referred to as the TTR. The stator used during the present turbine tests has converging type nozzles. Also available is a stator with converging-diverging type nozzles for supersonic stator discharge velocities. The three rotors and the two stators are interchangable, and any stator-rotor combination can be tested with the TTR. Of the six available combinations only one was tested because of time considerations and the delays because of the TTR modifications. Figures 1, 2, and 3 are photographs of the stator and rotor of the turbine stage tested. Scale drawings of the mean radius blade profiles of this stator and rotor are shown in Figs. 4 and 5, respectively. Pertinent turbine dimensions are listed in Table I. The blading parameters indicated in Table I are at the mean radius of the stage.

Another rotor which can be run in the TTR has double circular-arc blade profiles with blunt leading edges. This type of rotor, which is shown in Fig. 6, could be used in high temperature applications where blade cooling is necessary. A third rotor, whose blade profiles are shown in Fig.

7, has blade profiles with gradually changing curvature. Figure 8 is a photograph of the blade profiles of the converging-diverging stator.

TABLE I

IMPULSE TURBINE DIMENSIONS

Converging Stator and Circular-Arc Rotor with Sharp Leading Edges

ITEM	SYMBOL	STATOR	ROTOR
Number of Blades	Z	31	60
Blade Height (in)	h	0.690	0.932
Blade Width (in)	b	0.975	0.750
Hub Radius (in)	R_h	3.895	3.826
Mean Radius (in)	R_m	4.240	4.292
Tip Radius (in)	R_t	4.585	4.763
Blade Spacing (in)	s	0.8594	0.444
Trailing Edge Thickness (in)	t	0.024	0.020
Throat Diameter (in)	a	0.205	0.1313
Throat Area (in^2)	A_{th}	4.385	7.348
Axial Exit Area (in^2)	A_{ax}	18.382	25.134

SECTION 3

TEST INSTALLATION

The TTR installation and instrumentation has been described by Commons [2]. Therefore, the information presented here will be concerned with the salient features of the TTR only. However, modifications made to the TTR for the impulse turbine tests will be covered in more detail.

The working fluid for the TTR is air which is supplied by an Allis Chalmers VA 312 Compressor. As shown in Fig. 9, the supply air enters the turbine test cell through the inlet valve attached to tank 1 which is manually operated, and normally in the open position. The turbine inlet valve, which was originally a manually operated valve, was replaced by a remote controlled electrically operated butterfly valve. Both the turbine inlet valve and the exhauster inlet valve could then be operated simultaneously from the control room. This change reduces the time spent to set and maintain a desired pressure ratio if the TTR is operated with the exhauster.

A scale drawing of the cross-section of the TTR is shown in Fig. 10. Air enters the floating armature assembly radially from a plenum which is instrumented with total temperature and total pressure probes. Labyrinth seals, with 0.005 inch radial clearance between the armature assembly and the plenum, limit the leakage flow to about 7 per cent of the turbine flow rate. A conical screen is fitted in the armature assembly to reduce the possibility of

damage to the turbine by foreign objects. The air flows through the conical screen into the stator plenum which is instrumented with five fixed total pressure probes, one 3-hole survey probe, and two total temperature probes. In addition a so-called bullet probe is installed at the downstream end of the armature assembly, which measures total pressure and total temperature. The arrangement of these probes is shown in Fig. 11.

The closure plate assembly, also shown in Fig. 11, was completely redesigned for the impulse turbine tests. The moment on the closure plate was obtained from six equally spaced torque flexures. The flexures, which are 0.025 inch thick and extend radially from an inner support to an outer ring, are equipped with two strain gages. The strain gages are arranged to measure the bending moments on the flexures in the axial plane. The inner support is fastened to the closure plate force flexure. The force flexure consists of four webs of 0.080 inch thickness which are also instrumented with strain gages. These gages measure the bending moments applied to the flexure by the axial force acting on the closure plate. The signals from both sets of strain gages was read on a Daytronic model 700 strain gage digital indicator. Figure 12 is a photograph of the closure plate assembly which shows the force and torque flexures. The closure plate was calibrated on a specially built calibration rig by applying known forces and moments with various combinations of weights. The arrangement of the calibration rig is shown in Fig. 13. Figure 14 gives two views of the

closure plate assembly installed in the TTR.

Stator hub and tip static pressures are measured in the cavities between the stator assembly and the closure plate, and between the stator assembly and shroud, respectively. These static ports are shown in Fig. 11. The outer shroud is instrumented with seven static pressure taps, P_{15} through P_{21}, spaced at 0.25 inch intervals from about the mid-rotor plane to the downstream end of the shroud. The last four static taps determine the shroud pressures needed in the momentum analysis of the inlet guide vanes.

There are seven shroud inserts available with different inside diameters. All inserts are cylindrical with the exception of two, one with a five degree slant and the other with a ten degree slant, for tapered rotor blade tips. Only the cylindrical shroud insert with an inside diameter of 9.546 inches was used in the present tests. The arrangement of the shroud, the shroud insert, and the seven static pressure taps is shown in Fig. 15.

Different radial tip clearances are obtained with a particular shroud insert by reducing the rotor diameter. The radial clearance used for the present tests was 0.010 inch.

The turbine rotor, shown in Fig. 11, is supported by two sets of precision ball bearings which are lubricated by oil mist. Two photographs of the rotor in the bearing stand are shown in Fig. 16. The axial clearance between the stator and rotor is varied by sliding the rotor bearing

assembly in the bearing stand. The minimum axial clearance is limited by the distance by which the closure plate extends beyond the trailing edges of the inlet guide vanes. Operating at 20,000 rpm and pressure ratios of 4 or more, the minimum axial clearance is about 0.1 inch.

The stator assembly, shown in Fig. 17, is supported by flexures which permit measuring of the reactions of the stator discharge flow by means of reluctance type force gages. One of the flexures was instrumented with strain gages for the final three runs of the impulse turbine. The results obtained with the strain gage and the reluctance capsule measurements are discussed in Section 8.

An air dynamometer capable of absorbing 200 HP at 20,000 rpm is used to measure the turbine torque. The torque is measured by a reluctance type force capsule which is attached to a 20 inch long lever arm that is fitted to the dynamometer housing. The force gage limits the angular rotation of the dynamometer housing to about 0.25 degree. Originally a so-called direct reading spring capsule, which turns by about 30 degrees at maximum torque, was used as a bearing housing for the dynamometer. At the small rotation of the dynamometer housing it was believed that the coil spring which serves as the measuring element of the capsule would not affect the readings of the reluctance gage. This assumption was proven false and it was necessary to remove the coil spring (Section 8). Similar to the rotor bearings, the dynamometer bearings are lubricated by oil mist.

All pressures are measured by mercury manometers except the pressure difference across the flow nozzle, which is read on a water U-tube manometer. All temperatures are measured with Iron-Constantan thermocouples using an ice bath as a reference. The hood temperature, to which reference is made in this study, was measured by a thermocouple located in the plastic casing of the stator torque capsule. This casing shields the thermocouple from the flow of air in the hood. The location of the thermocouple is shown in Fig. 17.

SECTION 4

FLOW NOZZLE CALIBRATION

The turbine flow nozzle installation and the calibration techniques used are described by Eckert [3]. Early tests by Eckert indicated that the nozzle discharge coefficient was a function of nozzle supply pressure. Further investigation by Naviaux at nozzle supply pressures of 20, 22, and 24 psia showed that the nozzle coefficient was a function of Reynolds number only [4]. The latter result was obtained with the equations used by Eckert and an expansion factor Y_1 for nozzles instead of sharp edge orifices in accordance with the ASME Power Test Codes [5].

Nozzle supply pressures for the turbine performance tests normally vary between 30 and 42 psia. Because of past experience with the calibration of the TTR flow nozzle it was decided to carry out additional tests at supply pressures of 24, 29, 34, 39, and 42 psia to verify the results which Naviaux obtained at lower pressures. The test data were reduced by using the IBM 360 Computer of the Naval Postgraduate School. The data reduction program was similar to that of Naviaux with the exception that the specific gravities of mercury and water in the manometer were corrected for the temperatures in the control room and that only the flange taps of the sharp edge orifice in the calibration pipe were used. The specific gravities of water and mercury as a function of temperature, and the standard conversion factors used for data reduction, were

obtained from the International Critical Tables [6]. The program description and the reduced data are given in Appendix I. In Fig. 18 the results of the nozzle calibration tests are plotted as a function of Reynolds number. Above a Reynolds number of $7(10^5)$ these results differ by less than 1 per cent from those found by Naviaux. Below a Reynolds number of $7(10^5)$ Naviaux's nozzle coefficient decreases sharply to a value of 1.002 at a Reynolds number of $4.2(10^5)$. The nozzle coefficients obtained from the present tests decrease less sharply below a Reynolds number of $7(10^5)$ resulting in differences of between 2 and 4 per cent at Reynolds numbers between $4.2(10^5)$ and $6(10^5)$. Since the present study was concerned with flows over a wider range of Reynolds numbers, considerably more data were taken at Reynolds numbers below $6(10^5)$.

An analytical expression for the nozzle discharge coefficient as a function of Reynolds number was obtained by using the method of least squares. This expression, which represents a fourth order polynomial approximation to the reduced data and is also plotted in Fig. 18, is

$$K_n = 9.32928\times10^{-1} + 4.268322\times10^{-7} R_e - 6.151495\times10^{-13} R_e^{\,2} + 3.895006\times10^{-19} R_e^{\,3} - 9.138062\times10^{-26} R_e^{\,4} \qquad (1)$$

where

K_n = nozzle discharge coefficient

R_e = Reynolds number referred to nozzle diameter

The maximum deviation between reduced data points and the analytical curve in the operating range of the impulse turbine between Reynolds numbers of $4(10^5)$ and $8(10^5)$ is 0.3 per cent.

SECTION 5

PLENUM LABYRINTH SEAL LEAK RATE

The method used for the plenum labyrinth seal leak tests and the associated instrumentation are described by Eckert [3]. Although the measuring techniques remained unchanged, the tests were carried out over a wider range of operating conditions.

The purpose of these tests was to find a simple analytical expression for the determination of the leak rate as a function of the pressure ratio across the labyrinth. This expression should cover the entire operating range of the TTR. To accomplish this goal two series of labyrinth leak tests were performed. The so-called hooded configuration of the TTR was used for both test series. Figure 9 represents a schematic of the installation of the TTR and shows the exhauster with the necessary piping for hooded operation. Labyrinth leak rates at pressure ratios between 1 and 6 were measured in both series of tests.

The first test series was performed before the impulse turbine was tested. From these tests a referred leak rate as a function of labyrinth pressure ratio was determined which was based on the actual labyrinth flow rate obtained from the square-edged orifice data for different conditions in the plenum. The referred leak rate (in^2) is

$$\Phi_L = \frac{\dot{W}_L}{P_{tp}\sqrt{T_{tp}\,\frac{R}{g}}} \qquad (2)$$

where

$\dot{W}_L$ = labyrinth flow rate (lbm/sec)

P_{tp} = inlet plenum total pressure (lb_f/in^2)

T_{tp} = inlet plenum total temperature (^oR)

R = gas constant for air ($ft\text{-}lb_f/lbm\text{-}^oR$)

g = gravitational constant ($lbm\text{-}ft/lb_f\text{-}sec^2$)

The results of the first series of labyrinth leak tests and the analytical expression derived from them are shown in Fig. 19. It can be seen that the labyrinth leak rate becomes choked at a pressure ratio of about 3. The referred labyrinth leak rate for the choked condition is equal to 0.073. This value corresponds to a flow rate between 0.06 lbm/sec and 0.1 lbm/sec, depending on inlet total conditions.

After the first twelve test runs of the impulse turbine, inconsistent values of turbine flow rates were noted. Analysis of these runs indicated that the inconsistency was probably due to errors in the labyrinth leak rate (Section 8). Re-evaluating the data from the first series of labyrinth leak tests, it was noticed that the hood temperature from run to run did not vary by more than 8^oF and remained practically constant during each run. However, during normal operation of the TTR with the turbine installed, the hood temperature is a function of the turbine discharge temperature and varies with turbine speed. Furthermore, the variation of hood temperature at different pressure ratios can be as much as 90^oF. The difference in the range of hood temperatures during the first labyrinth tests and

during normal operations of the TTR made it necessary to perform a second series of leak tests. For this series a two inch pipe with a gate valve was connected from tank 1 to the TTR hood. Since the air temperature in tank 1 can be changed by about 100°F, it was possible to control the hood temperature.

Three tests were performed at hood temperatures of 59°F, 91°F and 116°F, each for the whole range of pressure ratios of the TTR. The results of these tests are given in Fig. 20, which shows the referred leak rate of Eq. (2) as a function of labyrinth pressure ratio. From this figure it is seen that the labyrinth leak rates depend on the hood temperature. Above a pressure ratio of 3 the referred leak rate varies by 12 per cent for a change in hood temperature of 57°F. Since this temperature can vary by 90°F during the turbine tests, an expression for the leak rate was empirically obtained which is independent of hood temperature and inlet plenum conditions. This expression is obtained by multiplying Eq. (2) with a correction factor which depends on the hood temperature and the inlet plenum total temperature. This so-called modified referred leak rate Φ_{LM} was found to be

$$\Phi_{LM} = \Phi_L \left[1 + 0.32 \left(\frac{t_{tp} - t_h}{t_{tp}} \right) \right]^{1.2} \qquad (3)$$

where

Φ_L = expression from Eq. (2)

t_{t_p} = inlet plenum total temperature ($^{\circ}F$)

t_h = hood temperature ($^{\circ}F$)

Figure 21 shows Φ_{LM} as a function of labyrinth pressure ratio from the tests at the three above-mentioned hood temperatures. An analytical expression for Φ_{LM} as a function of labyrinth pressure ratio was obtained from the method of least squares, by approximating the test data by a fifth order polynomial. The resulting expression is

$$\Phi_{LM} = -0.1004586 + 0.2122579r - 0.1081851r^2 + 0.0276576r^3 - 0.003489933r^4 + 0.0001726733r^5 \quad (4)$$

where

r = labyrinth pressure ratio = P_{t_p}/P_2

P_2 = hood static pressure (lb_f/in^2)

Equation (4) is plotted in Fig. 21. The maximum deviation between the test data and the analytical curve is 4 per cent for the operating range ($1.0 < r \leq 4.0$) of the impulse turbine.

The IBM 360 Computer was used to reduce the data for both series of labyrinth leak tests. The computer program for the data reduction is presented in Appendix I together with the output for the second series of tests.

SECTION 6

ANALYSIS AND DATA REDUCTION

6.1 General

The TTR is instrumented to obtain data for a one-dimensional performance analysis of single stage axial turbines. It is assumed that steady axisymmetric flow conditions exist at the entrance and exit of the blade rows and that the flow on the mean stream surface is representative of the flow through the whole stage. The mean stream surface is assumed to exist at the mean radius R_m

$$R_m = \frac{R_t + R_h}{2} \tag{5}$$

where

R_t = radius of stator blade tip (in)

R_h = radius of stator blade hub (in)

The TTR data were analyzed on the IBM 360 Computer at the Naval Postgraduate School. The computer program is described in Appendix I, which give samples of print-outs for runs 32, 33 and 34.

6.2 Flow Rate Determination

The flow rate through the turbine is the difference of the flow rate through the flow nozzle and the labyrinth leak rate,

$$\dot{W} = \dot{W}_n - \dot{W}_L \tag{6}$$

where

$\dot{W}_n$ = nozzle flow rate (lbm/sec)

$\dot{W}_L$ = labyrinth leak rate (lbm/sec)

The nozzle flow rate is obtained from the nozzle flow equation given by Commons (Reference 2, p. 46). However, the nozzle discharge coefficient K_n is determined from Eq. (1). Moreover, the constant in Commons' equation was found to be incorrect. The correct equation for the determination of $\dot{W}_n$ is

$$\dot{W}_n = 0.16384 D_n^2 \alpha_n K_n Y_1 \sqrt{\frac{P_{noz}\, h_w}{T_{noz}}} \tag{7}$$

where

D_n = nozzle throat diameter (in)

α_n = coefficient of thermal expansion of the flow nozzle (dimensionless)

K_n = nozzle discharge coefficient from Eq. (1) (dimensionless)

Y_1 = expansion factor (dimensionless)

h_w = differential pressure across the pressure taps at 68° F (in H_2O)

P_{noz} = absolute static pressure at upstream pressure tap (lb/in^2)

T_{noz} = temperature at upstream pressure tap (°R)

The leakage flow rate through the plenum labyrinths is obtained from

$$\dot{W}_L = \frac{\Phi_{LM}\, P_{tp}}{\sqrt{T_{tp} R/g}\left[1 + 0.32\left(\frac{T_{tp} - T_n}{T_{tp}}\right)\right]^{1.2}} \tag{8}$$

where Φ_{LM} is the modified referred labyrinth leak rate obtained from Eq. (4)

6.3 Stator Entrance Properties

The total pressure P_{to} at the stator entrance is taken as the average of the data obtained with the five fixed total pressure probes. A radial survey with the 3-hole flow probe at this location indicated a maximum variation of 0.75 per cent in total pressure from stator hub to stator tip. The results of this pressure survey are presented in Fig. 22. The total temperature T_{to} is obtained from two Temperature-Kiel probes.

6.4 Stator Discharge Properties

The stator discharge properties can be obtained from the momentum and moment of momentum equations applied to the fluid in the stator assembly. These two fundamental equations yield the axial and peripheral velocities from which the other discharge properties can be derived. In addition, the axial velocity component can be obtained also from the equation of continuity applied to the stator exit. The equations used in the stator analysis are presented here without derivation, since they are given by Messegee [7]. From the theorem of angular mementum

$$V_{ul} = 12(M_s + M_{cl})g/\dot{N} R_{ml} \qquad (9)$$

where

V_{ul} = peripheral component of absolute velocity at stator exit (ft/sec)

M_s = moment acting on stator assembly, measured by a reluctance gage ($ft\text{-}lb_f$)

M_{cl} = moment acting on closure plate ($ft\text{-}lb_f$)

R_{ml} = mean radius at stator discharge (in)

The two values of the average axial velocity component obtained from the momentum and continuity equations are used to establish a parabolic change of the pressure at the stator discharge between the measured pressures at hub and tip such that both methods yield the same results. These calculations are carried out by an iteration procedure of the computer program. However, the resulting pressure distribution cannot be verified experimentally. The stator exit pressure distribution is first assumed to be linear between the stator hub and tip pressures. From the momentum equation

$$V_{al} = g/\dot{W}\left[F_s + F_{cl} - F_o - 2\pi \int_{R_{hl}}^{R_{tl}} P_l r dr\right] \qquad (10)$$

where

V_{al} = axial velocity component at stator discharge (ft/sec)

F_s = force acting on stator assembly, measured by reluctance gage (lb_f)

F_{cl} = force acting on stator assembly by closure plate, measured by strain gages (lb_f)

F_o = sum of pressure forces acting on stator assembly less force due to the stator discharge pressure (lb_f)

P_1 = static pressure at radius r at stator exit (lb_f/in^2)

The last term of Eq. (10) is then evaluated by assuming that P_1 varies parabolically from hub to tip. A factor ϵ is introduced so that the shape of the parabola can be changed to satisfy continuity considerations. From the derivation presented in Appendix II

$$2\pi \int_{R_{hl}}^{R_{tl}} P_1 r\,dr = \frac{\pi}{3} P_{hl}\left[(1+\epsilon)R_{tl}^2 + R_{tl}R_{hl} - (2+\epsilon)R_{hl}^2\right] + \frac{\pi}{3} P_{tl}\left[(2+\epsilon)R_{tl}^2 - R_{tl}R_{hl} - (1+\epsilon)R_{hl}^2\right] \tag{11}$$

where

P_{hl} = hub static pressure at stator discharge (lb_f/in)

P_{tl} = tip static pressure at stator discharge (lb_f/in)

The integral of Eq. (10) can be represented by an average stator discharge pressure P_{lav}, multiplied by the stator exit axial area. Using Eq. (11),

$$P_{lav} = \frac{P_{hl}}{3}\left[\frac{(1+\epsilon)R_{tl}^2 + R_{tl}R_{hl} - (2+\epsilon)R_{hl}^2}{R_{tl}^2 - R_{hl}^2}\right] + \frac{P_{tl}}{3}\left[\frac{(2+\epsilon)R_{tl}^2 - R_{tl}R_{hl} - (1+\epsilon)R_{hl}^2}{R_{tl}^2 - R_{hl}^2}\right] \tag{12}$$

From the continuity equation

$$V_{al} = \left[C \left[T_{to} - \frac{CA_1^2 P_{1av}^2}{R^2 \dot{W}^2} \left(-1 + \left(1 - \frac{4\dot{W}^2 R^2}{CA_1^2 P_{1av}^2} \left(\frac{V_{ul}^2}{C} - T_{to} \right) \right)^{\frac{1}{2}} \right) \right] - V_{ul}^2 \right]^{\frac{1}{2}} \quad (13)$$

where

A_1 = effective axial flow area at stator exit (in^2)

C = conversion factor, $2gJc_p$ ($ft^2/sec^2 - {}^oR$)

c_p = specific heat at constant pressure (BTU/lbm-^oR)

The axial velocity component obtained from Eqs. (10) and (13) varies directly with the stator discharge pressure. Since this pressure is a function of the factor ϵ, an increase or decrease in ϵ will increase or decrease the axial velocity, respectively. The solutions of these equations are matched by varying ϵ until the velocity calculated with Eq. (10) equals the velocity calculated from Eq. (13). This iteration is possible because the value of Eq. (10) changes more rapidly for a change in ϵ than the value of Eq. (13). The absolute velocity at the stator exit is then

$$V_1 = \left[V_{al}^2 + V_{ul}^2 \right]^{\frac{1}{2}} \quad (14)$$

The static temperature T_1 at the stator exit is found from the energy equation, or

$$T_1 = T_{to} - \frac{V_1^2}{2gJc_p} \quad (15)$$

From Fig. 23, which represents a velocity diagram of a turbine stage, it can be seen that the angle of the absolute flow at the stator discharge is

$$\alpha_1 = \text{Tan}^{-1} (V_{ul}/V_{al}) \tag{16}$$

Further, the relative velocity W_1 at the rotor inlet has an axial component

$$W_{al} = V_{al} \tag{17}$$

and a peripheral component

$$W_{ul} = V_{ul} - U_1 \tag{18}$$

where, with N representing the rotor speed in rpm,

$$U_1 = \frac{N\pi R_{m1}}{360} \tag{19}$$

Thus, the relative velocity is

$$W_1 = [W_{al}^2 + W_{ul}^2]^{\frac{1}{2}} \tag{20}$$

The angle of the relative flow at the rotor inlet is

$$\beta_1 = \text{Tan}^{-1} (W_{ul}/W_{al}) \tag{21}$$

The speed of sound of the air at the stator exit is

$$a_1 = [\gamma g R T_1]^{\frac{1}{2}} \tag{22}$$

where γ is the ratio of the specific heats of the working fluid. The absolute and relative Mach numbers of the flow

at the stator discharge are

$$M_1 = V_1/a_1 \tag{23}$$

$$M_{R1} = W_1/a_1 \tag{24}$$

In accordance with Fig. 24, the stator loss coefficient ζ_s is defined as

$$\zeta_s = \frac{(T_1 - T_{1is})}{\Delta T_{1is}} = \frac{(T_1 - T_{1is})}{(T_{to} - T_{1is})} \tag{25}$$

where

$$T_{1is} = T_{to}\left(\frac{P_{1av}}{P_{to}}\right)^{\frac{\gamma-1}{\gamma}} \tag{26}$$

Also, from Fig. 24,

$$\zeta_s = 1 - \frac{V_1^2}{V_{1th}^2} \tag{27}$$

where

$$V_{1th}^2 = 2gJc_p\,(T_{to} - T_{1is}) \tag{28}$$

The stator efficiency is

$$\eta_s = 1 - \zeta_s \tag{29}$$

The so-called flow function Φ is given by Vavra (Reference 8, Pt. I, p. C24) as

$$\Phi = \frac{\dot{W}}{A_{th}P_{to}}\left[T_{to}\,R/g\right]^{\frac{1}{2}} \tag{30}$$

where A_{th} = stator throat area given in Table I (in^2).
For isentropic conditions the flow function Φ_{is} is obtained from

$$\Phi_{is} = \left[\frac{2\gamma}{\gamma-1}\left[\left(\frac{P_{th}}{P_{to}}\right)^{2/\gamma} - \left(\frac{P_{th}}{P_{to}}\right)^{\frac{\gamma+1}{\gamma}}\right]\right]^{\frac{1}{2}} \tag{31}$$

where P_{th} = stator throat static pressure (lb_f/in^2).
The stator throat pressure is assumed to equal P_{lav} until the flow through the stator becomes choked. For choked conditions the pressure ratio P_{th}/P_{to} in Eq. (31) is taken as the critical pressure ratio, which for air is equal to 0.5283. A stator blockage factor can now be defined by

$$\xi = \Phi / \Phi_{is} \tag{32}$$

Therefore, ξ represents that percentage of throat area which would be necessary to pass the flow if the expansion process through the stator were frictionless.

6.5 Rotor Discharge Properties

The rotor discharge properties are obtained by the application of the moment of momentum equation, the continuity equation, and the energy equation to the fluid passing through the rotor. The flow in the rotor will be treated with respect to a relative coordinate system. In this manner the fundamental laws, applied to the rotating row of blades, will yield discharge properties analogous to those obtained for the stator.

From the moment of momentum equation the peripheral component of the absolute discharge velocity is

$$V_{u2} = \frac{R_{m1}}{R_{m2}} V_{u1} - \frac{12 M_D g}{R_{m2} \dot{W}} \tag{33}$$

where

M_D = moment acting on the dynamometer measured by a reluctance gage (ft-lb_f)

R_{m2} = mean radius at rotor discharge (in)

The peripheral component of the relative velocity is

$$W_{u2} = V_{u2} - U_2 \tag{34}$$

with

$$U_2 = U_1 \frac{R_{m2}}{R_{m1}} \tag{35}$$

Introducing the so-called equivalent temperature T_E as defined by Vavra (Reference 8, Pt. III, p. G4), the energy equation for relative flows becomes

$$T_E = T_1 + \frac{W_1^2}{2gJc_p} + \frac{U_2^2 - U_1^2}{2gJc_p} = T_2 + \frac{W_2^2}{2gJc_p} \tag{36}$$

Using the energy equation in this form with the continuity equation, the static temperature at the rotor discharge is found as

$$T_2 = \frac{\gamma}{\gamma - 1} \frac{P_2^2 A_2^2 g}{\dot{W}^2 R} \left[\left[1 - \frac{2}{g} \left(\frac{\gamma - 1}{\gamma} \right) \frac{\dot{W}^2 R}{P_2^2 A_2^2} \left(\frac{W_{u2}^2}{2gJc_p} - T_E \right) \right]^{\frac{1}{2}} - 1 \right] \tag{37}$$

where

P_2 = hood static pressure (lb_f/in^2)

A_2 = effective axial flow area at rotor discharge (in^2)

From Fig. 24, the total temperature at the rotor discharge is

$$T_{t2} = T_{to} - \Delta T_W \tag{38}$$

The temperature drop ΔT_W is proportional to the work generated by the turbine stage or

$$\Delta T_W = \frac{M_D(\omega)}{\dot{W} c_p J} \tag{39}$$

where

ω = rotational speed of rotor (rad/sec).

From Euler's turbine equation, ΔT_W is also

$$\Delta T_W = \frac{U_1 V_{u1} - U_2 V_{u2}}{g J c_p} \tag{40}$$

In accordance with Fig. 24, the absolute and relative velocities at the rotor discharge are

$$V_2 = \left[(T_{t2} - T_2) 2 g J c_p\right]^{\frac{1}{2}} \tag{41}$$

$$W_2 = \left[(T_E - T_2) 2 g J c_p\right]^{\frac{1}{2}} \tag{42}$$

The axial velocity components of V_2 and W_2 are

$$V_{a2} = W_{a2} = \left[V_2^2 - V_{u2}^2\right]^{\frac{1}{2}} \tag{43}$$

From Fig. 23, the angles of the absolute and relative velocities at the rotor discharge are

$$\alpha_2 = \text{Tan}^{-1} \left(V_{u2}/V_{a2}\right) \tag{44}$$

$$\beta_2 = \text{Tan}^{-1} \left(W_{u2}/W_{a2}\right) \tag{45}$$

With the equivalent temperature of Eq. (12), the rotor loss coefficient is obtained from

$$\zeta_R = \frac{T_2 - T_{2is}}{T_E - T_{2is}} \tag{46}$$

with

$$T_{2is} = T_E\left(\frac{P_2}{P_{El}}\right)^{\frac{\gamma-1}{\gamma}} = T_1\left(\frac{P_2}{P_{1av}}\right)^{\frac{\gamma-1}{\gamma}} \tag{47}$$

where

P_{El} = total equivalent pressure at the stator discharge (lb_f/in^2). From Fig. 24, the rotor loss coefficient of Eq. (46) is also

$$\zeta_R = 1 - \frac{W_2^2}{W_{2th}^2} \tag{48}$$

where

$$W_{2th}^2 = 2gJ_{cp}(T_1 - T_{2is}) + W_1^2 + U_2^2 - U_1^2 = 2gJc_p(T_E - T_{2is}) \tag{49}$$

The rotor efficiency is

$$\eta_R = 1 - \zeta_R \tag{50}$$

6.6 Performance Parameters

For the evaluating of the overall performance of a turbine stage it is advantageous to use dimensionless coefficients. The performance parameters presented in this section are those given by Vavra [9].

The overall stage efficiency is the ratio of the work generated by the turbine stage and the isentropic enthalpy drop across the turbine from the total conditions at the stator inlet to the static conditions at the rotor discharge. Therefore, the so-called total-static efficiency is obtained from

$$\eta = \frac{\Delta T_W}{\Delta T_{is}} = \frac{\frac{M_D \omega}{\dot{W} c_p J}}{\Delta T_{is}} \tag{51}$$

where, as shown by Fig. 24,

$$\Delta T_{is} = T_{to}\left[1 - \left(\frac{P_2}{P_{to}}\right)^{\frac{\gamma-1}{\gamma}}\right] \tag{52}$$

ΔT_{is} can be expressed also by

$$\Delta T_{is} = \frac{C_o^2}{2gJc_p} \tag{53}$$

where C_o is the theoretical velocity obtained by an isentropic expansion from P_{to} to P_2.

The theoretical degree of reaction r* is that fraction of the isentropic enthalpy drop of the turbine stage which is used up by the rotating row of blades. It is a measure

for the acceleration of the relative flow in the rotor. From Fig. 24

$$r^* = 1 - \frac{V_{1th}^2}{C_o^2} \tag{54}$$

Using Eqs. (26), (28), (52) and (53) the degree of reaction at the hub or the tip of the blading can be expressed by

$$r^* = \frac{\left(\frac{P'}{P_2}\right)^{\frac{\gamma-1}{\gamma}} - 1}{\left(\frac{P_{to}}{P_2}\right)^{\frac{\gamma-1}{\gamma}} - 1} \tag{55}$$

where $P' = P_{h1}$ or P_{t1} (lb_f/in^2).

The isentropic head coefficient K_{is} is used to estimate the number of stages necessary to handle a given isentropic enthalpy drop at a given speed U_1. It is defined as

$$K_{is} = \left(\frac{C_o}{U_1}\right)^2 \tag{56}$$

The work coefficient K is a measure of the actual work that the stage generates per unit mass of fluid at a given speed U_1, or

$$K = \frac{\Delta T_w}{U_1^2/2gJc_p} \tag{57}$$

The peripheral speed U_1 was selected to make K_{is} and K dimensionless since it is usually a fixed quantity determined by rotor stress considerations.

Referred values of flow rate, rotational speed, dynamometer moment, and horsepower are obtained by using the NASA reference system. They are defined by

$$W_{REF} = \frac{\dot{W}\sqrt{\theta}}{\delta} \tag{58}$$

$$N_{REF} = N/\sqrt{\theta} \tag{59}$$

$$M_{DREF} = M_D/\delta \tag{60}$$

$$HP_{REF} = \frac{HP}{\delta\sqrt{\theta}} = \frac{M_D\,\omega}{550\,\delta\sqrt{\theta}} \tag{61}$$

with

$$\theta = T_{to}/518.4 \tag{62}$$

$$\delta = P_{to}/14.7 \tag{63}$$

SECTION 7

DESCRIPTION OF TURBINE TESTS

During the present study the TTR was operated for 191 hours, 84 of which were used for calibration tests with the impulse turbine installed. The initial tests consisted of the runs conducted before the second series of labyrinth leak tests, and the final tests consisted of three turbine test runs that followed these labyrinth tests.

During the first run of the impulse turbine foreign object damage to the circular-arc rotor blading was encountered. The damaged rotor, however, could be saved by cutting back the leading edge of the blade row by 0.125 inch and shaping each blade as shown in Fig. 6. Another circular-arc rotor with sharp leading edges was installed, and the tests were resumed.

The next five runs were carried out without the exhauster system at a pressure ratio of 2.0 and different axial clearance $\triangle X$ between the stator and the rotor. The turbine was tested at $\triangle X$ equal to 0.200, 0.250, 0.265, 0.300 and 0.350 inch. As stated in Section 3 the radial rotor tip clearance was 0.010 inch for all runs. Data were taken at rotor speeds between 14,000 and 20,000 rpm, where the lower speed was imposed by the maximum torque absorption of the dynamometer.

After the optimum clearance $\triangle X$ was determined, the exhauster was installed for so-called hooded operation of the TTR. Tests were conducted at turbine pressure ratios

of 1.5, 2.0, 2.5, 3.0, 3.5, and 4.0 at speeds up to 20,000 rpm. Several runs were conducted at pressure ratios of 2.0 and 3.0 to insure that consistent results could be obtained. The minimum speed possible with the presently installed dynamometer varies with pressure ratio. The minimum speeds for the above-listed pressure ratios were 9,000; 11,000; 12,500; 14,000; 15,000 and 16,900 rpm, respectively.

A particular turbine pressure ratio can be set by different combinations of stator inlet pressure and hood pressure. However, to adopt a standard procedure, the stator inlet pressure was kept at 5 inches of mercury above the atmosphere, and the pressure in the exhauster was varied to obtain the desired pressure ratio up to a value of about 2.7. For higher pressure ratios the maximum vacuum of about 17 in. Hg was maintained and the stator inlet pressure was increased.

From the initial test results, discrepancies were found in the turbine flow rates and the loss coefficients of stator and rotor. As discussed in Section 8, the second series of labyrinth leak tests was then undertaken to investigate the leakage flow problem. The unrealistic loss coefficients could be attributed to inaccurate measurement of the torque which is exserted on the stator assembly. Inaccurate stator hub and tip static pressures were thought to be a secondary cause for this discrepancy.

For the final three runs the reluctance type force capsule used for measuring the stator torque was disconnected

and one of the horizontal torque flexure shown in Fig. 17 was instrumented with strain gages to measure the torque of the stator assembly. Additionally the static taps for the measuring of the hub and tip pressures at the stator discharge were modified and static taps were arranged to determine the pressures at the hub and tip radius of the stator throat section as shown in Fig. 15.

The final tests were conducted with the hooded configuration of the TTR. For two of the three runs data were recorded at various speeds between the minimum possible and 20,000 rpm at pressure ratios of 2.0 and 2.5. The third run was carried out at a fixed speed of 13,080 rpm and a constant pressure ratio of 2.5. For this run the stator inlet total temperature was varied between 135° and 165° F. Appendix I lists the raw data that were recorded for each run.

SECTION 8

RESULTS AND DISCUSSION OF TURBINE TESTS

Figure 25 gives the measured total-static turbine efficiencies as a function of the referred speed at different values of the axial clearance ΔX. It is seen that the maximum efficiency of 83.0 per cent was obtained for an axial clearance of 0.250 inch.

Increasing ΔX to 0.265 and 0.30 inch produced optimum efficiencies of 82.2 per cent and 82.8 per cent, respectively, indicating that the values obtained for $\Delta X = 0.265$ inch might be doubtful. At a reduced axial clearance of 0.20 inch the optimum efficiency is about 82.2 per cent, equal to that obtained for $\Delta X = 0.35$ inch.

The efficiency, as defined by Eq. (51), depends on the dynamometer torque M_D and the mass flow rate $\dot{W}$, for given values of turbine pressure ratio P_{to}/P_2, inlet total temperature T_{to}, and rotational speed N. The influence of dynamometer torque can be seen by the plot of referred dynamometer moment against referred rotor speed of Fig. 26. Figure 26 shows these data for values of ΔX of 0.250, 0.265 and 0.300 inch. The graph shows that the values of referred dynamometer moment at $\Delta X = 0.250$ inch and $\Delta X = 0.300$ inch lie on the same curve, whereas the data for $\Delta X = 0.265$ inch form a curve that is parallel to but below the curve for the other clearances. Therefore, it can be concluded that the low efficiency obtained with $\Delta X = 0.265$ inch was due to low values of measured

dynamometer torque. During the tests the dynamometer seemed to be functioning normally, and no reason could be found to explain the lower readings. However, during the next several runs it was noticed that the dynamometer readings would sometimes fluctuate by 10 or more counts as the temperature of the dynamometer housing increased. It was found that the fluctuations were due to expansion and contraction with temperature of the coil spring that was located inside the capsule which served as the bearing housing of the dynamometer. After removing this spring consistent values of dynamometer torque were obtained. The results of the runs with the hood attached with $\Delta X = 0.250$ inch indicated that there were inconsistencies in the data necessary for the calculation of the efficiencies and the stator and rotor loss coefficients. These discrepancies will be discussed by comparing the data of runs 21, 23 and 24 carried out with the hood, with the data obtained from run 20 where the turbine discharged into the atmosphere. Runs 20 and 21 were carried out at a pressure ratio of 2.0, and runs 23 and 24 at a pressure ratio of 3.0.

The efficiency as a function of head coefficient K_{is} for the four runs is shown in Fig. 27. It can be noted that the efficiency was different for the runs at equal pressure ratios. Moreover, the maximum efficiency was obtained at a value of K_{is} of about 3.7 for runs 20, 21, and 23 whereas for run 24 the maximum efficiency occurred at $K_{is} = 4.3$.

Figure 28 shows the referred dynamometer moment as a function of referred speed. It is evident from this graph that the difference in efficiencies at a pressure ratio of 3.0 was due to the higher values of the referred dynamometer moment obtained during run 24. The non-linear shape of the referred moment curve accounts for the different value of K_{is} at which the maximum efficiency for run 24 was obtained.

During later runs it was noticed that fluctuations occurred in the dynamometer moment readings. Examination of the reluctance gage showed that a lead from a cannon plug to the gage had broken within the insulation. This faulty lead may have affected the dynamometer readings during run 24.

The referred moments for runs 20 and 21 plotted against referred speed lie on the same curve. Equal referred moments for a given referred speed and pressure ratio indicate that the difference in efficiency must be due to differences in mass flow rates. Since it was believed that errors in turbine flow rate were due to wrong values of labyrinth leakage, the second series of labyrinth leak tests was undertaken as discussed in Section 5. As stated earlier it was found from these tests that the labyrinth leak rate is a function of hood temperature. However, the new labyrinth leak rates used for the reduction of the data from runs 20 and 21 did not account for the difference in efficiency of 1.7 per cent since the variation in hood temperature between the two runs was only $12^{\circ}F$. Without

further testing it is not possible to explain the differences in the efficiencies of Fig. 26.

Equation (25), (27), (46) and (48) show that the stator and rotor loss coefficients depend on the discharge properties after the rows of blades and can be obtained from the calculated velocities. These velocities are obtained with the methods explained in Section 6. The peripheral component of the absolute velocity after the stator is determined primarily from the stator torque measurements. It is about 3 to 4 times larger than the axial velocity component. Thus a variation in peripheral velocity influences the losses more than an equal percentage variation in axial velocity. Figure 29 shows the stator torque reading as a function of speed for runs 20, 21, 23, 24 and 25. All the runs clearly indicate a decrease of the order of 15 per cent in the stator moment as the speed is increased from the minimum rotor speed to 20,000 rpm. It can be shown that a 3.5 per cent variation in the stator moment will change the rotor loss coefficient by about 0.10, hence it can be concluded that the measured stator moments are responsible for the inconsistent values of the losses. Therefore, it was decided to monitor the read-out of the stator torque capsule during the second series of labyrinth leak tests to determine if a change in hood temperature would influence its reading. Since a closure plate was placed over the stator discharge during these tests, any variation of the stator torque capsule reading from its calibration setting had to occur because of different

thermal expansion of the capsule and the frame to which the capsule is attached. Figure 30 is a plot of the torque capsule readings for different hood temperatures. The latter are given in millivolts above the electrical read-out of the instrument at the calibration temperature. The calibration temperature, which changed for each run, was the hood temperature at which the capsule was set to zero. Figure 30 shows that the read-outs of the stator torque capsule are strongly affected by the hood temperature. The read-outs varied by 10 to 15 per cent of full scale read-out over a $56^{\circ}F$ temperature range. To separate the overall losses into stator and rotor losses with a sufficient degree of accuracy, the variation of the stator torque must be less than 2.5 per cent of full scale read-out. The axial stator force, which was monitored also during these tests, varied by less than 1 per cent of full scale read-out in the same temperature range. Since both reluctance capsules are identical except for their operating range, it was concluded that the large variation in the stator torque capsule read-out was due to the thermal expansion of the frame to which the capsule is fastened. This conclusion is supported by Fig. 17 since the U-shaped frame to which the capsule is attached is made of aluminum whose coefficient of thermal expansion is at least twice that of the capsule and its attachment rods.

For the final series of tests one of the horizontal torque flexures shown in Fig. 17 was instrumented with strain gages to measure the stator torque, and the

reluctance torque capsule was removed. Additionally, as shown in Fig. 15, the outer diameter of the closure plate rim was reduced by about 0.030 inch to avoid impingement of flow on the rim which could falsify the readings of the static hub pressure. This modification was necessary since the closure plate assembly could not be centered perfectly with the stator assembly. Moreover, as shown in Fig. 15, a cylindrical shim was placed behind the upstream end of the shroud insert which blocked the upper portion of the stator tip static port, reducing its radial width from 0.069 inch to about 0.025 inch, to ensure a more accurate measurement of the stator tip pressure. From Eq. (10) it is evident that correct measurements of the hub and tip pressures are necessary to obtain accurate values of the axial velocity component after the stator.

Results of tests indicated that the readings obtained by the strain gages attached to the torque flexure were influenced by the hood temperature also. Figure 31 shows the stator and rotor loss coefficients obtained from the data of a run at a constant rotor speed and constant pressure ratio. In Fig. 31 these loss coefficients are shown as functions of the measured hood temperature. It is seen that reasonable values of the loss coefficients were obtained only if the hood temperature did not differ by more than about $2^{\circ}F$ from the temperature at which the torque flexure strain gages were calibrated. During this test it was noticed also that the temperature difference along the flexure was about $70^{\circ}F$, which made it impossible

to compensate the strain gage circuit for temperature. Thus it can be concluded that accurate measurements of the stator moment are not possible with the torque flexure or the reluctance capsule as presently installed in the TTR. However, it is felt that accurate measurements can be obtained with the reluctance capsule if it is relocated as recommended in Section 9.

The change in the axial velocity due to the modifications to the stator hub and tip static pressure ports was negligible. It was found that the tip pressure decreased by about 2 per cent and that the hub pressure remained unchanged from values recorded for similar runs during earlier turbine tests.

As stated in Section 7 the stator throat was instrumented with static pressure taps at the hub and tip radii. The throat hub static pressure was found to be the same as the hub pressure measured in the gap between the closure plate and the stator hub. Whether this condition truly occurs or whether it occurs because of a leak in the measuring line can be verified only by additional tests. The throat tip pressures measured at an overall turbine pressure ratio of 2.5 were 15 per cent higher than the theoretical pressure for choked conditions. The theoretical critical pressure ratio for air is 1.89 and that obtained from the measured stator throat tip pressure was 1.60. This indicates that either the flow is not choked at the tip at a overall turbine pressure ratio of 2.5 or that

the pressure tap is located upstream of the actual stator throat. Tests at higher pressure ratios would show whether the last-mentioned condition exists.

SECTION 9

RECOMMENDATIONS

The rotor and stator losses cannot be separated accurately with the present instrumentation of the TTR because of the difficulties associated with the measurement of the moments that act on the stator assembly. It is felt, however, that accurate measurements of the stator torque are possible if the force capsule is arranged near the back strut of the cradle that supports the stator.

The capsule should be mounted vertically with one end connected to an arm attached to the cylindrical inlet pipe and the other end to a steel frame which is bolted to the cradle. Using steel for the frame reduces the differential thermal expansion of the frame and the capsule. To reduce temperature effects further, an enclosure should be built around the frame and the capsule into which a small amount of ambient air would be blown from the atmosphere to keep the capsule and frame at constant temperature. A similar arrangement has been successful in reducing the temperature effects on the dynamometer force capsule (Reference 2, p.33).

Further tests should be carried out at a number of turbine pressure ratios between 2.0 and 4.0 to determine whether accurate measurements of static pressure can be obtained from the stator throat hub and tip taps as presently installed, or whether these taps need to be relocated. It is suspected that the static pressure line to the stator

throat hub tap has become disconnected in the cavity between the closure plate assembly and the stator hub. This possibility should be investigated before further tests are carried out.



FIGURE 1

BLADE PROFILES
CIRCULAR – ARC ROTOR
CONVERGING STATOR

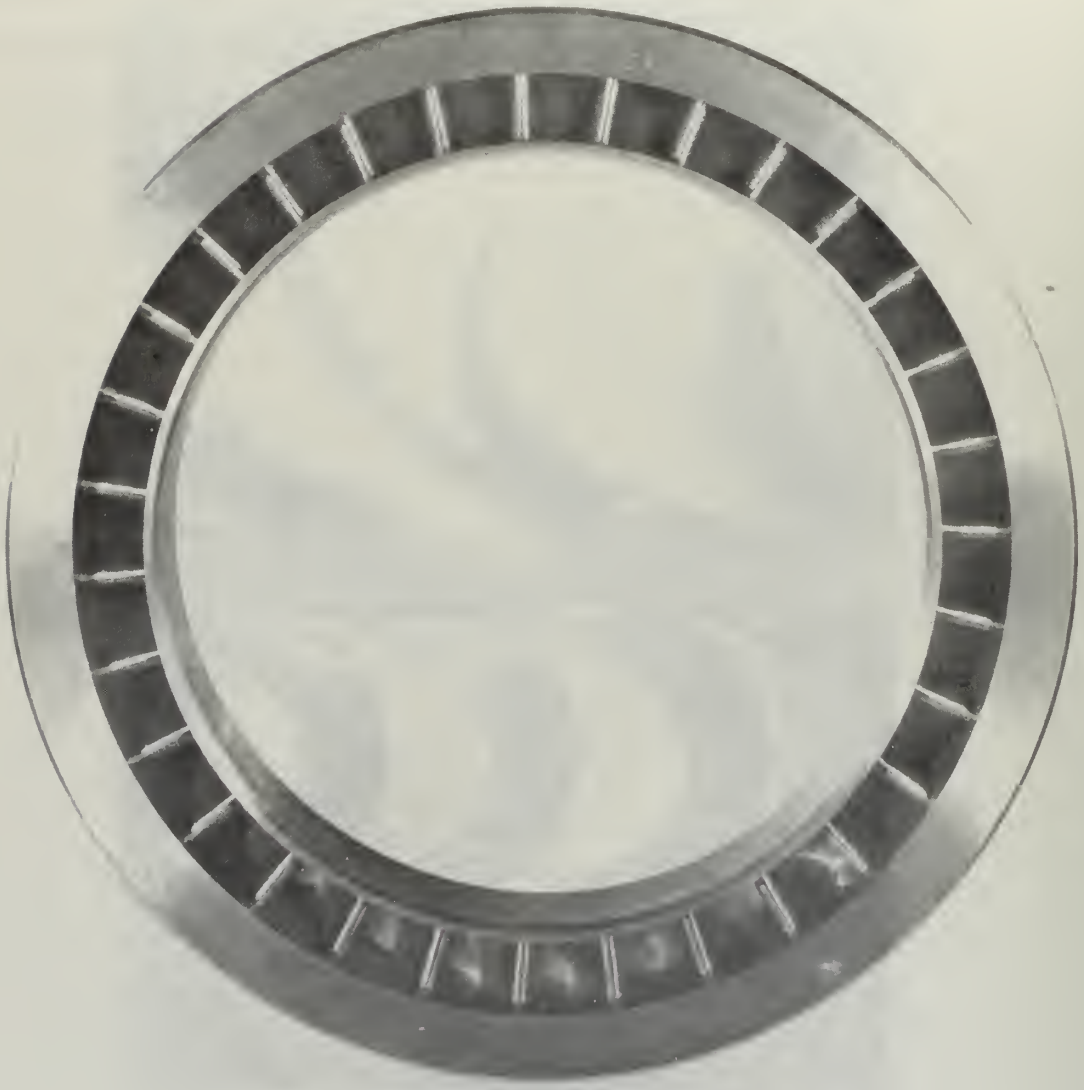


FIGURE 2

CONVERGING STATOR
(VIEW SHOWING STATOR ENTRANCE)



FIGURE 3

CIRCULAR-ARC ROTOR
(VIEW SHOWING ROTOR ENTRANCE)

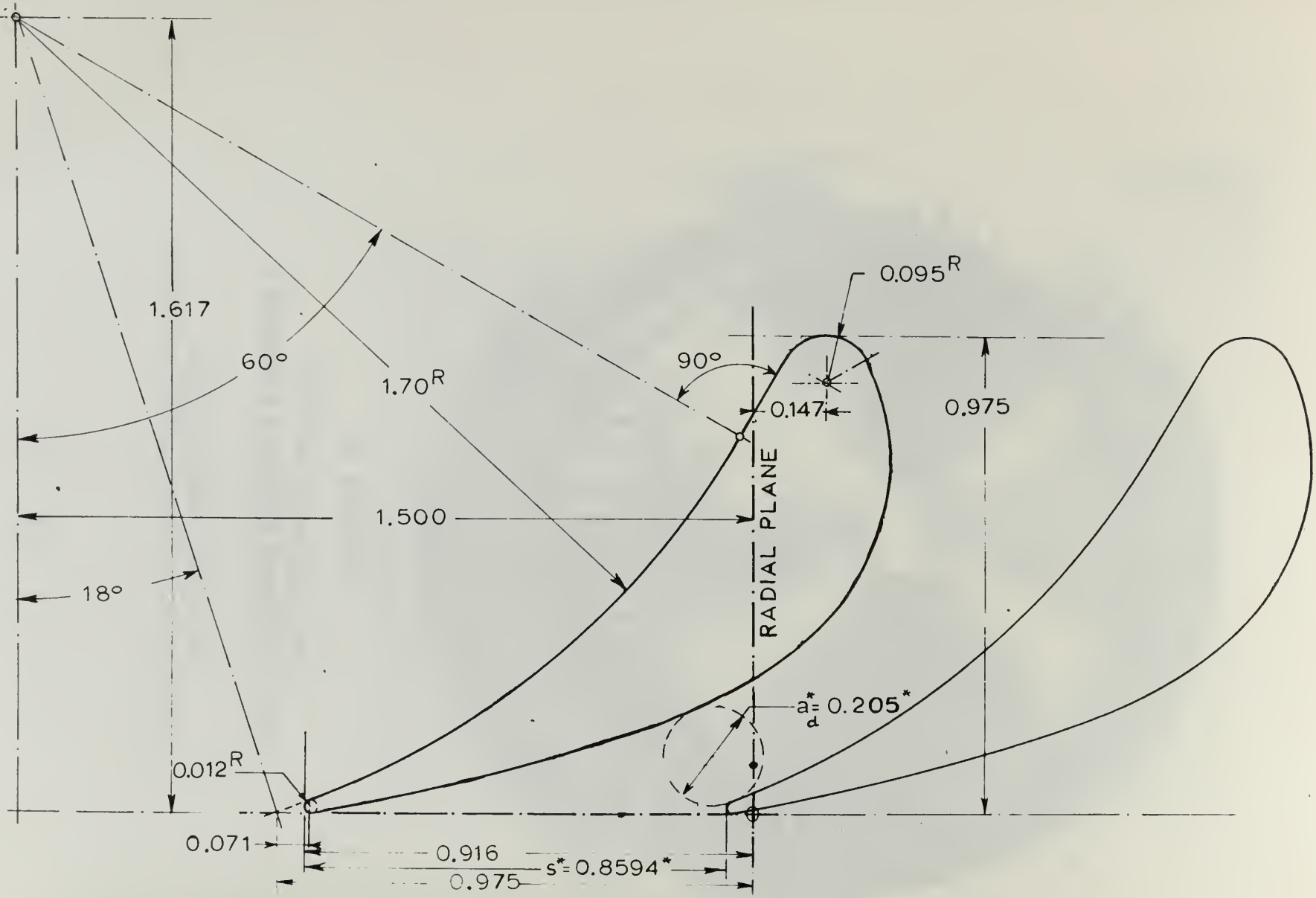


FIGURE 4

MEAN RADIUS BLADE PROFILE

CONVERGING STATOR

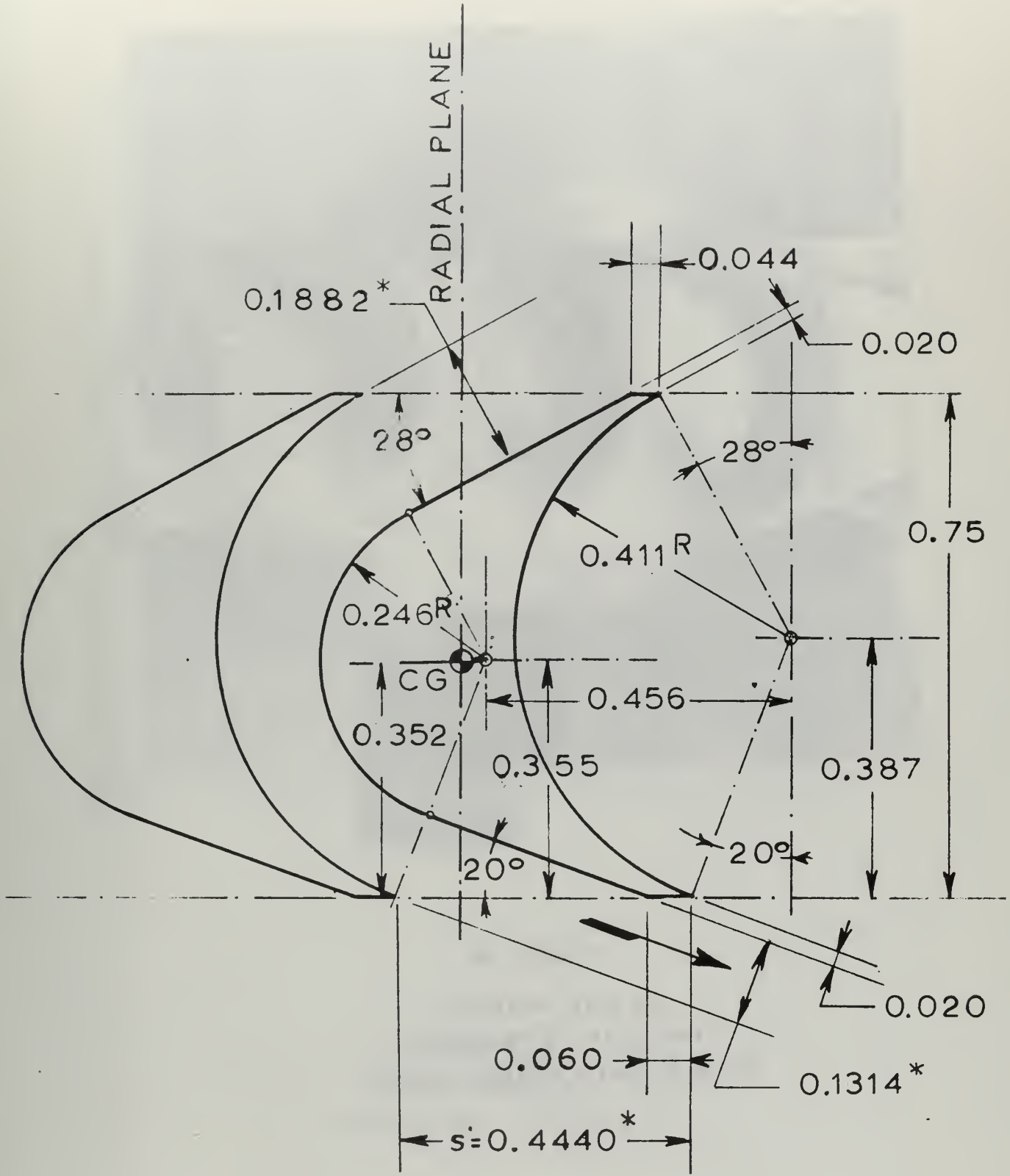


FIGURE 5

MEAN RADIUS BLADE PROFILE

CIRCULAR-ARC ROTOR WITH SHARP LEADING EDGES



FIGURE 6

BLADE PROFILE
CIRCULAR-ARC ROTOR
WITH BLUNT LEADING EDGES



FIGURE 7

BLADE PROFILE
CONTOURED ROTOR

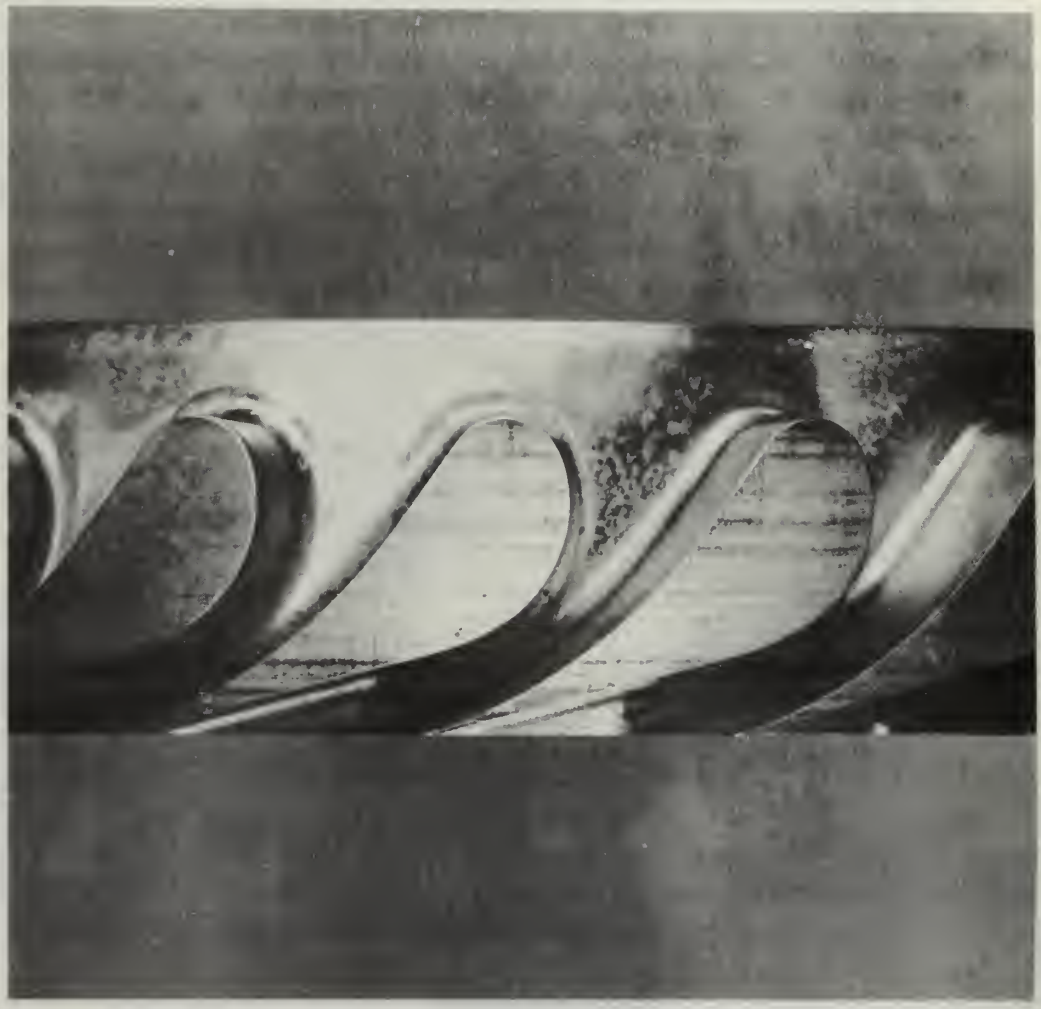


FIGURE 8

BLADE PROFILE
CONVERGING — DIVERGING STATOR

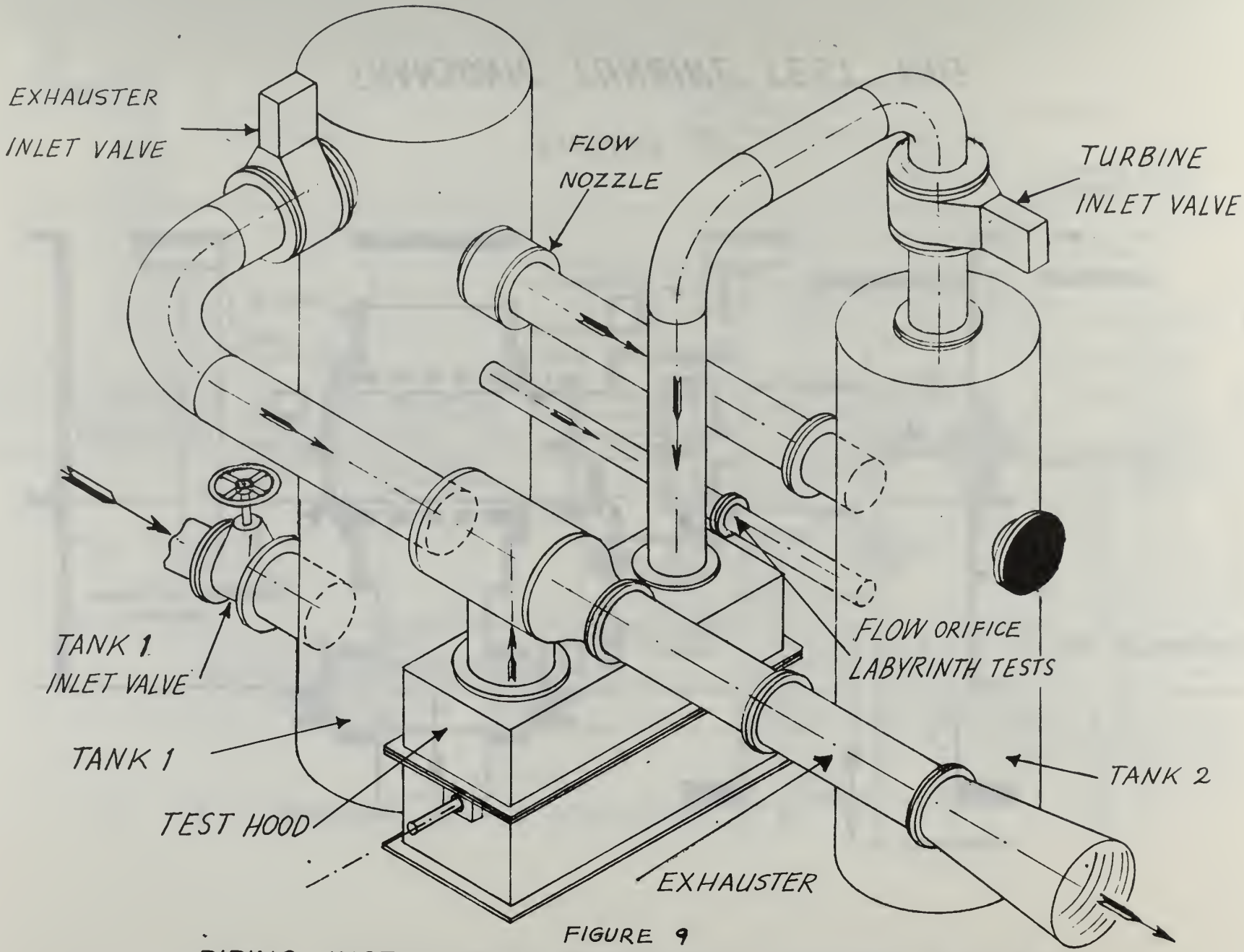


FIGURE 9

PIPING INSTALLATION, TRANSONIC TURBINE TEST RIG

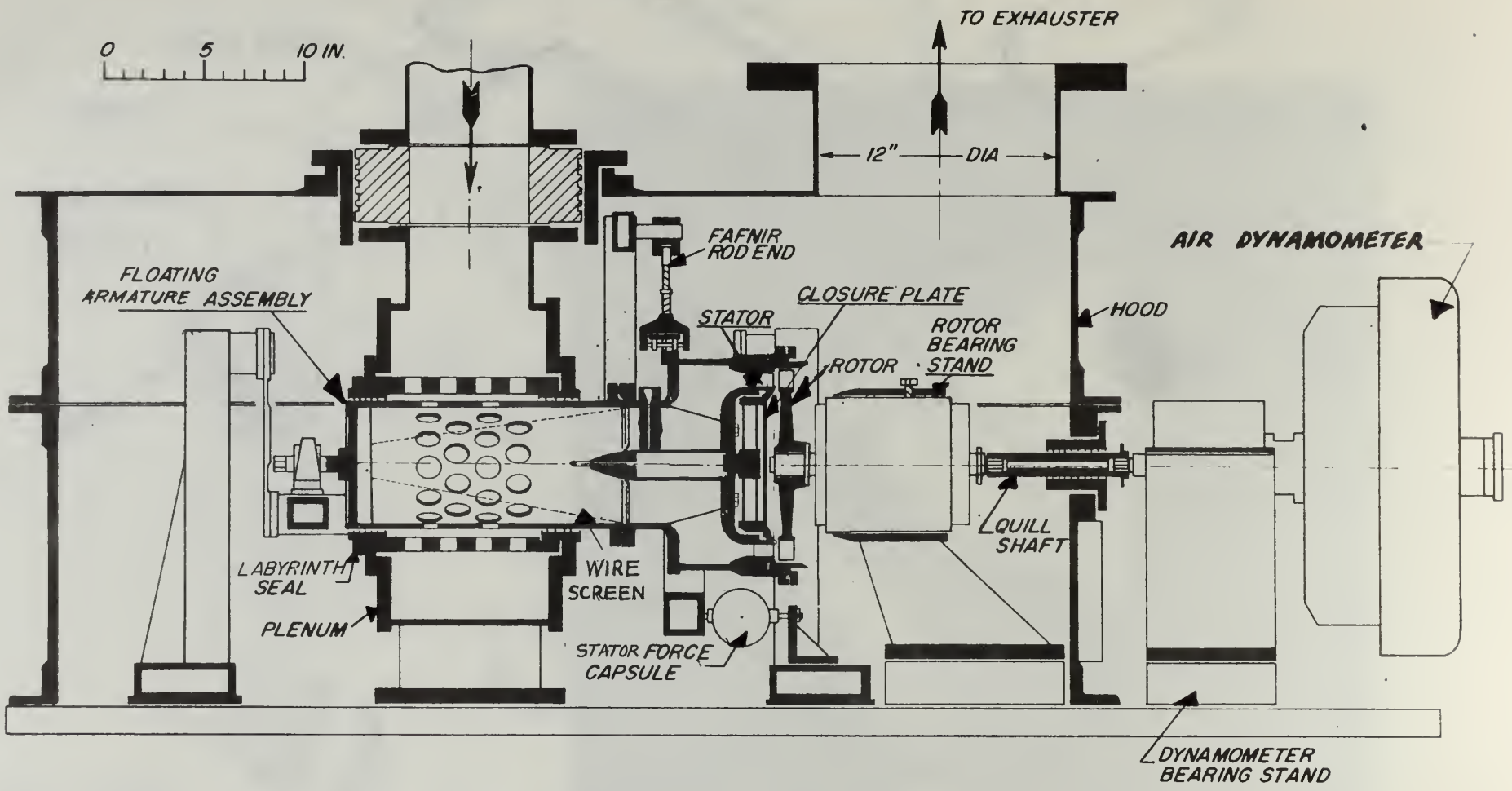


FIGURE 10

TRANSONIC TURBINE TEST RIG

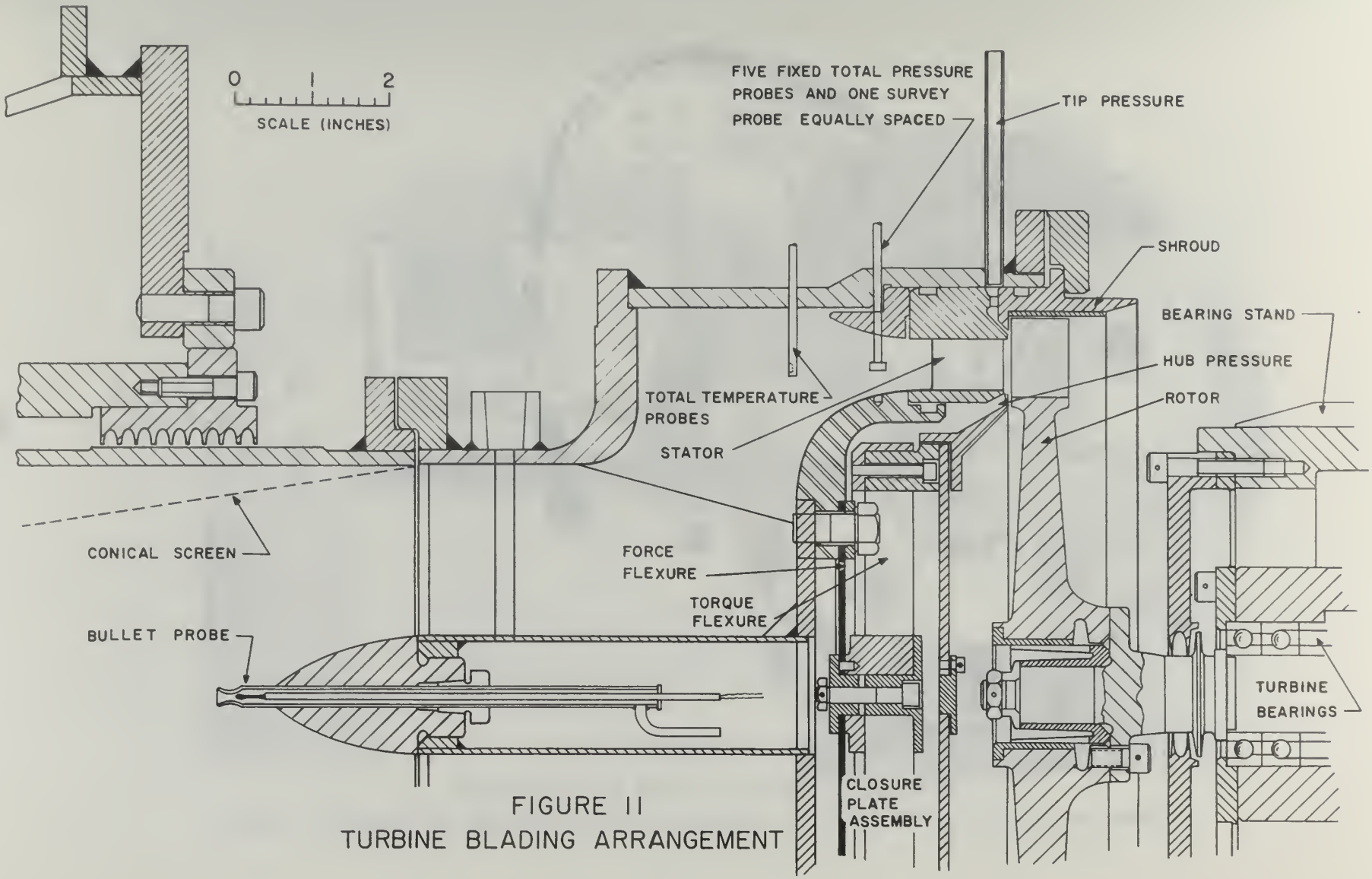


FIGURE 11
TURBINE BLADING ARRANGEMENT

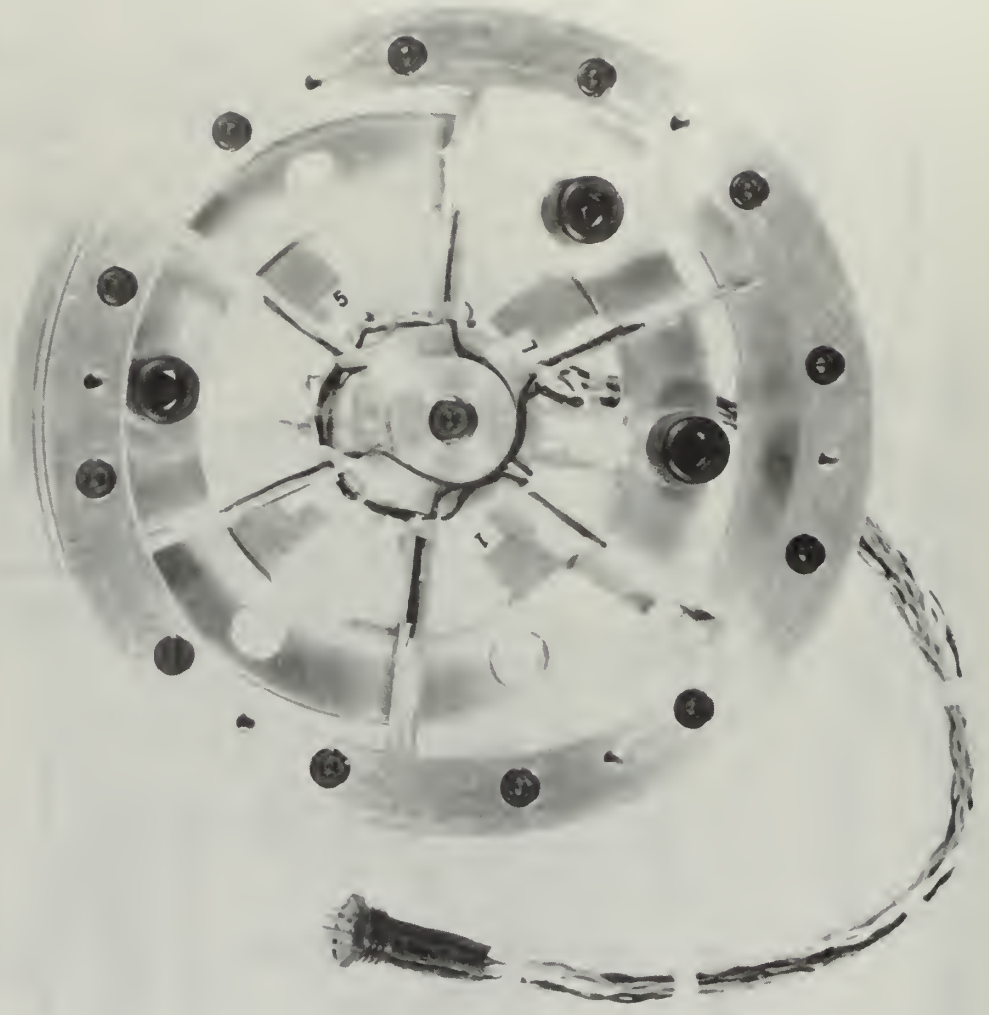


FIGURE 12

CLOSURE PLATE ASSEMBLY
TRANSONIC TURBINE TEST RIG

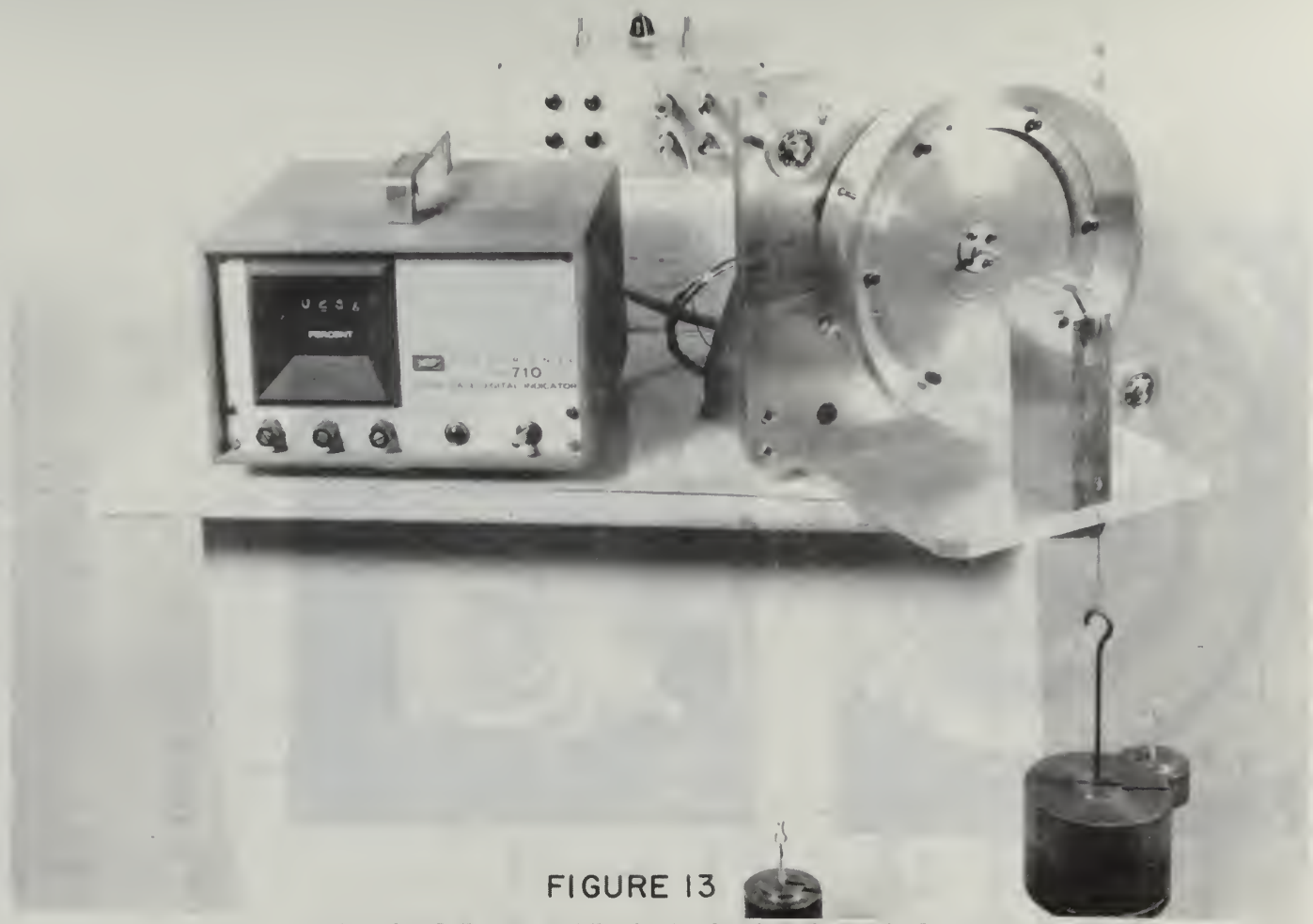
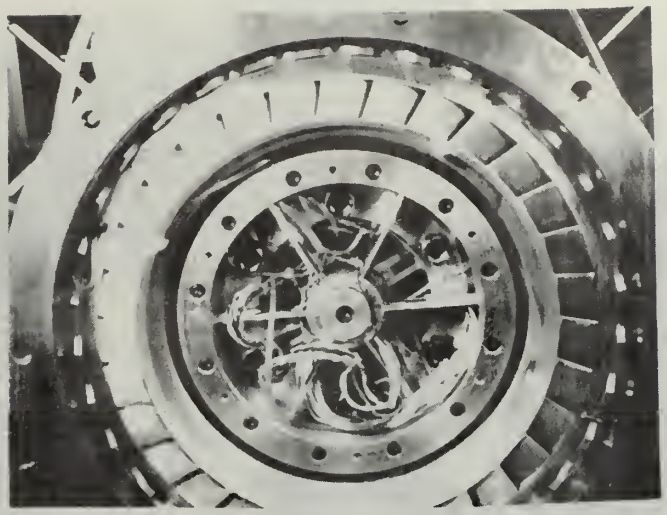


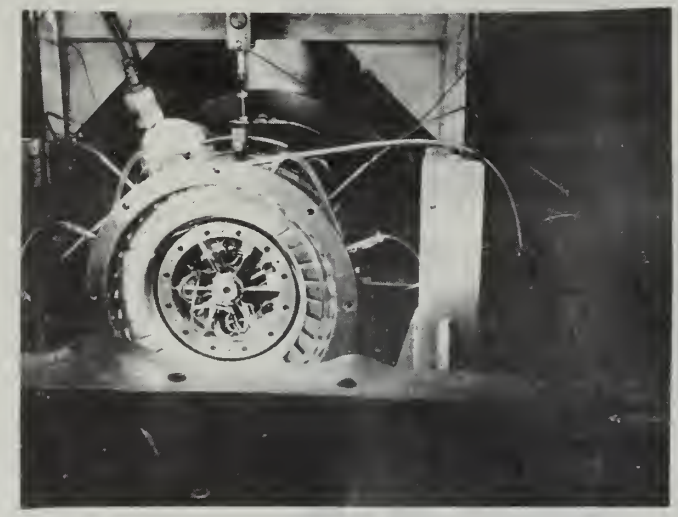
FIGURE 13

CLOSURE PLATE CALIBRATION RIG

(VIEW SHOWING CLOSURE PLATE ASSEMBLY SETUP FOR CALIBRATION RUN)



View a



View b

FIGURE 14

CLOSURE PLATE ASSEMBLY INSTALLATION
TRANSONIC TURBINE TEST RIG

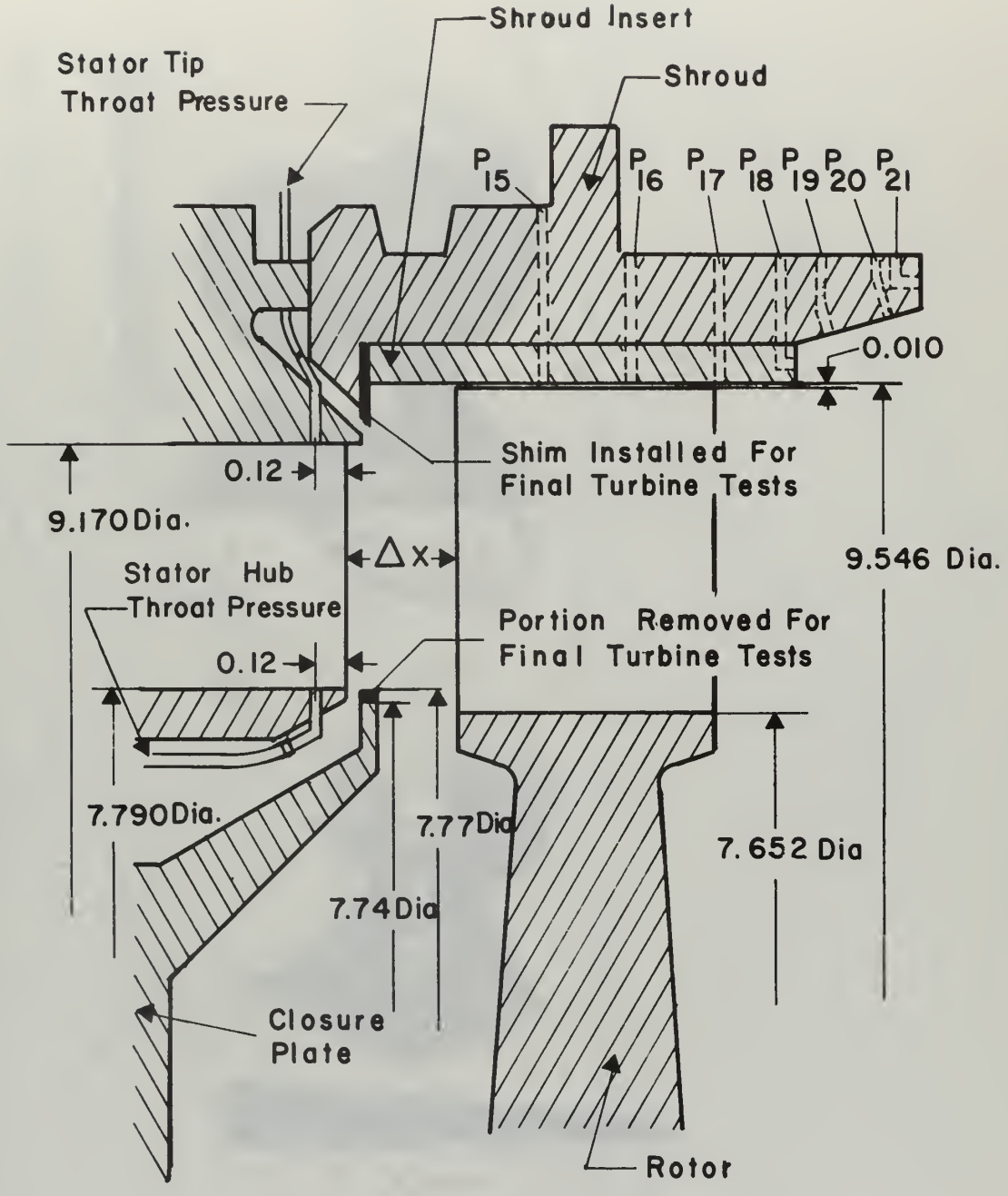
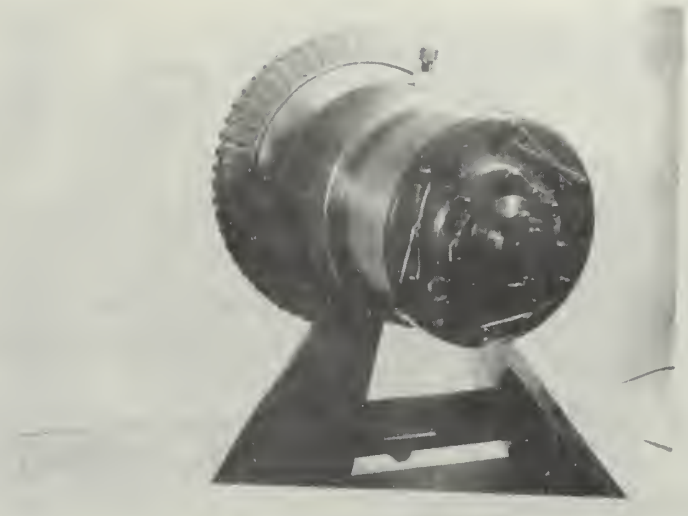


FIGURE 15

TURBINE AND SHROUD DETAILS



View a



View b

FIGURE 16

CIRCULAR-ARC ROTOR AND BEARING ASSEMBLY MOUNTED IN ROTOR BEARING STAND

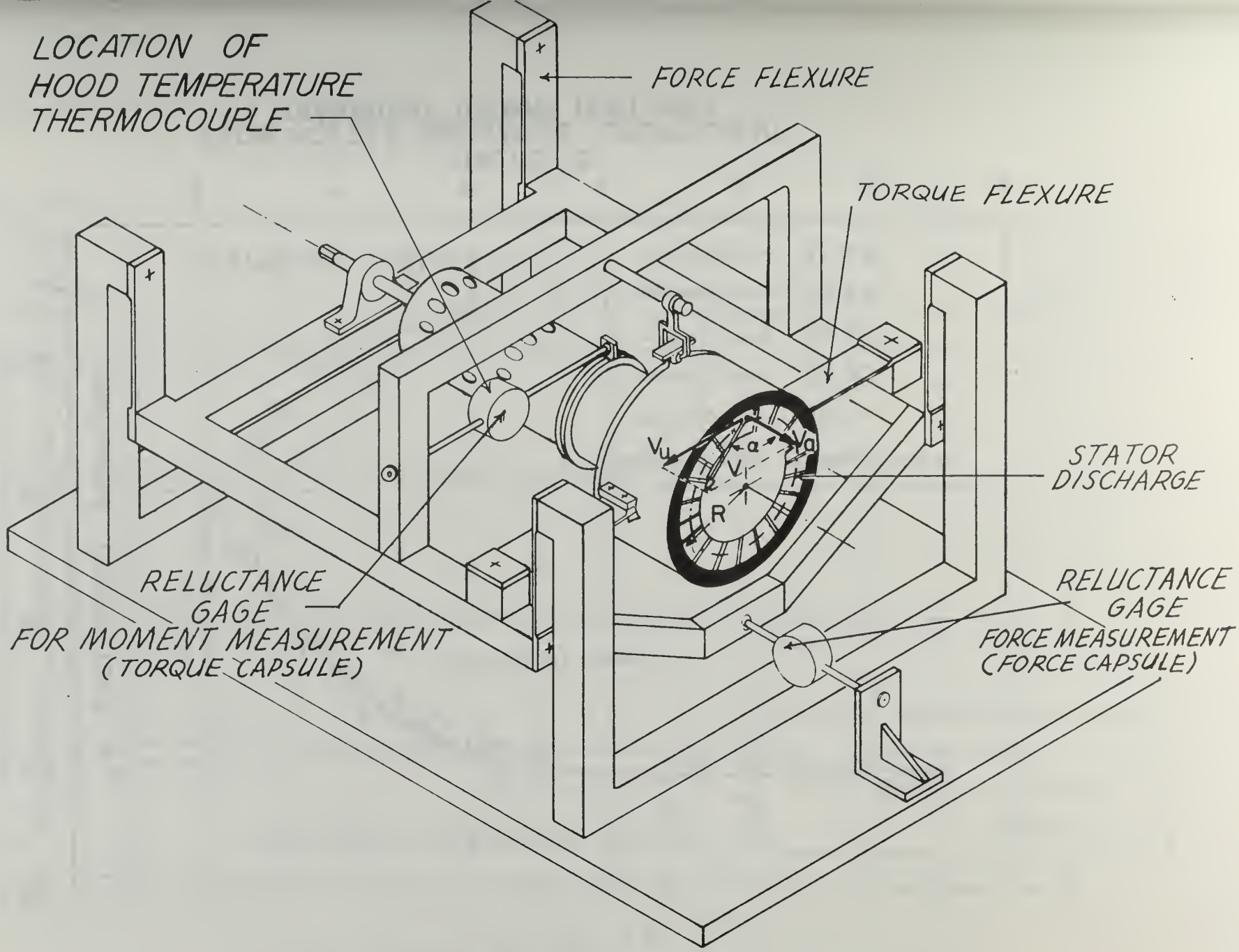


FIGURE 17
FLOATING STATOR ASSEMBLY

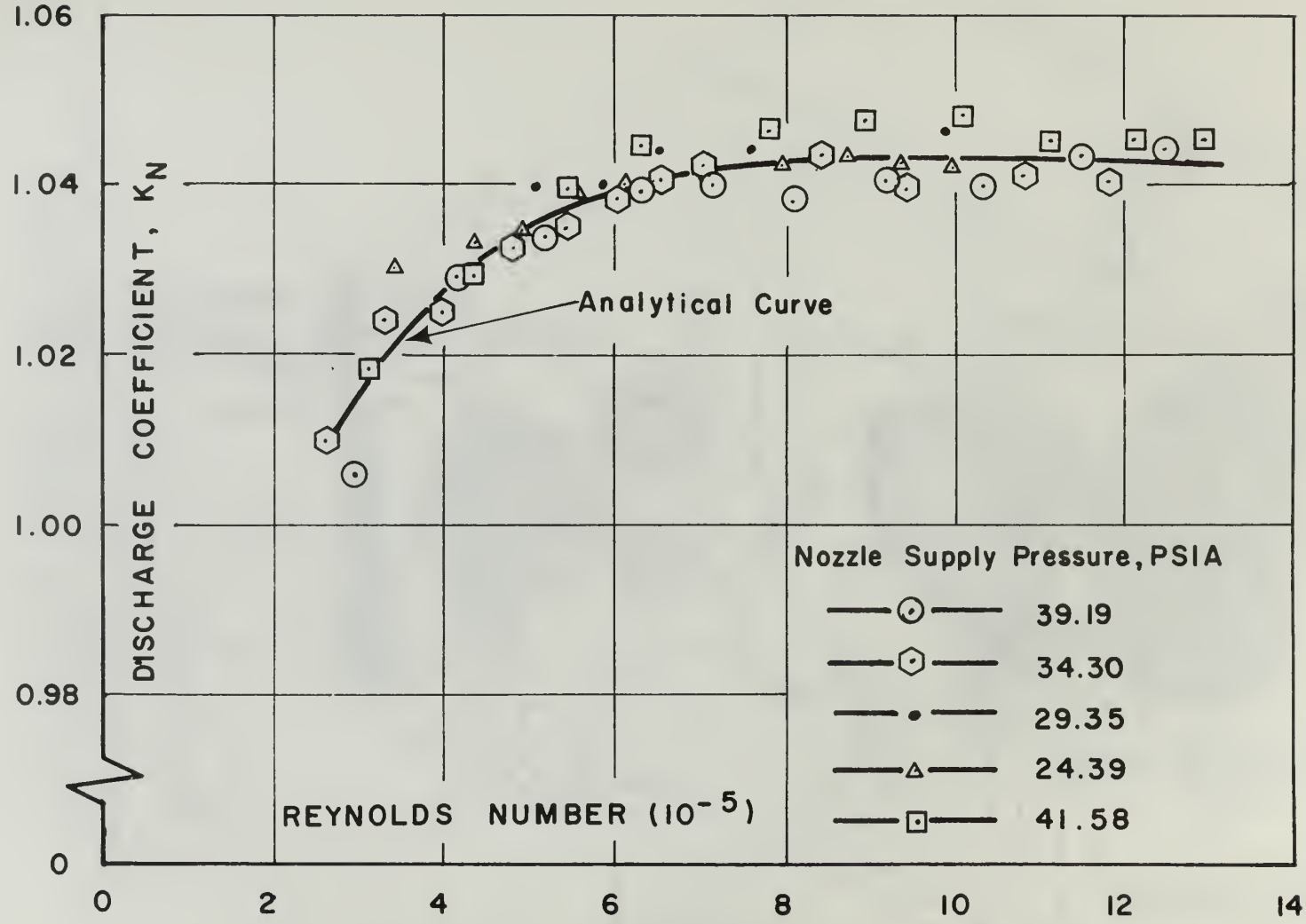


FIGURE 18
FLOW NOZZLE DISCHARGE COEFFICIENT
TRANSONIC TURBINE TEST RIG

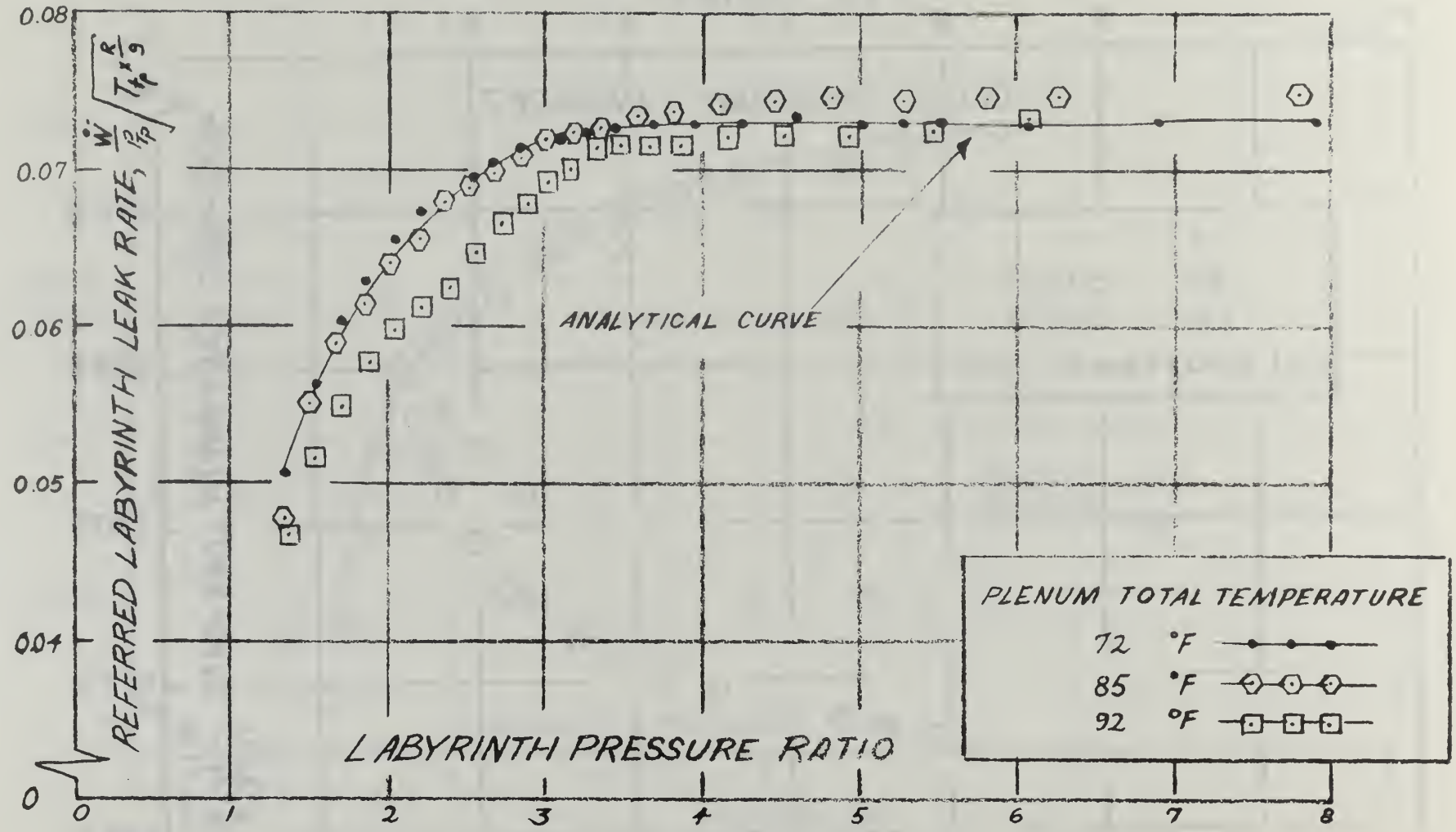


FIGURE 19
REFERRED LABYRINTH SEAL LEAK RATE
TRANSONIC TURBINE TEST RIG

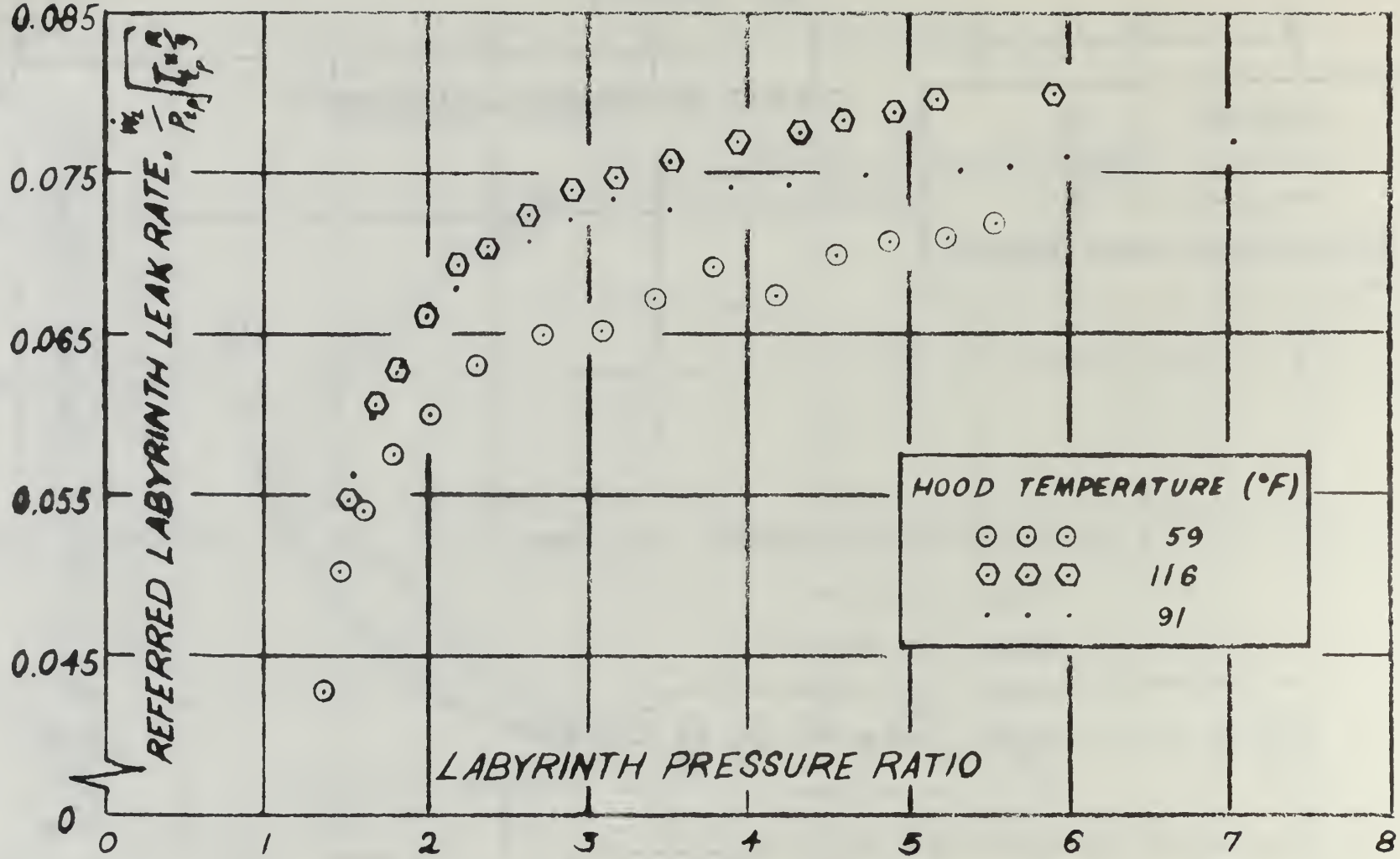


FIGURE 20
REFERRED LABYRINTH SEAL LEAK RATE
TRANSONIC TURBINE TEST RIG

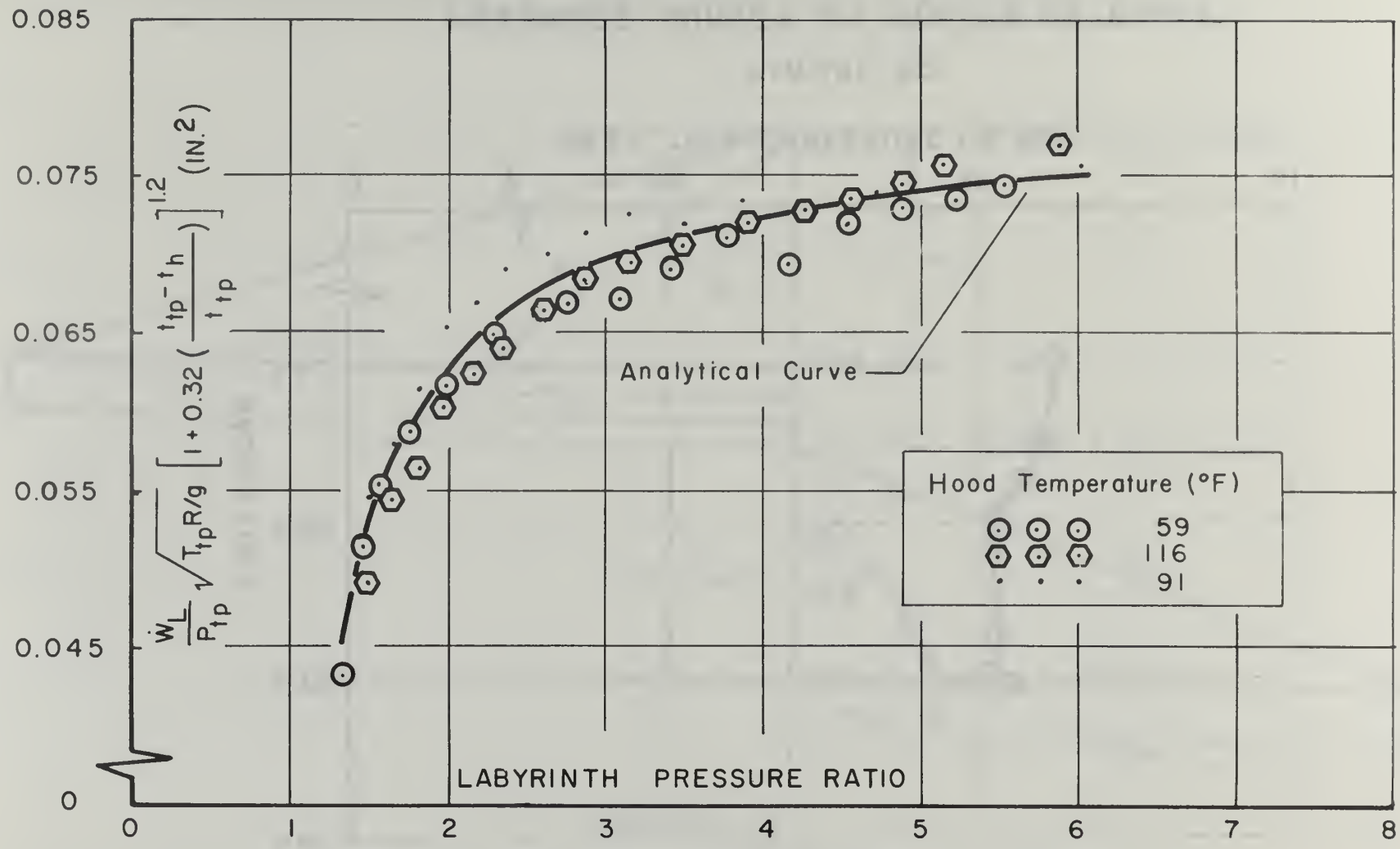


FIGURE 21

MODIFIED REFERRED LABYRINTH SEAL LEAK RATE

TRANSONIC TURBINE TEST RIG

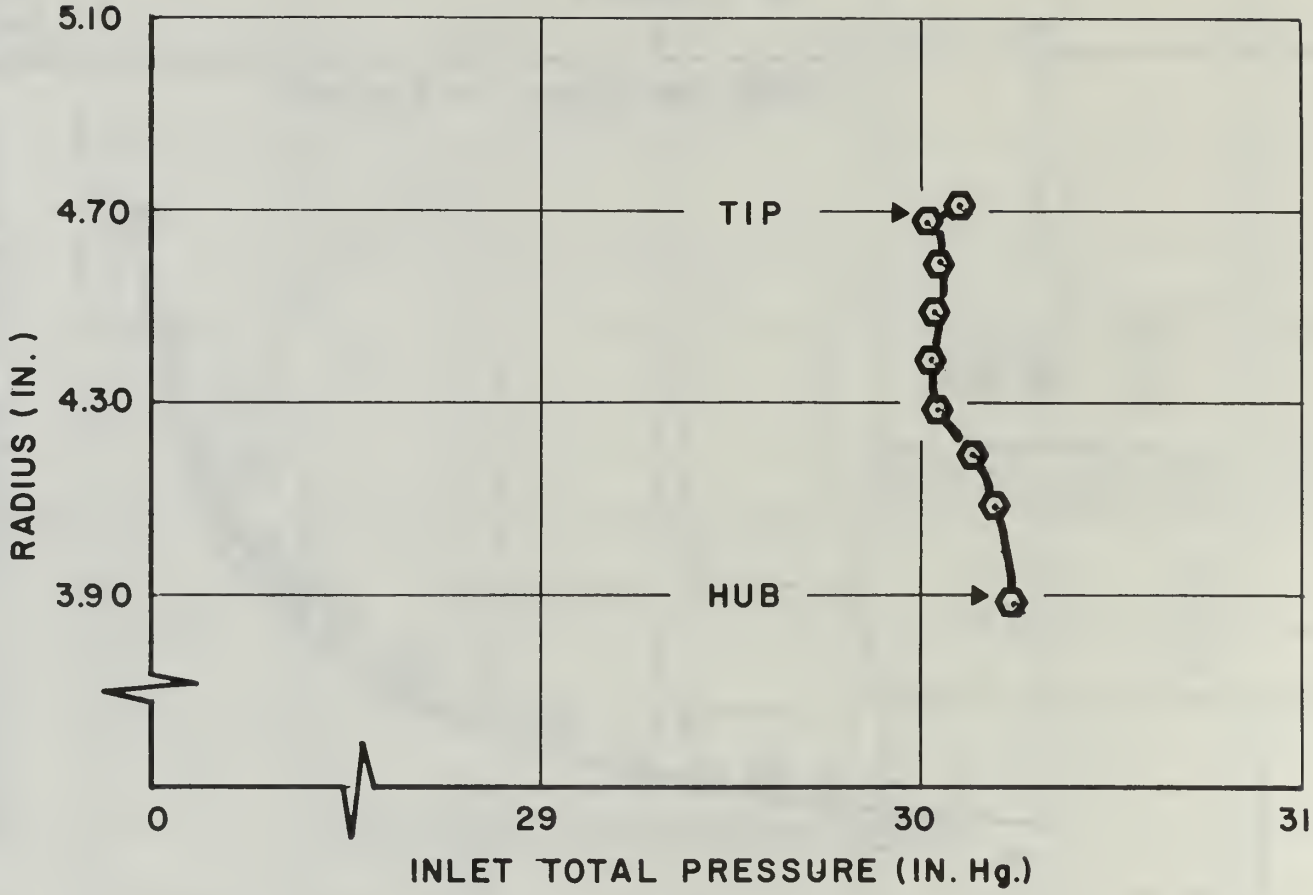


FIGURE 22

PRESSURE SURVEY AT STATOR ENTRANCE

PRESSURE RATIO = 2.0

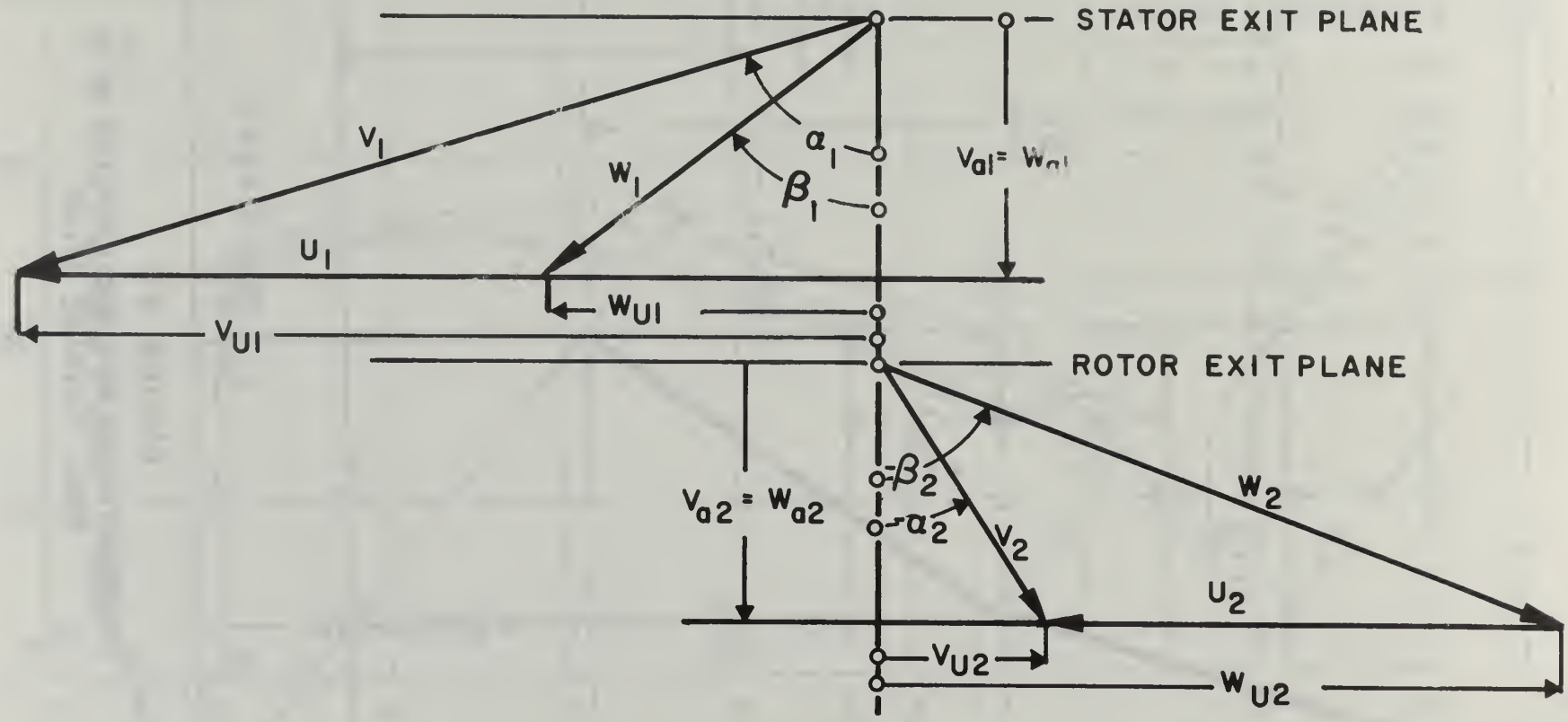


FIGURE 23

VELOCITY DIAGRAM OF TURBINE STAGE

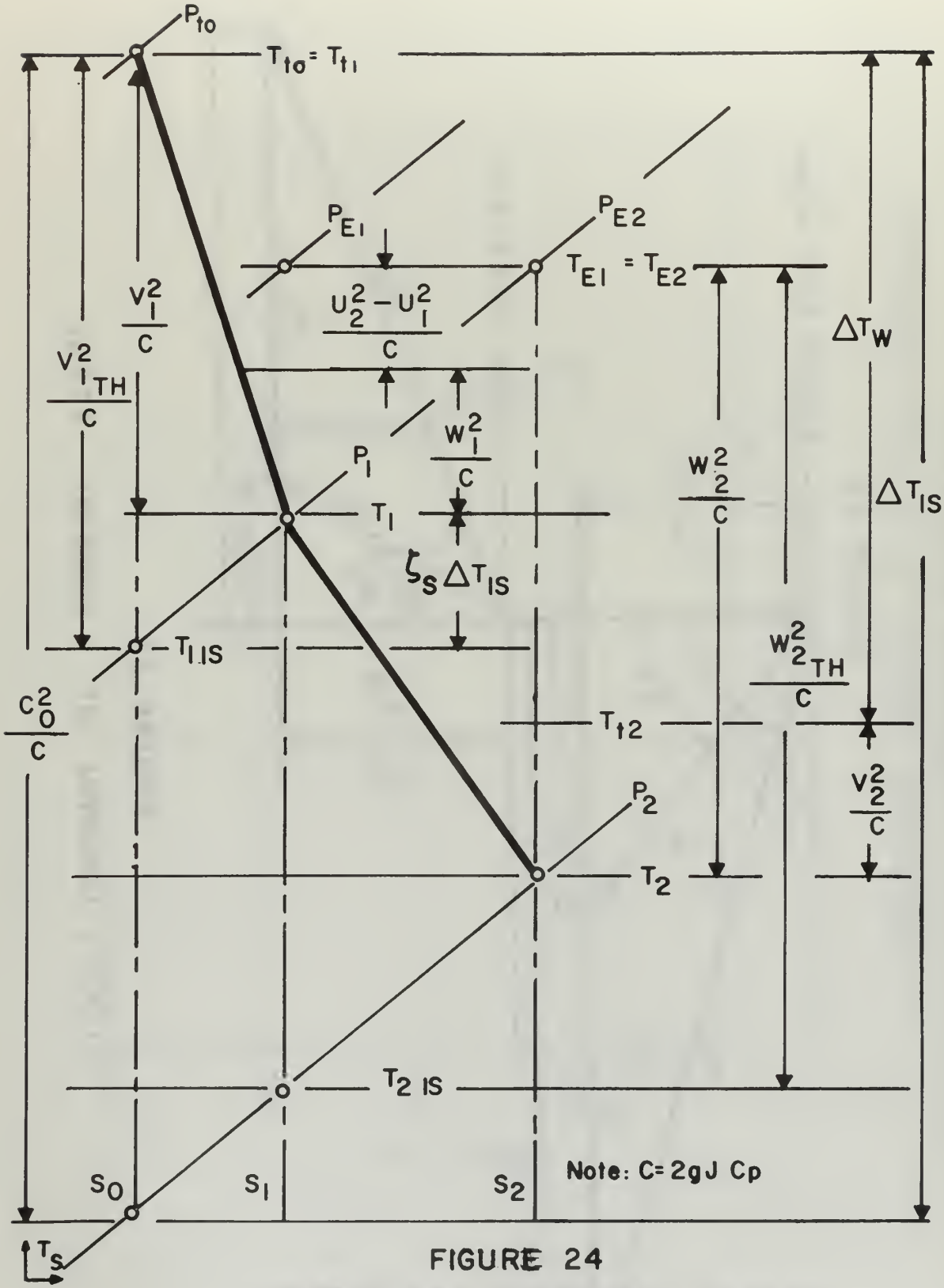


FIGURE 24

THERMODYNAMIC PROCESS OF FLUID IN AN AXIAL TURBINE STAGE

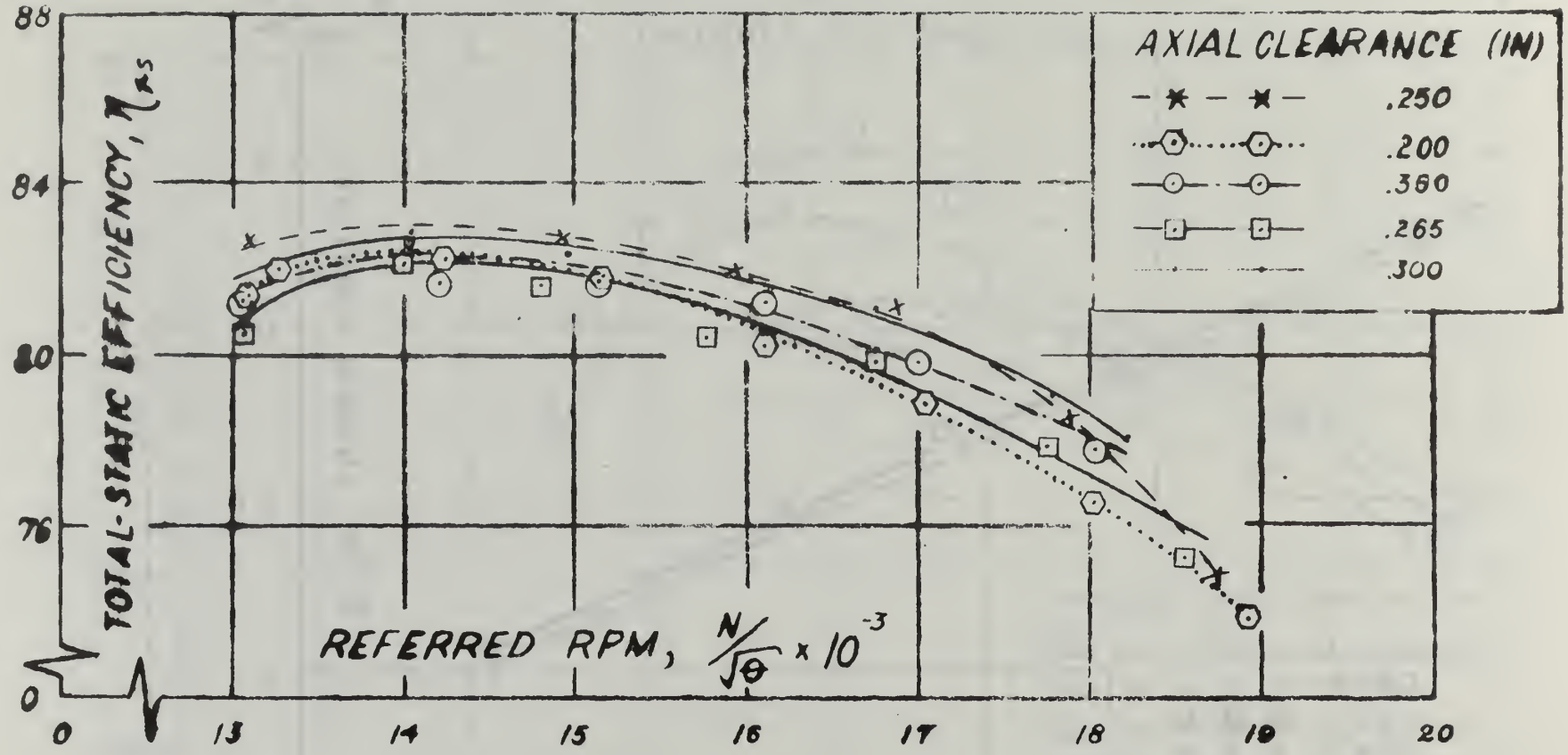


FIGURE 25

TOTAL-STATIC EFFICIENCY AT VARIOUS AXIAL CLEARANCES

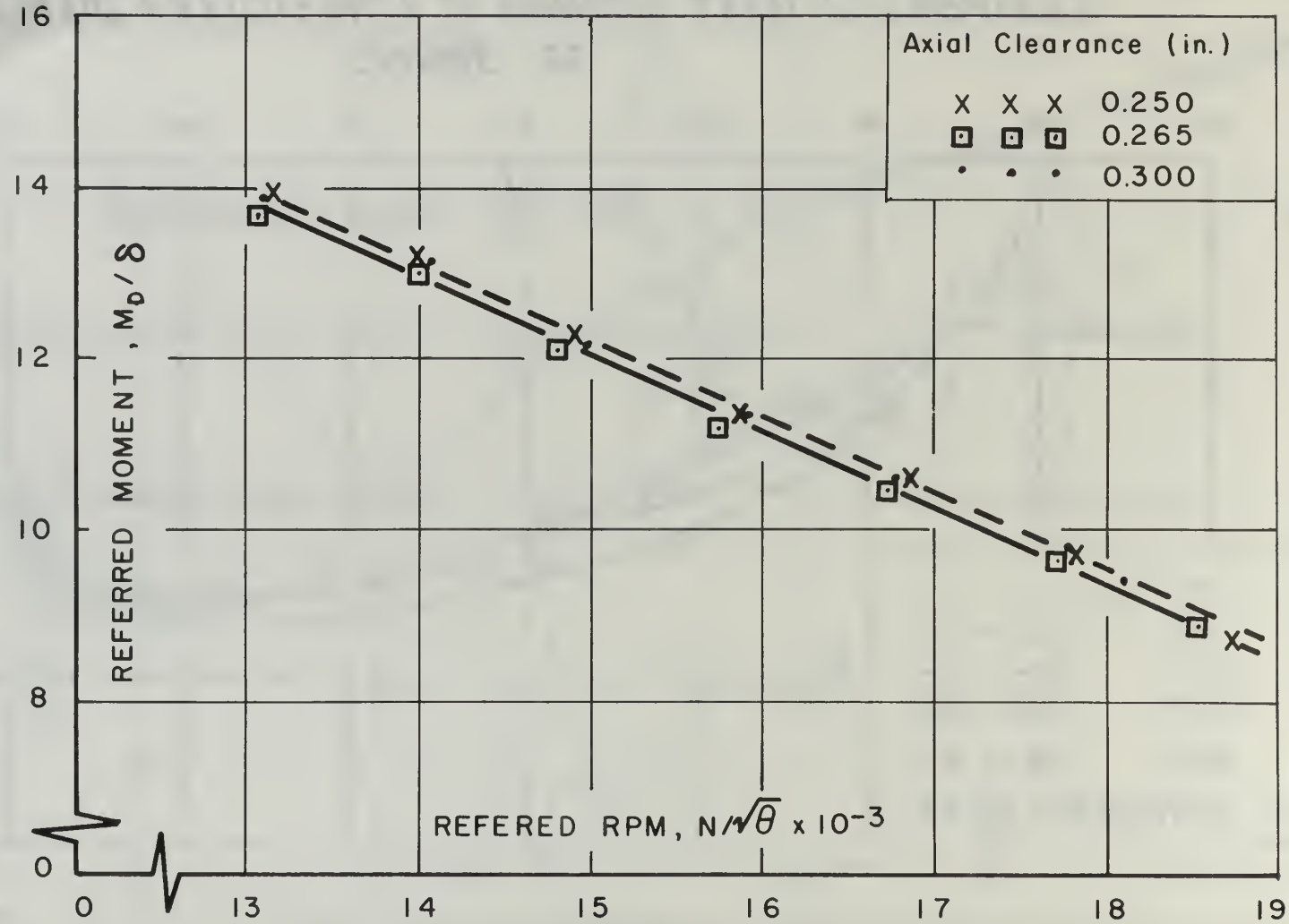


FIGURE 26
REFERRED MOMENT VERSUS REFERRED RPM
PRESSURE RATIO = 2.0

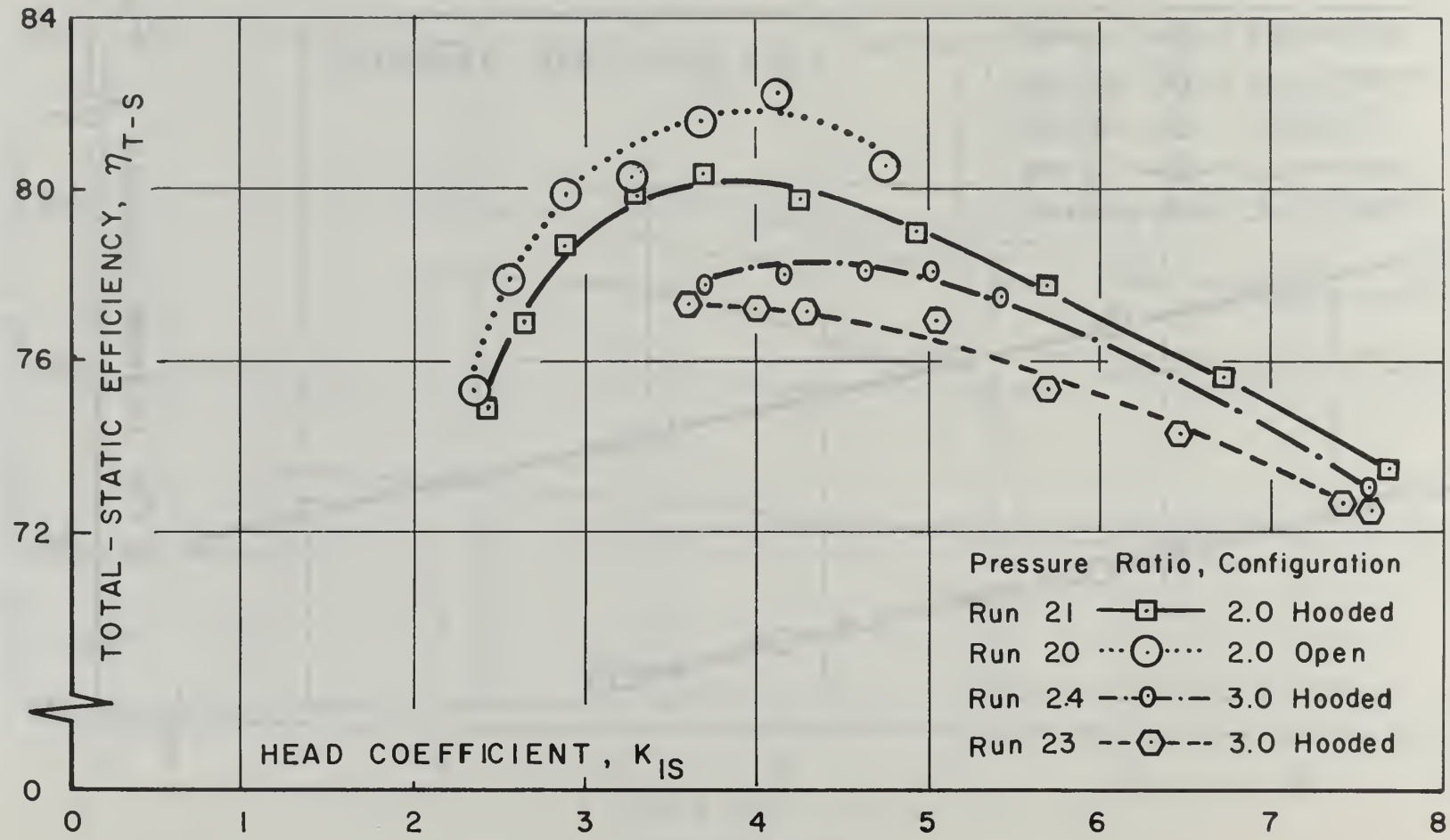


FIGURE 27

EFFICIENCY TOTAL-STATIC
INITIAL TURBINE TESTS

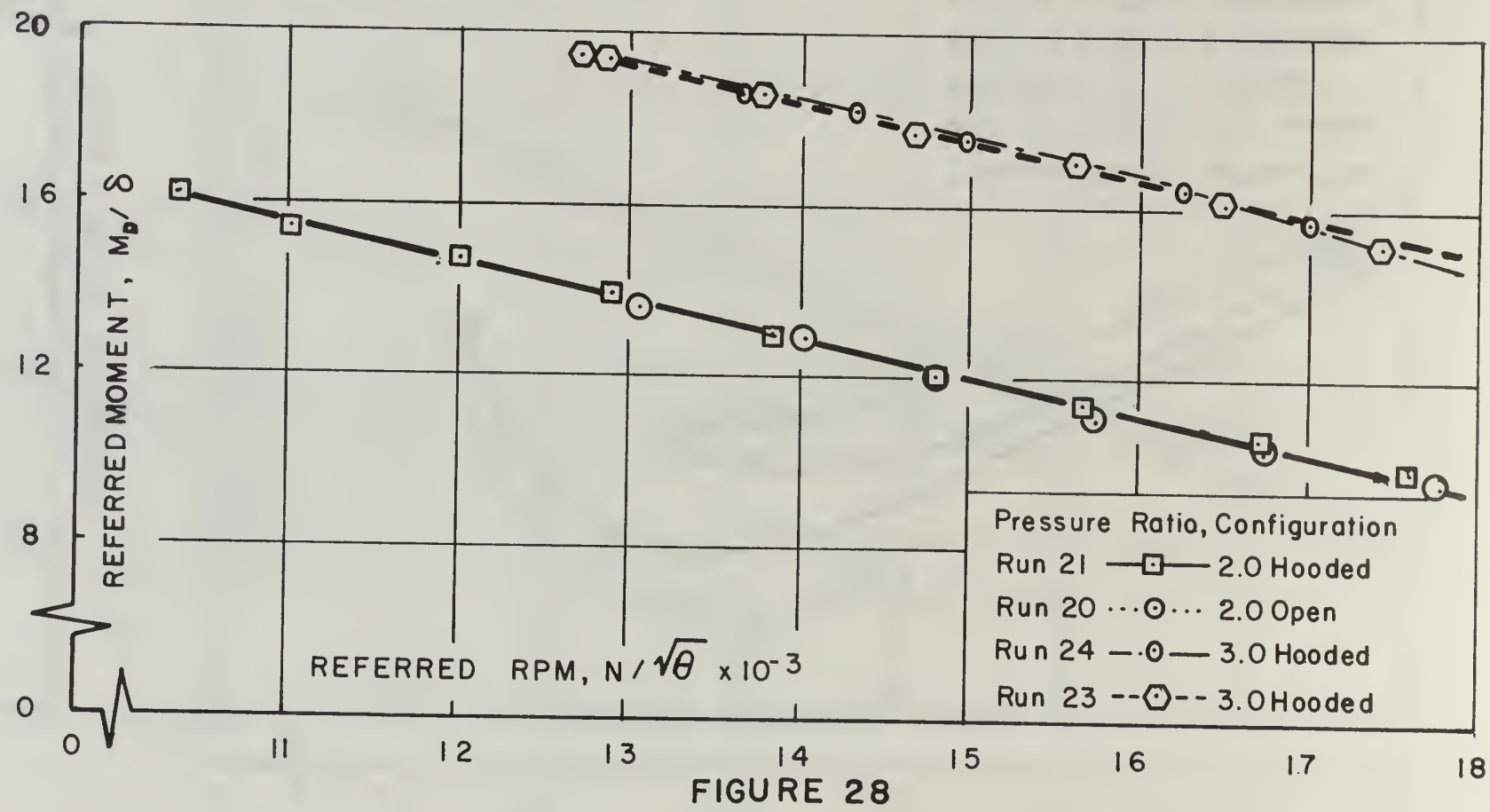


FIGURE 28

REFERRED MOMENT VERSUS REFERRED RPM
INITIAL TURBINE TESTS

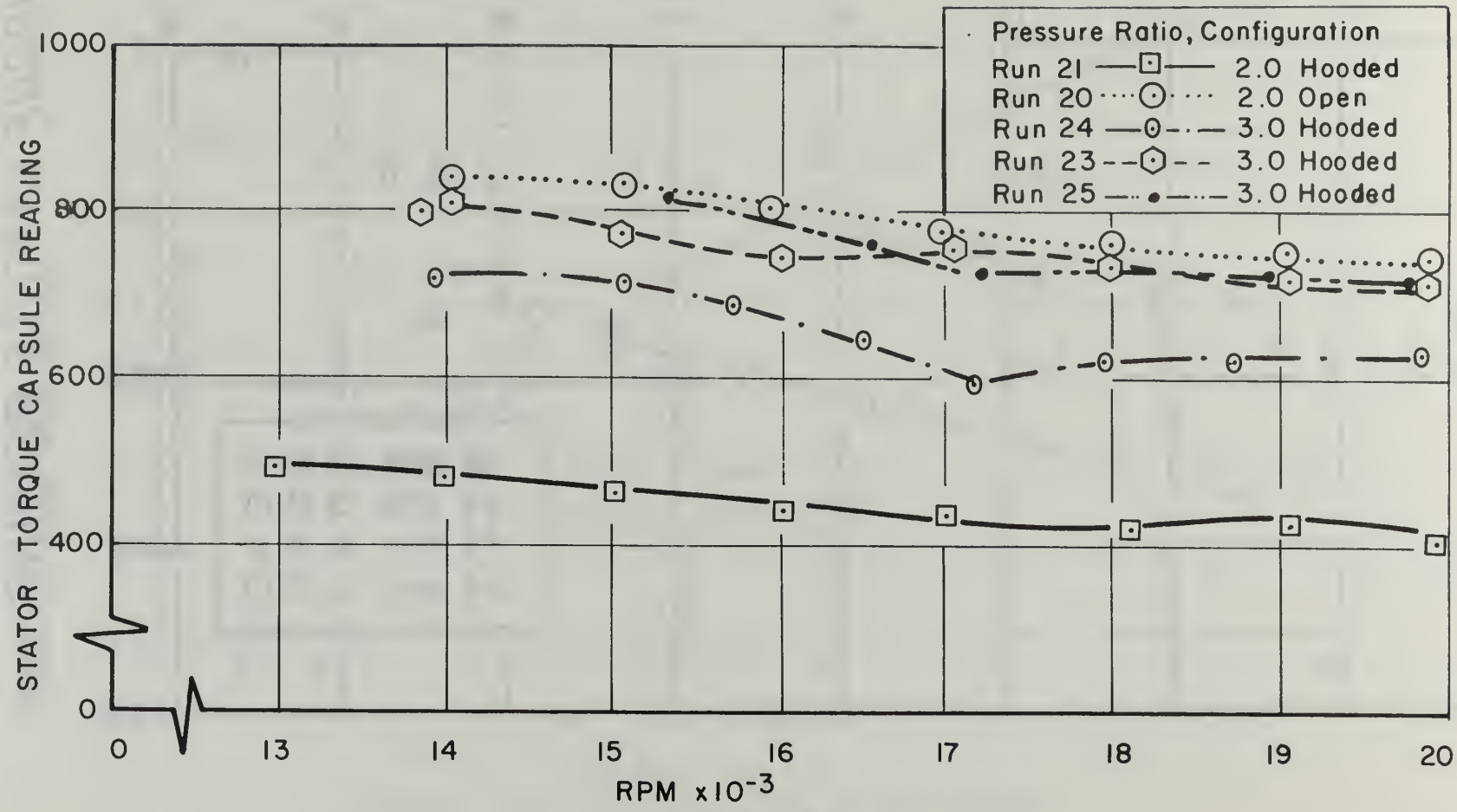


FIGURE 29

STATOR TORQUE CAPSULE VARIATION WITH RPM
TRANSONIC TURBINE TEST RIG

FIGURE 30
STATOR TORQUE CAPSULE
VARIATION WITH TEMPERATURE
TRANSONIC TURBINE TEST RIG

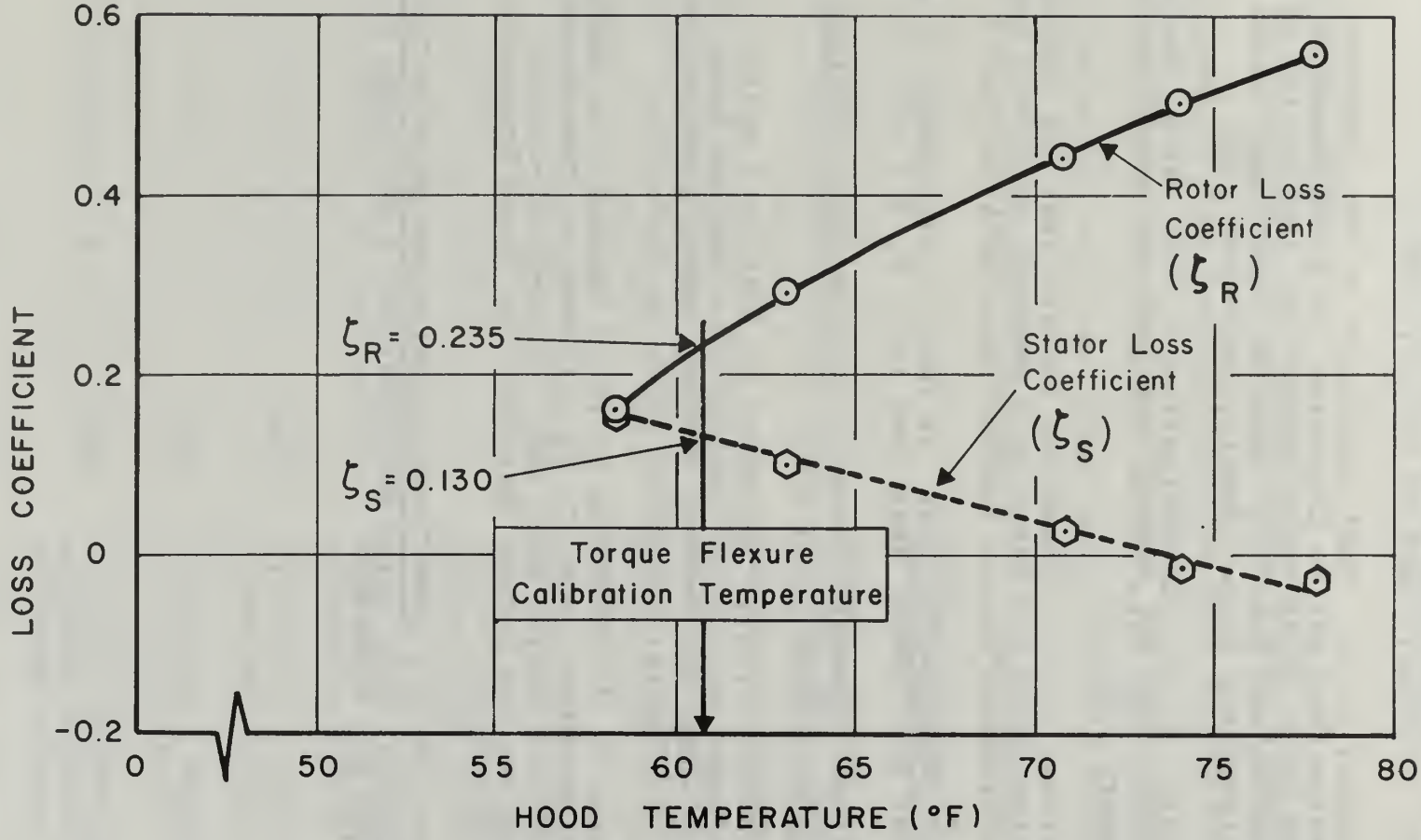


FIGURE 31
STATOR AND ROTOR LOSS COEFFICIENT
VERSUS
HOOD TEMPERATURE
AT 13080 RPM AND PRESSURE RATIO OF 2.5

REFERENCES

1. Vanco, M. r., "Thermodynamic and Turbine Characteristics of Hydrogen-Fueled Open-Cycle Auxiliary Space Power Systems," NASA TM X-1337, 1967.

2. Commons, P. M., "Instrumentation of the Transonic Turbine Test Rig to Determine the Performance of Turbine Inlet Guide Vanes through the Application of the Momentum and Moment of Momentum Equations," Naval Postgraduate School Thesis, September 1967.

3. Eckert, R. H., "Determination of Flow Rates, Transonic Turbine Test Rig," Naval Postgraduate School TN 66T-1, January 1966.

4. Naviaux, J. C., "Transonic Turbine Test Rig Exhauster System Tests and Tests of a Reaction Turbine," Naval Postgraduate School Thesis, December 1966, p. 68.

5. Flow Measurement, Chap. 4, Part 5, Supplement to ASME Power Test Codes, ASME, New York, N. Y., 1959, p. 74.

6. National Research Council, International Critical Tables, McGraw Hill, 1928.

7. Messegee, J. A., "Influence of Axial and Radial Clearance on the Performance of a Turbine Stage with Blunt-Edge Non-Twisted Blades," Naval Postgraduate School Thesis, September 1967, pp. 112-119.

8. Vavra, M. H., Problems of Fluid Mechanics in Radial Turbomachines, Pts. I, II, III and IV, "Von Karman Institute Course Note 55a," Rhode-Saint-Genese, Belgium, Von Karman Institute for Fluid Dynamics, March 1965.

9. Vavra, M. H., Aero-Thermodynamics and Flow in Turbomachines, John Wiley and Sons, Inc., New York, N.Y., 1960, pp. 418-438.

APPENDIX I

COMPUTER PROGRAMS FOR FLOW RATE DETERMINATION AND TURBINE TEST DATA REDUCTION

A. Program FLOCAL.

This program calculates the flow nozzle discharge coefficient of the Transonic Turbine Test Rig by comparing the flow through the nozzle with that through a standard ASME square-edge orifice. The inputs for this program are:

Card No.	Format	Units	Fortran	Description
1	I3		L	Number of runs to be processed.
2	I3		N	Number of data points in a given run. Entries on cards 2 through 11 are repeated for each run.
3	3F10.4	in.Hg.	PBAR	Barometric pressure.
		^{o}F	TCL	Temperature of Hg. of barometer
		^{o}F	TCR	Control room temperature.
4	8F10.4	in.H_2O	DH	Differential pressure across flow nozzle, multiple entries.
5	8F10.4	in.Hg.	PATM	Reference for nozzle pressure, multiple entries.
6	8F10.4	in.Hg.	PNOZ	Flow nozzle upstream static pressure, multiple entries.
7	8F10.4	m.v.	TNOZ	Flow nozzle temperature, multiple entries.
8	8F10.4	m.v.	TTD1	Orifice temperature at upstream pressure tap, multiple entries.
9	8F10.4	in.Hg.	PFL	Orifice upstream static pressure, multiple entries.

10	8F10.4	in.Hg.	PREF	Reference for orifice pressure, multiple entries.
11	8F10.4	cm.H_2O	DPFL	Pressure difference across orifice with flange taps, multiple entries.

B. Program LABLEK.

This program calculates the labyrinth leak rate of the Transonic Turbine Test Rig. The referred labyrinth leakage is computed and compared with the values obtained from the analytical expression of Section 5. The variation between these two values in percentage is included as output. The inputs for this program are:

Card No.	Format	Units	Fortran	Description
1	I3		L	Number of runs to be processed.
2	F10.4	in.Hg.	PBAR	Barometric pressure.
	I2		N	Number of data points in the given run. Entries on cards 2 through 12 are repeated for each run.
	I3		NRUN	Run number.
3	2F10.4	^oF	TCL	Temperature of Hg. of barometer.
		^oF	TCR	Control room temperature
4	8F10.4	in.Hg.	PATM	Reference of labyrinth plenum pressure and hood pressure, multiple entries.
5	8F10.4	in.Hg.	PSPL	Labyrinth plenum total pressure, multiple entries.
6	8F10.4	in.Hg.	PHD	Hood static pressure, multiple entries.
7	8F10.4	m.v.	TTPLD	Labyrinth plenum total temperature, multiple entries.

8	8F10.4	m.v.	TTD1	Total temperature at upstream pressure tap of the flow orifice, multiple entries.
9	8F10.4	m.v.	THD	Hood temperature, multiple entries.
10	8F10.4	in.Hg.	PFL	Orifice upstream static pressure, multiple entries.
11	8F10.4	in.Hg.	PREF	Reference for orifice pressure, multiple entries.
12	8F10.4	cm.H_2O	HWFL	Pressure difference across orifice with flange taps, multiple entries.

C. Program TTRSS.

This program reduces the data obtained with the Transonic Turbine Test Rig. The program consists of an executive routine and 10 subroutines. The executive routine provides the calling sequence for the subroutines. This sequence is:

1. INPUT. This subroutine reads the input test data. The data items which have multiple entries are so indicated in the item description, all others are single entry items. Each test run may consist of a maximum of 50 data points. The input data consists of the following items:

Card No.	Format	Units	Fortran	Description
1	I10		MM	Number of runs to be processed
2	I10		NRUN	Run number. Entries on cards 2 through 37 are repeated for each run.
3	2F10.4	in.	AXCLR	Axial clearance.

		in.	RADCR	Radial clearance.
4	F10.4	in.Hg.	PBAR	Barometric pressure.
5	I10		N	Number of data points in the given run.
6	2F10.4	^{o}F	TCL	Temperature of Hg of barometer.
		^{o}F	TCR	Control room temperature
7	8F10.4	in.Hg.	PREF2	Reference for stator plenum pressure and shroud pressures, multiple entries.
8	8F10.4	in.Hg.	PTPL	Stator plenum total pressure, multiple entries.
9-15	8F10.4	in.Hg.	P15-P21	Shroud pressures, multiple entries.
16	8F10.4	in.H_2O	DH	Differential pressure across the flow nozzle, multiple entries.
17	8F10.4	in.Hg.	PATM	Reference for the nozzle pressure, labyrinth plenum pressure, stator hub and tip pressures and the hood pressure, multiple entries.
18	8F10.4	in.Hg.	PNOZ	Flow nozzle upstream static pressure, multiple entries.
19	8F10.4	in.Hg.	PSPL	Labyrinth plenum total pressure, multiple entries.
20	8F10.4	in.Hg.	PHUB	Stator hub static pressure, multiple entries.
21	8F10.4	in.Hg.	PTIP	Stator tip static pressure, multiple entries.
22	8F10.4	in.Hg.	PHD	Hood static pressure, multiple entries.

23	8F10.4	m.v.	TNOZ	Flow nozzle temperature, multiple entries.
24	8F10.4	m.v.	TTPLD	Labyrinth plenum total temperature, multiple entries.
25	8F10.4	m.v.	TTPL	Stator plenum total temperature, multiple entries.
26	8F10.4	m.v.	THD	Hood temperature, multiple entries.
27	8F10.4	RPM	RPM	Turbine rotational speed, multiple entries.
28	8F10.4	counts	AXIL	Stator assembly axial force, multiple entries.
29	8F10.4	counts	TORQR	Stator assembly torque, multiple entries.
30	8F10.4	counts	DYNAR	Dynamometer torque, multiple entries.
31	8F10.4	counts	CLAXIL	Closure plate force, multiple entries.
32	8F10.4	counts	CLTRQR	Closure plate torque, multiple entries.
33	10X,4A2		DATE	Month/Day/Year.
34	15X,3A2		TTYPEB	I (circular-arc rotor with sharp leading edges) or II (circular-arc rotor with blunt leading edges).
			STATOR	I (converging stator) or II (converging-diverging stator).
			METHOD	MF (V_{a1} determined using momentum and continuity) or CF (V_{a1} determined using continuity alone).
35	F5.3	in.	RMEAN	Stator mean radius.
36	I1		J	Number of pressure ratios tested in given run.

37	8(2I5)	NPTS(K)	First data point at particular pressure ratio.
		NPTSS(K)	Last data point at particular pressure ratio. These two entries repeat in pairs, one pair for each pressure ratio tested in given run.

2. SETCON. This subroutine consists of all the constant factors used in the data reduction calculations.

3. CONVERT. This subroutine converts the units of the input data into a single system compatible with the equations of Section 6.

4. FLORAT. This subroutine computes the turbine flow rate using the equations of Subsection 6.2.

5. STATOR. This subroutine uses the equation of Subsection 6.4 to calculate the stator discharge properties. Subroutine MOMENT is called from STATOR when using momentum and continuity to compute the axial velocity component.

6. MOMENT. This subroutine determines the axial component of absolute velocity by the application of the momentum equation to the fluid within the stator assembly.

7. ROTOR. This subroutine computes the rotor discharge properties using the equations of Subsection 6.5.

8. PERFRM. This subroutine computes the performance parameters and the referred quantities of Subsection 6.6.

9. OUTPTA. This subroutine gives a detailed printed output consising of the stator and rotor discharge properties and the performance parameters.

10. OUTPUT. This subroutine prints the turbine performance parameters in report form.

```
      DIMENSION TNOZ(100),TTD1(100),DH(100),PNOZ(100),PATM(100),PFL(100)
     1,PREF(100),DPFL(100),RE(100),W(100),FLOCO(100),TTD1R(100),TNOZR(10
     20)
CTHIS PROGRAM CALCULATES THE DISCHARGE COEFFICIENT OF THE TRANSONIC
CTURBINE TEST RIG FLOW RATE NOZZLE BY MATCHING THE FLOW THROUGH THE
CNOZZLE WITH THAT OF A STANDARD SHARP EDGE ORIFICE. INPUT DATA DH(IN.
CH2O),PATM(IN HG),PNOZ(IN HG),PFL(IN HG),PREF(IN HG),DPFL(CM H2O),TCR
C(DEGREES F),TCL(DEGREES F),TNOZ(MV),TTD1(MV),PBAR(IN HG),L(NUMBER OF
CDATA SETS),N(NUMBER OF DATA POINTS WITHIN EACH SET)
      WRITE(6,101)
      READ(5,99)L
      DO 90 M=1,L
      READ(5,99)N
      READ(5,100)PBAR,TCL,TCR
      READ(5,100) (DH(I),I=1,N)
      READ(5,100) (PATM(I),I=1,N)
      READ(5,100) (PNOZ(I),I=1,N)
      READ(5,100) (TNOZ(I),I=1,N)
      READ(5,100) (TTD1(I),I=1,N)
      READ(5,100) (PFL(I),I=1,N)
      READ(5,100) (PREF(I),I=1,N)
      READ(5,100) (DPFL(I),I=1,N)
      D1O=6.065
      D1N=7.975
      D2O=4.2425
      D2N=4.25
      BO=D2O/D1O
      BN=D2N/D1N
      B=BN**4
      GAM=1.4
      EX1=GAM/(GAM-1.)
      EX2=(GAM-1.)/GAM
      EX3=2./GAM
      QKINF=0.689556
      A=D2O*(830.-5000.*BO+9000.*BO**2-4200.*BO**3+530./SQRT(D1O))
      GHGCL=13.63905-.0013630303*TCL
      GHGRM=13.63905-.0013630303*TCR
      CHGC=0.4891585*GHGCL/13.54
      CHGCR=0.4891585*GHGRM/13.54
      GW68=0.99837633+1.0605756*68./10000.-1.5931861*68.**2/1000000.
      GWRM=0.99837633+1.0605756*TCR/10000.-1.5931861*TCR**2/1000000.
      RATGW=GWRM/GW68
      PAMB=PBAR
      PAMB=PAMB*CHGC
      DO 50 I=1,N
```

```
      QDH=DH(I)
      QDPFL=DPFL(I)
      TTD1(I)=32.+35.98*TTD1(I)-.425*TTD1(I)**2
      TTD1R(I)=TTD1(I)+459.7
      TNOZ(I)=32.+35.98*TNOZ(I)-.425*TNOZ(I)**2
      TNOZR(I)=TNOZ(I)+459.7
      ALPHO=1.+0.00193*((TTD1(I)-68.)/100.)
      ALPHN=1.+0.00252*((TNOZ(I)-68.)/100.)
      DPFL(I)=QDPFL/2.54*GWRM*62.42732/1728.
      PFL(I)=CHGCR*(PREF(I)-PFL(I))+PAMB
      YO=1.-(.41+.35*BO**4)*DPFL(I)/(GAM*PFL(I))
      DH(I)=QDH*GWRM/12.*62.42732/144.
      PNOZ(I)=CHGCR*(PATM(I)-PNOZ(I))+PAMB
      XR=1.-(DH(I)/PNOZ(I))
      YN=SQRT(XR**EX3*EX1*((1.-XR**EX2)/(1.-XR))*((1.-B)/(1.-B*XR**EX3))
     1)
      HW68=QDPFL/2.54*RATGW
      Z=0.019+0.0024*(TTD1(I)/100.-1.)
      WPART=0.163842658*D2O**2*ALPHO*YO*SQRT(PFL(I)*HW68/TTD1R(I))
      C1=WPART*QKINF
      C2=C1*A*Z/5359.48144
      W(I)=C1/2.+SQRT((C1**2/4.)+C2)
      HW68N=QDH*RATGW
      FLOCO(I)=6.1034166*W(I)/(D2N**2*YN*ALPHN)*SQRT(TNOZR(I)/(HW68N*PNO
     1Z(I)))
      RE(I)=5359.48144*W(I)/Z
   50 CONTINUE
      WRITE(6,102)
      WRITE(6,103)M,PNOZ(1)
      WRITE(6,104)
      WRITE(6,105)PAMB,N,GAM
      WRITE(6,106)
      DO 90 I=1,N
      WRITE(6,107)I,W(I),FLOCO(I),RE(I)
   90 CONTINUE
   99 FORMAT(I3)
  100 FORMAT(8F10.4)
  101 FORMAT(1H1///32X,58HFLOW NOZZLE CALIBRATION FOR THE TRANSONIC TURB
     1INE TEST RIG)
  102 FORMAT (////32X,11HTEST SERIES25X,22HNOZZLE SUPPLY PRESSURE)
  103 FORMAT(/35X,I3,38X,F5.2)
  104 FORMAT(/32X,13HATMOS. PRESS.11X,11HDATA POINTS11X,5HGAMMA)
  105 FORMAT(/35X,F6.3,19X,I2,17X,F3.1)
  106 FORMAT(//34X,5HPOINT8X,9HFLOW RATE8X,9HDISCHARGE8X,8HREYNOLDS/47X,
     19H(LBM/SEC)7X,11HCOEFFICIENT8X,6HNUMBER//)
```

```
107 FORMAT(36X,I2,9X,F8.4,8X,F9.5,7X,F11.2)
    STOP
    END
```

FLOW NOZZLE CALIBRATION FOR THE TRANSONIC TURBINE TEST RIG

TEST SERIES		NOZZLE SUPPLY PRESSURE
1		39.19
ATMOS. PRESS.	DATA POINTS	GAMMA
14.766	10	1.4

POINT	FLOW RATE (LBM/SEC)	DISCHARGE COEFFICIENT	REYNOLDS NUMBER
1	4.5470	1.04389	1249496.00
2	4.1810	1.04332	1150119.00
3	3.7625	1.03974	1036495.37
4	3.3435	1.04034	921833.00
5	2.9460	1.03806	812751.44
6	2.6033	1.04049	718826.87
7	2.2851	1.03916	631762.94
8	1.8747	1.03327	519366.69
9	1.4961	1.02885	415375.44
10	1.0637	1.00591	295950.94

TEST SERIES		NOZZLE SUPPLY PRESSURE
2		41.95
ATMOS. PRESS.	DATA POINTS	GAMMA
14.767	10	1.4

POINT	FLOW RATE (LBM/SEC)	DISCHARGE COEFFICIENT	REYNOLDS NUMBER
1	4.6679	1.03796	1284592.00
2	4.2442	1.03850	1167508.00
3	3.8877	1.03734	1069204.00
4	3.4127	1.04024	939151.62
5	2.8829	1.03816	793691.87
6	2.5549	1.03302	703979.37
7	2.2868	1.03217	630379.37
8	1.9506	1.02720	538148.44
9	1.5451	1.01220	426719.87
10	1.0399	0.98741	287806.31

TEST SERIES		NOZZLE SUPPLY PRESSURE
3		34.30
ATMOS. PRESS.	DATA POINTS	GAMMA
14.735	2	1.4

POINT	FLOW RATE (LBM/SEC)	DISCHARGE COEFFICIENT	REYNOLDS NUMBER
1	4.2561	1.04044	1182130.00
2	3.9094	1.04132	1085137.00

TEST SERIES		NOZZLE SUPPLY PRESSURE
4		34.25
ATMOS. PRESS.	DATA POINTS	GAMMA
14.700	10	1.4

POINT	FLOW RATE (LBM/SEC)	DISCHARGE COEFFICIENT	REYNOLDS NUMBER
1	3.4087	1.03932	944578.00
2	3.0387	1.04327	842217.06
3	2.5675	1.04209	711613.37
4	2.3839	1.04038	660725.44
5	2.1594	1.03792	598632.69
6	1.9635	1.03493	544912.75
7	1.7285	1.03260	479896.50
8	1.4205	1.02484	395303.19
9	1.1926	1.02393	332649.62
10	0.9363	1.00979	261676.87

TEST SERIES		NOZZLE SUPPLY PRESSURE
5		29.35
ATMOS. PRESS.	DATA POINTS	GAMMA
14.682	9	1.4

POINT	FLOW RATE (LBM/SEC)	DISCHARGE COEFFICIENT	REYNOLDS NUMBER
1	3.9243	1.04078	1094621.00
2	3.5504	1.04636	990741.62
3	3.1456	1.04380	878523.81
4	2.7296	1.04415	762850.12
5	2.3435	1.04390	655627.62
6	2.0941	1.04002	586375.50
7	1.8079	1.03963	506764.06
8	1.4423	1.02582	404797.87
9	0.9900	1.02611	278830.06

TEST SERIES 6

NOZZLE SUPPLY PRESSURE 24.39

ATMOS. PRESS. 14.603

DATA POINTS 4

GAMMA 1.4

POINT	FLOW RATE (LBM/SEC)	DISCHARGE COEFFICIENT	REYNOLDS NUMBER
1	3.5521	1.04187	994823.81
2	3.3403	1.04228	935497.94
3	3.1144	1.04286	872236.44
4	2.8472	1.04237	796562.81

TEST SERIES 7

NOZZLE SUPPLY PRESSURE 24.32

ATMOS. PRESS. 14.574

DATA POINTS 6

GAMMA 1.4

POINT	FLOW RATE (LBM/SEC)	DISCHARGE COEFFICIENT	REYNOLDS NUMBER
1	2.5438	1.04131	711068.44
2	2.2157	1.03960	619473.12
3	1.9886	1.03860	556218.69
4	1.7660	1.03475	493973.37
5	1.5451	1.03297	432556.75
6	1.2198	1.03049	342052.44

TEST SERIES 8

NOZZLE SUPPLY PRESSURE 41.58

ATMOS. PRESS. 14.654

DATA POINTS 11

GAMMA 1.4

POINT	FLOW RATE (LBM/SEC)	DISCHARGE COEFFICIENT	REYNOLDS NUMBER
1	4.6614	1.04521	1294436.00
2	4.3785	1.04539	1216127.00
3	4.0059	1.04457	1112648.00
4	3.6474	1.04790	1013286.12
5	3.2227	1.04723	896041.56
6	2.8031	1.04634	779872.37
7	2.5465	1.04855	708955.31
8	2.2738	1.04442	633425.87
9	1.9652	1.03927	547810.06
10	1.5387	1.02991	429389.37
11	1.1206	1.01809	313372.31

PROGRAM LABLEK

```
      DIMENSION PATM(80),PSPL(80),PHD(80),TTPLD(80),ERROR(80),TTD1(80),
     1PEL(80),HWEL(80),WREET(80),          WLABR(80),WREE(80),PE(80),PR(80)
     2,PREE(80),THD(80)
CTHIS PROGRAM CALCULATES THE LABYRINTH LEAK RATE OF THE TRANSONIC TURBIN
CRIG. INPUT DATA PATM(IN.HG.),PSPL(IN.HG.),PHD(IN.HG.),TTPLD(MV),THD(MV)
CTTD1(MV),PEL(IN.HG.),              HWEL(CM.H2O),              PBAR(IN.HG.)
CTCL(DEGREES F.),TCR(DEGREES F.),PREE(IN.HG.)
      A1=-1.004586E-01
      A2=2.122579E-01
      A3=-1.081851E-01
      A4=2.767576E-02
      A5=-3.489933E-03
      A6=1.726733E-04
      READ(5,99)L
      DO 50 M=1,L
      READ(5,100)PBAR,N,NRUN
      WRITE (6,199)NRUN
      WRITE(6,200)
      READ(5,101)TCL,TCR
      READ(5,101) (PATM(I),I=1,N)
      READ(5,101) (PSPL(I),I=1,N)
      READ(5,101) (PHD(I),I=1,N)
      READ(5,101) (TTPLD(I),I=1,N)
      READ(5,101) (TTD1(I),I=1,N)
      READ(5,101) (THD(I),I=1,N)
      READ(5,101) (PEL(I),I=1,N)
      READ(5,101) (PREE(I),I=1,N)
      READ(5,101) (HWEL(I),I=1,N)
      EN(1)=1.0
      EN(2)=1.1
      EN(3)=1.2
      EN(4)=1.3
      EN(5)=1.4
      D1= 2.067
      D2= 0.825
      B= D2/D1
      QKINE=0.608913
      A=D2*(830.-5000.*B+9000.*B**2-4200.*B**3+530./SQRT(D1))
      GAM=1.4
      GHGRM=13.63905-.0013630303*TCR
      GHGCL=13.63905-.0013630303*TCL
      CHGC=0.4891585*GHGCL/13.54
      CHGCR=0.4891585*GHGRM/13.54
      GW68=0.99837633+1.0605756*68./10000.-1.593186*68.**2/1000000.
      GWRM=0.99837633+1.0605756*TCR/10000.-1.593186*TCR**2/1000000.
```

```
      RATGW=GWRM/GW68
      PAMB=PBAR
      PAMB=PAMB*CHGC
      R=53.3448
      G=32.174
      DO 49 I=1,N
      OPATM=PATM(I)
      OPSPL=PSPL(I)
      OPHD=PHD(I)
      OTTPLD=TTPLD(I)
      OTTD1=TTD1(I)
      OPEL=PEL(I)
      OPREF=PREF(I)
      OHWEL=HWEL(I)
      THD(I)=32.+35.98*THD(I)-.435*THD(I)**2
      TTPLD(I)=32.+35.98*OTTPLD-.435*OTTPLD**2
      OTTD1=32.+35.98*OTTD1-.435*OTTD1**2
      ALPH=1.+.00193*((OTTD1-68.)/100.)
      DPEL=OHWEL/2.54*GWRM/12.*62.42732/144.
      OPEL=CHGCR*(OPREF-OPEL)+PAMB
      Y=1.-(0.41+0.35*B**4)*DPEL/(GAM*OPEL)
      HW68=OHWEL/2.54*RATGW
      TTD1R=OTTD1+459.7
      WPART=0.1115154*ALPH*Y*SQRT(OPEL*HW68/TTD1R)
      Z=0.019+0.0024*(OTTD1/100.-1.)
      C1=WPART*OKINE
      C2=C1*A*7/27560.727
      WLABR(I)=C1/2.+SQRT((C1**2/4.)+C2)
      RE(I)=27560.727*WLABR(I)/7
      OPSPL=CHGCR*(OPATM-OPSPL)+PAMB
      OPHD=CHGCR*(OPATM-OPHD)+PAMB
      PR(I)=OPSPL/OPHD
      TTPLDR=TTPLD(I)+459.7
      PHI=WLABR(I)/OPSPL*SQRT(TTPLDR*R/G)
      CORR=(1.0+.32*((TTPLD(I)-THD(I))/TTPLD(I)))
        WREF(I)=PHI*CORR**1.2
  504 WREFR=A1+A2*PR(I)+A3*PR(I)**2+A4*PR(I)**3+A5*PR(I)**4+A6*PR(I)**5
      WREFT(I)=WREFR
      IF(WREFT(I)-WREF(I))20,20,30
   20 ERROR(I)=-(WREF(I)-WREFT(I))/WREF(I)*100.
      GO TO 51
   30 ERROR(I)=(WREFT(I)-WREF(I))/WREFT(I)*100.
   51 WRITE(6,201)I,WLABR(I),PR(I),TTPLD(I),RE(I),WREF(I),WREFT(I),ERROR
     1(I),THD(I)
   49 CONTINUE
```

```
 50 CONTINUE
 99 FORMAT(I3)
100 FORMAT(F10.4,I2,I3)
101 FORMAT(8F10.4)
199 FORMAT (1H1//54X,16HTTRSS RUN NUMBER3X,I3)
200 FORMAT (    ///39X,53HLABYRINTH LEAK RATE OF THE TRANSONIC TURBINE
   1TEST RIG//2X,5HPOINT6X,9HLABYRINTH7X,9HLABYRINTH4X,12HPLENUM TOTAL
   26X,8HREYNOLDS 9X,8HREFERRED8X,11HANALYTICAL 6X,7HPERCENT9X,4HHOOD/
   313X,9HLEAK RATE7X,8HPRESSURE5X,11HTEMPERATURE8X,6HNUMBER10X,9HLEAK
   4 RATE8X,8HREFERRED9X,5HERROR5X,11HTEMPERATURE/13X,9H(LBM/SEC)9X,5H
   5RATIO8X,7H(DEG F)27X,7H(SQ IN)9X,9HLEAK RATE21X,7H(DEG F)//)
201 FORMAT(3X,I2,8X,F8.6,8X,F7.4,8X,F7.3,8X,F10.2,7X,F9.5, 9X,F8.6,7X,
   1F8.4,7X,F7.3)
    STOP
    END
```

TTRSS RUN NUMBER 27

LABYRINTH LEAK RATE OF THE TRANSONIC TURBINE TEST RIG

POINT	LABYRINTH LEAK RATE (LBM/SEC)	LABYRINTH PRESSURE RATIO	PLENUM TOTAL TEMPERATURE (DEG F)	REYNOLDS NUMBER	REFERRED LEAK RATE (SQ IN)	ANALYTICAL REFERRED LEAK RATE	PERCENT ERROR	HOOP TEMPERATURE (DEG F)
1	0.084465	5.5690	107.005	109630.50	0.077182	0.074548	-3.4135	115.864
2	0.085082	5.4678	111.093	111805.52	0.078407	0.074400	-5.0939	118.217
3	0.085526	5.3559	109.391	114077.25	0.078310	0.074303	-5.7305	116.524
4	0.086093	5.4566	107.858	115708.56	0.078304	0.074395	-5.7145	113.811
5	0.086881	5.4628	104.956	118244.31	0.078340	0.074402	-5.2232	110.072
6	0.085693	5.3829	101.364	117920.44	0.078370	0.074324	-5.1527	105.081
7	0.085647	5.4171	97.590	119213.56	0.078365	0.074355	-5.1180	101.706
8	0.086158	5.4059	95.699	121205.87	0.078509	0.074346	-5.4241	99.135
9	0.086213	5.3674	92.771	123121.12	0.078215	0.074311	-4.9999	96.043
10	0.085482	5.3376	88.454	123918.19	0.077360	0.074288	-3.9834	91.219
11	0.085284	5.3551	84.124	125485.44	0.077194	0.074301	-3.7480	85.685
12	0.083399	5.3962	80.824	123203.31	0.075873	0.074336	-2.0253	81.867
13	0.082868	5.3913	78.039	122473.37	0.075522	0.074333	-1.5741	77.965
14	0.068396	3.2336	74.200	101152.37	0.062417	0.060027	-4.7532	72.277
15	0.067472	3.2175	74.550	98774.94	0.062402	0.060081	-3.4825	73.326
16	0.067640	3.2334	76.121	97631.50	0.062388	0.060030	-3.6133	75.248
17	0.067689	3.2164	79.084	96251.00	0.061366	0.060076	-2.0870	80.000
18	0.068397	3.2312	84.471	95023.56	0.062264	0.060024	-3.2330	88.800
19	0.068580	3.2192	87.070	96161.69	0.062606	0.060085	-1.0214	96.730

TTRSS RUN NUMBER 28

LABYRINTH LEAK RATE OF THE TRANSONIC TURBINE TEST RIG

POINT	LABYRINTH LEAK RATE (LBM/SEC)	LABYRINTH PRESSURE RATIO	PLENUM TOTAL TEMPERATURE (DEG F)	REYNOLDS NUMBER	PREDICTED LEAK RATE (SQ IN)	ANALYTICAL PREDICTED LEAK RATE	PERCENT ERROR	HOOP TEMPERATURE (DEG F)
1	0.021826	1.3314	61.123	32578.10	0.043589	0.045445	4.0859	59.740
2	0.025725	1.4502	61.299	38363.04	0.051375	0.049017	-3.3389	59.554
3	0.027210	1.5885	61.564	40503.99	0.055252	0.054195	-1.0393	59.544
4	0.028948	1.7786	61.828	43033.96	0.058863	0.058605	-0.3959	59.740
5	0.030337	2.0187	62.092	45067.64	0.061507	0.062663	1.7006	59.544
6	0.031957	2.3155	62.357	47452.64	0.064824	0.065743	1.3973	59.740
7	0.033083	2.7261	62.709	49113.49	0.066714	0.068133	2.0817	59.740
8	0.037032	3.1010	63.061	54939.91	0.073049	0.075507	3.3352	59.917
9	0.042354	3.4257	63.414	62778.99	0.080137	0.080520	1.9026	59.934
10	0.048026	3.7731	63.766	71170.50	0.087130	0.086022	-0.5622	59.279
11	0.051290	4.1759	64.118	75972.62	0.090340	0.092720	4.4594	59.447
12	0.058159	4.5450	64.557	86127.87	0.097033	0.093531	-3.0357	59.800
13	0.063139	4.8767	65.085	93481.63	0.102017	0.103060	1.0234	59.976
14	0.068072	5.2587	65.788	100786.62	0.107402	0.104235	-2.9136	60.153
15	0.073451	5.5364	66.491	108725.06	0.114466	0.114497	0.0411	60.506
16	0.071527	5.4391	68.861	104049.37	0.114589	0.114376	-0.4184	61.564
17	0.073983	5.6582	70.526	105991.75	0.115503	0.114730	-1.0358	62.269
18	0.073608	5.5273	73.501	103679.44	0.116063	0.114483	-2.0756	63.679
19	0.073249	5.5528	78.300	101545.25	0.117049	0.114533	-3.2773	66.316
20	0.073991	5.5957	81.172	101495.94	0.117667	0.114594	-3.0558	67.896
21	0.074626	5.5415	82.996	101963.75	0.118477	0.114595	-5.0515	68.940
22	0.073963	5.5279	87.070	100251.94	0.115874	0.114485	-1.8335	81.519
23	0.075382	5.6280	92.426	99242.12	0.116623	0.114655	-2.5819	87.762
24	0.075741	5.5308	95.699	99335.75	0.116865	0.114490	-3.2158	92.254
25	0.075677	5.5054	100.164	100111.25	0.115702	0.114454	-1.6473	102.229
26	0.076396	5.4655	104.956	100837.13	0.116641	0.114406	-2.3153	114.151
27	0.078033	5.2217	108.028	103093.75	0.116590	0.116211	-0.5089	120.004

TTRSS RUN NUMBER 22

LABYRINTH LEAK RATE OF THE TRANSONIC TURBINE TEST 216

POINT	LABYRINTH LEAK RATE (LBM/SEC)	LABYRINTH PRESSURE RATIO	PLENUM TOTAL TEMPERATURE (DEG F)	REYNOLDS NUMBER	CORRECTED LEAK RATE (SQ IN)	ANALYTICAL CORRECTED LEAK RATE	PERCENT ERROR	WORK TEMPERATURE (DEG F)
1	0.033354	1.4001	85.944	45456.91	0.048082	0.051243	6.2141	105.221
2	0.039216	1.6586	87.742	53278.64	0.054357	0.056014	2.9534	111.243
3	0.042311	1.8030	89.146	57360.87	0.056265	0.058175	4.0184	113.649
4	0.047126	1.9774	91.132	63013.36	0.059085	0.061000	3.2318	114.208
5	0.051266	2.1702	91.823	69653.81	0.062503	0.064434	2.8572	115.677
6	0.054204	2.3658	93.288	73728.25	0.064019	0.066124	3.1949	115.846
7	0.058356	2.6177	95.255	79297.37	0.066442	0.067632	1.7411	116.602
8	0.061834	2.8781	97.419	84024.12	0.068336	0.069737	2.0833	117.022
9	0.065040	3.1677	97.932	88571.00	0.069269	0.069722	0.6046	116.602
10	0.068253	3.4081	98.534	93018.94	0.070533	0.070752	0.3243	116.185
11	0.071632	3.9077	99.564	97129.75	0.071819	0.071991	0.2386	116.863
12	0.074619	4.2892	101.364	100306.62	0.072701	0.073007	0.3967	118.248
13	0.080311	4.5743	101.702	108067.75	0.073575	0.073570	0.0050	117.709
14	0.086070	4.8939	102.562	117185.81	0.074529	0.073987	-0.7277	117.232
15	0.091794	5.1605	103.418	124979.64	0.075713	0.074176	-2.0305	116.602
16	0.099423	5.9089	105.640	135438.81	0.076834	0.075611	-1.7861	116.185

TTRSS RUN NUMBER 30

LABYRINTH LEAK RATE OF THE TRANSONIC TURBINE TEST SIG

POINT	LABYRINTH LEAK RATE (LBM/SEC)	LABYRINTH PRESSURE RATIO	PLENUM TOTAL TEMPERATURE (DEG F)	REYNOLDS NUMBER	REFERRED LEAK RATE (SQ IN)	ANALYTICAL REFERRED LEAK RATE	PERCENT ERROR	HOOD TEMPERATURE (DEG F)
1	0.034971	1.5151	85.511	48596.26	0.054604	0.052035	-4.7049	93.288
2	0.038855	1.6533	85.858	54115.61	0.058001	0.055883	-3.6527	93.288
3	0.043203	1.8195	86.551	60220.97	0.061528	0.059630	-3.1124	93.590
4	0.047854	1.9881	86.897	66744.00	0.065422	0.062744	-4.0575	93.256
5	0.050789	2.1750	87.416	71069.06	0.066702	0.064483	-3.4570	91.736
6	0.054682	2.3702	87.935	76800.25	0.069124	0.066156	-4.2979	91.736
7	0.057763	2.6285	88.281	81295.00	0.070003	0.067696	-3.3111	91.564
8	0.061205	2.8761	88.627	86621.56	0.071436	0.068730	-3.7876	91.564
9	0.064549	3.1589	88.108	92105.31	0.072462	0.069693	-3.8295	91.219
10	0.066266	3.4865	87.935	94574.69	0.071703	0.070717	-1.5099	90.873
11	0.070279	3.8718	87.762	100195.94	0.073326	0.071985	-1.8651	90.873
12	0.072579	4.2467	87.762	103496.81	0.073382	0.072906	-0.6433	90.873
13	0.075610	4.7290	87.762	107932.62	0.073869	0.073806	-0.0859	91.044
14	0.078390	5.3212	87.762	111760.44	0.074150	0.074276	0.1632	90.873
15	0.083899	5.6315	87.940	119715.44	0.074592	0.074664	0.0965	90.873
16	0.090341	6.0351	88.281	128907.44	0.075311	0.076289	1.4113	90.873

```
C       PROGRAM TTRSS
C       COMPUTES EXPERIMENTAL PERFORMANCE CHARACTERISTICS OF THE
C       TURBINE TEST RIG
C       INPUT DATA DH(IN H20),PNOZ(IN HG),TNOZ(MV),PTPL(IN HG),PHUB(IN HG)
C       PTIP(IN HG),          ,TTPL(MV),PATM(IN HG),RPM(RPM),TORQR(COUNTS)
C       AXIL(COUNTS),DYNAR(COUNTS),PHD(IN HG),          ,PSPL(IN HG),
C       CLAXIL(COUNTS),CLTROR(COUNTS),PRE2(IN HG),THD(MV),P15 TH2U P21
C       (IN HG),TCL(DEGREES F),TCR(DEGREES F).
        DIMENSION DH(50),PNOZ(50),TNOZ(50),PTPL(50),PHUB(50),PTIP(50),
       1        TTPL(50),PATM(50),RPM(50),TORQR(50),AXIL(50),DYNAR(50),
       2PHD(50),        PSPL(50),CLAXIL(50), CLTROR(50),PRE2(50)
       3,P18(50),P15(50),P16(50),P17(50),P19(50),P20(50),TTPLD(50),
       4HW68(50),P21(50),THD(50)
        DIMENSION FLOWT(50),PR(50),HP(50),XKTS(50),COEFL(50),COEFM(50),
       1COEFP(50),COEFS(50),V1(50),V2(50),W1(50),W2(50),U1(50),U2(50),
       2T1(50),T2(50),T2IS(50),TT2(50),ALPH1(50),ALPH2(50),BETA1(50),
       3BETA2(50),DBETA(50),ETA(50),ETAT(50),ZETAP(50),ZETAS(50),ZETA(50),
       4REACHB (50),REACMN(50),REACTP (50),VM1(50),WM1(50),PHI(50),
       5        XI(50),PRS(50)
        COMMON G,R,C2,EX2,RM1,RM2,AAX,ATH,QFLOWT,QTTPL,T1IS,QT1,QPTPL,
       1QPTIP,QPHUB,P1AV,QP18,QP15,QP16,QP17,QPRS,TORQ,CLTORQ,QV1,VA1,VU1,
       2QZETAS,QPHI,QXI,GAM,QALPH1,QBETA1,QRPM,QU1,QW1,QVM1,QWM1,QPHD,
       3 CLEAX,EAX,RTIP1,RHUB1,SKT,PAMB,QP19,QP20,EX3,QP21,EX1
        READ 20,MM
   20 FORMAT(I10)
        CALL CANCEL (2)
        DO 99 M=1,MM
        CALL INPUT(NRUN,AXCLR,RADCLR,PBAR,N,TCL,TCR,DH,PNOZ,TNOZ,PTPL,
       1PHUB,PTIP,     TTPL,PATM,RPM,TORQR,AXIL,DYNAR,PHD,      PSPL,
       2CLAXIL,CLTROR,PRE2,P18,P15,P16,P17,P19,P20,P21,TTPLD,THD)
        CALL SETCON(BETA,D1,D2,AAXR,AAX,ATH,R,GAM,G,CP,CJ,C1,C2,EX2,EX1,
       1RTIP1,RHUB1,RTIP2,RHUB2,RM1,RM2,RADCLR,SKT,PKT,B,EX3,A,B1,B2,B3,B4
       2,B5,A1,A2,A3,A4,A5,A6,CL1,CL2,CL3,CL4,CE1,CE2,CE3,CE4)
        DO 90 I=1,N
        QDH=DH(I)
        QPNOZ=PNOZ(I)
        QTNOZ=TNOZ(I)
        QPTPL=PTPL(I)
        QPHUB=PHUB(I)
        QPTIP=PTIP(I)
        QTTPL=TTPL(I)
        QTTPLD=TTPLD(I)
        QTHD=THD(I)
        QPATM=PATM(I)
        QRPM=RPM(I)
```

```
      QTORQR=TORQR(I)
      QAXIL=AXIL(I)
      QDYNAR=DYNAR(I)
      QPHD=PHD(I)
      QPSPL=PSPL(I)
      QCLXIL=CLAXIL(I)
      QLTRQR=CLTRQR(I)
      QPRF2=PRF2(I)
      QP18=P18(I)
      QP15=P15(I)
      QP16=P16(I)
      QP17=P17(I)
      QP19=P19(I)
      QP20=P20(I)
      QP21=P21(I)
      CALL  CNVERT(QDH,QPNOZ,QTNOZ,QPTPL,QPHUB,QPTIP,QTTPLD,QTTPL,QPATM,
     1QRPM,QTORQR,QAXIL,QDYNAR,QPHD,QTHD, QPSPL, QLTRQR, QCLXIL,P1AV,P2,
     2QP18,QP15,QP16,QP17,TORQ,CLTORQ,FAX,CLFAX,DYNA,PRAR,QPRF2,TCL,
     3TCR,   PAMB,QP19,QP20,QHW6R,QP21,CL1,CL2,CL3,CL4,CF1,CF2,CF3,CF4)
      CALL FLORAT(A,R,D2,BETA,EX1,EX2,EX3,R,G,GAM,QPNOZ,QPSPL,QTNOZ,
     1QTTPLD,QPHD,QDH,QHW6R,NRUN,B1,B2,B3,B4,B5,A1,A2,A3,A4,A5,A6,
     2QFLOWT,QTHD,I)
      CALL STATOR
      CALL ROTOR(G,R,CP,CJ,C2,EX2,RM1,RM2,AAXR,QFLOWT,QTTPL,QRPM,DYNA,
     1QDP,P1AV,P2,QT1,QT2,QTT2,QT2IS,VA1,VU1,QV2,QW1,QW2,QU1,QU2,QALPH2,
     2QBETA1,QBETA2,EX1,RKT)
      CALL  PERFM(G,R,CP,C1,C2,EX2,GAM,QTTPL,QPTPL,QPHUB,QPTIP,QPHD,
     1QRPM,QFLOWT,DYNA,QDP,P2,T1IS,QT1,QT2IS,QPR,QETA,QXKIS,QCOEFL,
     2QCOEFM,QCOEFP,QCOEFS, QEACMN,QEACHB ,QEACTP ,QZETAR,QALPH1,QALPH2,
     3QBETA1,QBETA2,QDBETA,QHP,QU2,QW1,QW2,EX1,QTT2,QT2,QETAT,QU1)
      FLOWT(I)=QFLOWT
      PR(I)=QPR
      HP(I)=QHP
      XKIS(I)=QXKIS
      COEFL(I)=QCOEFL
      COEFM(I)=QCOEFM
      COEFP(I)=QCOEFP
      COEFS(I)=QCOEFS
      V1(I)=QV1
      V2(I)=QV2
      W1(I)=QW1
      W2(I)=QW2
      U1(I)=QU1
      U2(I)=QU2
      TTPL(I)=QTTPL
```

```
      T1(I)=QT1
      T2(I)=QT2
      T2IS(I)=QT2IS
      TT2(I)=QTT2
      ALPH1(I)=QALPH1
      ALPH2(I)=QALPH2
      BETA1(I)=QBETA1
      BETA2(I)=QBETA2
      QBETA(I)=QQBETA
      ETA(I)=QETA
      ETAT(I)=QETAT
      ZETAR(I)=QZETAR
      ZETAS(I)=QZETAS
      REACHB (I)=QREACHB
      REACMN(I)= QREACMN
      REACTP (I)=QREACTP
      VM1(I)=QVM1
      WM1(I)=QWM1
      PHI(I)=QPHI
      XI(I)=QXI
      PRS(I)=QPRS
      PTPL(I)=QPTPL
   90 CONTINUE
      CALL OUTPTA (NRUN,AXCLR,RADCLR,FLOWT,N ,HP,XKIS,COEFL,COEFM,COEFD,
     1COEFS,V1,V2,W1,W2,U1,U2,T1,T2,T2IS,TT2,ALPH1,ALPH2,BETA1,BETA2,
     2DBETA,ETA,ETAT,ZETAR,ZETAS,     REACHB ,REACMN,REACTP ,VM1,WM1,
     3PHI,     XI,PRS,RPM,TTPL,PR)
      CALL OUTPUT(NRUN,AXCLR,RADCLR,N,PR,XKIS,ETA,COEFL,COEFM,COEFD,
     1COEFS,REACHB ,REACTP ,PTPL)
   99 CONTINUE
      STOP
      END



      SUBROUTINE INPUT(NRUN,AXCLR,RADCLR,PRAR,N,TCL,TCP,DH,PNOZ,TNOZ,
     1PTPL,PHUB,PTIP,     TTPL,PATM,RPM,TORQR,AXIL,DYNAR,PHD,     PSPL,
     2CLAXIL, CLTRQR,PRE2,P18,P15,P16,P17,P19,P20,P21,TTPLD,THD)
      DIMENSION DH(50),PNOZ(50),TNOZ(50),PTPL(50),PHUB(50),PTIP(50),
     1 TTPLD(50)       ,PATM(50),RPM(50),TORQR(50),AXIL(50),DYNAR(50),
     2PHD(50),TTPL(50),PSPL(50),CLAXIL(50), CLTRQR(50),PRE2(50),
     3P18(50),P15(50),P16(50),P17(50),P19(50),P20(50),P21(50),THD(50)
      READ (5,101)NRUN
```

```
      READ (5,102)AXCLR,RADCLR
      READ (5,102)PBAR
      READ (5,101)N
      READ (5,102)TCL,TCR
      READ (5,102)(PRE2(I),I=1,N)
      READ (5,102)(PTPL(I),I=1,N)
      READ (5,102)(P15 (I),I=1,N)
      READ (5,102)(P16 (I),I=1,N)
      READ (5,102)(P17 (I),I=1,N)
      READ (5,102)(P18 (I),I=1,N)
      READ (5,102)(P19 (I),I=1,N)
      READ (5,102)(P20 (I),I=1,N)
      READ (5,102)(P21(I),I=1,N)
      READ (5,102)(DH(I),I=1,N)
      READ (5,102)(PATM(I),I=1,N)
      READ (5,102)(PNOZ(I),I=1,N)
      READ (5,102)(PSPL(I),I=1,N)
      READ (5,102)(PHUB(I),I=1,N)
      READ (5,102)(PTIP(I),I=1,N)
      READ (5,102)(PHD (I),I=1,N)
      READ (5,102)(TNOZ(I),I=1,N)
      READ (5,102)(TTPLD(I),I=1,N)
      READ (5,102)(TTPL(I),I=1,N)
      READ (5,102)(THD(I),I=1,N)
      READ (5,102)(RPM(I),I=1,N)
      READ (5,102)(AXIL(I),I=1,N)
      READ (5,102)(TORQR(I),I=1,N)
      READ (5,102)(DYNAR(I),I=1,N)
      READ (5,102)(CLAXIL(I),I=1,N)
      READ (5,102)(CLTRQR(I),I=1,N)
      WRITE(6,105)NRUN,PBAR
      WRITE(6,107)(PRE2(I),I=1,N)
      WRITE(6,107)(PTPL(I),I=1,N)
      WRITE(6,107)(P15(I),I=1,N)
      WRITE(6,107)(P16(I),I=1,N)
      WRITE(6,107)(P17(I),I=1,N)
      WRITE(6,107)(P18(I),I=1,N)
      WRITE(6,107)(P19(I),I=1,N)
      WRITE(6,107)(P20(I),I=1,N)
      WRITE(6,107)(P21(I),I=1,N)
      WRITE(6,107)(DH(I),I=1,N)
      WRITE(6,107)(PATM(I),I=1,N)
      WRITE(6,107)(PNOZ(I),I=1,N)
      WRITE(6,107)(PSPL(I),I=1,N)
      WRITE(6,107)(PHUB(I),I=1,N)
```

```
      WRITE(6,107)(PTIP(I),I=1,N)
      WRITE(6,107)(PHD(I),I=1,N)
      WRITE(6,107)(TNO7(I),I=1,N)
      WRITE(6,107)(TTPLO(I),I=1,N)
      WRITE(6,107)(TTPL(I),I=1,N)
      WRITE(6,107)(THD(I),I=1,N)
      WRITE(6,107)(RPM(I),I=1,N)
      WRITE(6,107)(AXIL(I),I=1,N)
      WRITE(6,107)(TORQR(I),I=1,N)
      WRITE(6,107)(DYNAR(I),I=1,N)
      WRITE(6,107)(CLAXIL(I),I=1,N)
      WRITE(6,107)(CLTRQR(I),I=1,N)
101   FORMAT(I10)
102   FORMAT(8E10.4)
105   FORMAT(1H1,//5X,11H RUN NUMBER,I5,//5X,40H INPUT DATA, CARD IMAGE,
     1 1 LINE = 1 CARD //,5X,6H PRAR=,F6.3/)
107   FORMAT(8E15.5)
      RETURN
      END


      SUBROUTINE SETCON(BETA,D1,D2,AAXR,AAX,ATH,R,GAM,G,CP,CJ,C1,C2,EX2,
     1EX1,RTIP1,RHUB1,RTIP2,RHUB2,RM1,RM2,RADCLR,SKT,BKT,B,EX3,A,B1,B2,
     2B3,B4,B5,A1,A2,A3,A4,A5,A6,CL1,CL2,CL3,CL4,CE1,CE2,CE3,CE4)
      BETA=0.163842658
      D1=7.975
      D2=4.250
      R=53.3448
      GAM=1.4
      G=32.174
      CP=0.24
      CJ=778.16
      C1=2.*G*CJ
      C2=2.*G*CJ*CP
      EX1=GAM/(GAM-1.)
      EX2=(GAM-1.)/GAM
      PI=3.14159
      ZN1=31.
      ASTAT=0.205
      SSTAT=0.8594
      THKS=0.024
      AROTR=0.1314
```

```
      SROTR=0.4440
      THKR=0.020
      RTIP1=4.584
      RHUB1=3.896
      RTIP2=9.516/2.
      RHUB2=7.652/2.
      AAX=PI*((RTIP1)**2-(RHUB1)**2)
      AAXR=PI*((RTIP2)**2-(RHUB2)**2)
      ATH=ASTAT*(RTIP1-RHUB1)*ZN1
      RM1=(RTIP1+RHUB1)/2.
      RM2=(RTIP2+RHUB2)/2.
      SKT=1.-(2.7/1000.)*(THKS/SSTAT*100.)**3.3*ASTAT/SSTAT
      RKT=(1.-(2.7/1000.)*(THKR/SROTR*100.)**3.3*AROTR/SROTR)*((AAXR+
     13.14159*RADCLR*(RTIP2+RADCLR/2.))/AAXR)
      B=(D2/D1)**4
      EX3=2./GAM
      A=6.316*3600./D2
      B1=0.93292874
      B2=4.268322E-07
      B3=-6.151495E-13
      B4=3.895006E-19
      B5=-9.138062E-26
      A1=-1.004586E-01
      A2=2.122579E-01
      A3=-1.081851E-01
      A4=2.767576E-02
      A5=-3.489933E-03
      A6=1.726733E-04
      CL1=-4.901048E-02
      CL2=7.376791E-03
      CL3=-4.121890E-06
      CL4=1.661981E-08
      CE1=-2.631117E-01
      CE2=3.890573E-02
      CE3=-2.068711E-06
      CE4=2.281905E-09
      RETURN
      END



      SUBROUTINE CNVERT(DH,PNOZ,TNOZ,PTPL,PHUB,PTIP,TTPLD,TTPL,PATM,PDM,
     1TORQR,AXIL,DYNAR,PHD,THD, PSPL, CLTROR,CLAXIL,P1AV,P2,P18,P15,P16,
```

```
2P17,TORQ,CLTORQ,FAX,CLFAX,DYNA,PBAR,PRE2,TCL,TCR,   PAMB,P1R,P2C,
3HW68,P21,CL1,CL2,CL3,CL4,CF1,CF2,CF3,CF4)
 TEMP(X)=32.+35.98*X-.435*X**2
 GWRM=0.99837633+1.0605756*TCR/10000.-1.5931861*TCR**2/10000000.
 GW68=0.99837633+1.0605756*68./10000.-1.5931861*68.**2/10000000.
 RATGW=GWRM/GW68
 GHGCL=13.63905-0.0013630303*TCL
 GHGCR=13.63905-0.0013630303*TCR
 CHGC =0.4891585*GHGCL/13.54
 CHGCR=0.4891585*GHGCR/13.54
 PAMB=PBAR
 PAMB=PAMB*CHGC
 HW68=DH*RATGW
 DH=DH*GWRM/12.*62.42732/144.
 PNOZ=CHGCR*(PATM-PNOZ)+PAMB
 PTPL=CHGCR*(PRE2-PTPL)+PAMB
 PHUB=CHGCR*(PATM-PHUB)+PAMB
 PTIP=CHGCR*(PATM-PTIP)+PAMB
 P15=CHGCR*(PRE2-P15)+PAMB
 P16=CHGCR*(PRE2-P16)+PAMB
 P17=CHGCR*(PRE2-P17)+PAMB
 P18=CHGCR*(PRE2-P18)+PAMB
 P19=CHGCR*(PRE2-P19)+PAMB
 P20=CHGCR*(PRE2-P20)+PAMB
 P21=CHGCR*(PRE2-P21)+PAMB
 PSPL=CHGCR*(PATM-PSPL)+PAMB
 PHD=CHGCR*(PATM-PHD)+PAMB
 P2=PHD
 TTPL= TEMP(TTPL)+459.7
 TNOZ=TEMP(TNOZ)
 TTPLD=TEMP(TTPLD)
 THD=TEMP(THD)
 ST1=-4.955933E-01
 ST2=4.451445E-01
 ST3=-4.259542E-05
 ST4=4.823251E-08
 TORQ=(ST1+ST2*TORQR+ST3*TORQR**2+ST4*TORQR**3)/12.
 CLTORQ=(CL1+CL2*CLTRQR+CL3*CLTRQR**2+CL4*CLTRQR**3)/12.
 FAX=0.1*AXIL
 CLFAX=CF1+CF2*CLAXIL+CF3*CLAXIL**2+CF4*CLAXIL**3
 DYNA=DYNAR/30.
 RETURN
 END
```

```
      SUBROUTINE FLORAT (A,B,D2,BETA,EX1,EX2,EX3,R,G,GAM,PNOZ,PSPL,TNOZ,
     1TTPLD,PHD,DH,HW68,NRUN,B1,B2,B3,B4,B5,A1,A2,A3,A4,A5,A6,FLOWT,THD,
     2I)
      ALPHN=1.+0.00252*(TNOZ-68.)/100.
      XR=1.-(DH/PNOZ)
      YN=SQRT(XR**EX3*EX1*((1.-XR**EX2)/(1.-XR))*((1.-B)/(1.-B*XR**EX3))
     1)
      Z=0.019+0.0024*(TNOZ/100.-1.)
      TNOZR=TNOZ+459.7
      EPS=0.0
   48 WG=1.0+EPS
      RE=A*WG/7
      IF(RE.GT.1300000.)GO TO 52
      CN=B1+B2*RE+B3*RE**2+B4*RE**3+B5*RE**4
      W=BETA*D2**2*ALPHN*YN*CN*SQRT(PNOZ*HW68/TNOZR)
      WD=W-WG
      IF(WD.LT..0001)GO TO 50
      EPS=EPS+0.88*WD
      GO TO 48
   52 WRITE(6,100)NRUN,I
  100 FORMAT  (/33X,I4,7X,I2,7X,36HFLOW RATE TOO HIGH, CHECK INPUT DATA/
     1)
   50 FLOW=W
      PR=PSPL/PHD
      WREF=A1+A2*PR+A3*PR**2+A4*PR**3+A5*PR**4+A6*PR**5
      CORR=(1.0+0.32*((TTPLD-THD)/TTPLD))**1.2
      TTPLDR=TTPLD+459.7
      WLAB=WREF*PSPL/SQRT(TTPLDR*R/G)/CORR
      FLOWT=FLOW-WLAB
      RETURN
      END



      SUBROUTINE STATOR
      COMMON G,R,C2,EX2,RM1,RM2,AAX,ATH, FLOWT, TTPL,TITS, T1, PTPL,
     1PTIP,PHUB,P14V,P18,P15,P16,P17,PRS,TORQ,CLTORQ,V1,VA1,VU1,
     2 ZETAS, PHI, XI,GAM, ALPHI, BETA1, RPM, U1, W1, VM1, WM1, PHD,
     3 CLEAX,EAX,RTIP1,RHUB1,SKT,PAMB,P19,P20,EX3,P21,EX1
      RR=0.0
```

911

```
      WRITE (6,55) SKT
   55 FORMAT (///10X,6HKTE =  ,F7.5//9X,3HEPS8X,4HP1AV9X,3HT1M10X,3HT1C9X,
     14HVA1M9X,4HVA1C10X,4HVM1M9X,4HVM1C7X,8HALPHA 1M5X,8HALPHA 1C//)
   97 EPS=RR
      P1AV=PHUB/3.*(((1.+EPS)*(2.*RTIP1)**2+(2.*RHUB1)*(2.*RTIP1)-(2.+
     1EPS)*(2.*RHUB1)**2)/((2.*RTIP1)**2-(2.*RHUB1)**2))+PTIP/3.*(((2.+
     2EPS)*(2.*RTIP1)**2-(2.*RHUB1)*(2.*RTIP1)-(1.+EPS)*(2.*RHUB1)**2)/
     3((2.*RTIP1)**2-(2.*RHUB1)**2))
      CALL MOMENT(G,C2,AAX,RM1,PHD,PTIP,P1AV,PHUB,P18,P15,P16,P17,
     1FLOWT,TORQ,CLEAX,EAX,TTPL,VU1,VA1,V1,ALPH1,T1,RTIP1,RHUB1,CPTORQ,
     2RADCLR,PBAR,DELP1,EX2,SKT,R,EPS,P19,P20,P21)
      T1C=EX1*G*(P1AV*AAX*SKT)**2/(R*FLOWT**2)*(SQRT(1.-2.*EX2*R*FLOWT**
     12/(G*(P1AV*AAX*SKT)**2)*(VU1**2/C2-TTPL))-1.)
      V1C=SQRT((TTPL-T1C)*C2)
      VA1C=SQRT(V1C**2-VU1**2)
      ALPH1C=ATAN(VU1/VA1C)
      AL1C=ALPH1C*57.295779
      AL1M=ALPH1*57.295779
      VM1C=V1C/SQRT(GAM*G*R*T1C)
      VM1M=V1/SQRT(GAM*G*R*T1)
      WRITE (6,58)EPS,P1AV,T1,T1C,VA1,VA1C,VM1M,VM1C,AL1M,AL1C
   58 FORMAT (10F13.5)
      DIFF=ABS(T1C-T1)
      IF (DIFF-0.02)98,98,50
   50 IF (T1C.LT.T1) GO TO 47
      RR=RR+DIFF/250.
      GO TO 97
   47 RR=RR-DIFF/250.
      GO TO 97
   98 PRS=P1AV/PTPL
      T1IS=TTPL*PRS**EX2
      ZETAS=(T1-T1IS)/(TTPL-T1IS)
      PHI=FLOWT/PTPL/ATH *SQRT (TTPL* R/G)
      PRST=PRS
      IF (PRST.LT.0.52828) PRST=0.52828
      XI=PHI/SQRT(2./EX2*(PRST**EX2-  PRST**((GAM+1.)/GAM)))
      RAD=.10471967*RPM
      U1=RM1*RAD/12.
      WU1=VU1-U1
      WA1=VA1
      BETA1=ATAN (WU1/WA1)
      W1=WA1/COS (BETA1)
      VM1=V1/SQRT (GAM*G* R*T1)
      WM1=W1/SQRT (GAM*G* R*T1)
      RETURN
```

```
      END


      SUBROUTINE MOMENT(G,C2,AAX,RM1,PHD,PTIP,P1AV,PHUB,P18,P15,P16,P17,
     1FLOWT,TORQ,CLEAX,FAX,TTPL,VU1,VA1,V1,ALPH1,T1,RTIP1,RHUB1,CLTORQ,
     2RADCLR,PBAR,DELP1,EX2,SKT,R,EPS,P19,P20,P21)
      VU1=(TORQ+CLTORQ)*G/FLOWT/RM1*12.
      PI=3.14159
      A1=PI*(5.125)**2
      A2=PI*((5.125)**2-(5.003)**2)
      A3=PI*(5.003**2-4.901**2)
      A3A=PI*(4.901**2-4.773**2)
      A4=PI*(4.773**2-RTIP1**2)
      A5=PI*(RTIP1**2-RHUB1**2)
      A6=PI*RHUB1**2
      F1=A1*PHD
      F2=A2*P21
      F3=A3*((P20+P19)/2.)
      F3A=A3A*P18
      F4=A4*PTIP
      F5=A5*P1AV
      F6=A6*PHUB
      FNET=F1+FAX+CLEAX-F2-F3-F4-F5-F6-F3A
       VA1=G*FNET/FLOWT
      ALPH1=ATAN (VU1/VA1)
      V1=SQRT (VA1**2+VU1**2)
      T1=TTPL-V1**2/C2
      RETURN
      END



      SUBROUTINE ROTOR(G,R,CP,CJ,C2,EX2,RM1,RM2,AAXR,FLOWT,TTPL,RPM,
     1DYNA,DP,P1AV,P2,T1,T2,TT2,T2IS,VA1,VU1,V2,W1,W2,U1,U2,ALPH2,BETA1,
     2BETA2,EX1,RKT)
      RAD=.104719667*RPM
      DP=DYNA*RAD/CJ
      VU2=RM1/RM2*VU1-DYNA*G/RM2/FLOWT*12.
      TT2=TTPL-DP/CP/FLOWT
      T2IS=T1*(P2/P1AV)**EX2
```

```
      U2=RM2*RAD/12.
      WU2=VU2-U2
      TE=T1+(W1**2.-U1**2.+U2**2.)/C2
      T2=EX1*G*(P2*AAXR*RKT)**2/(R*FLOWT**2)*(SQRT(1.-2.*EX2*R*FLOWT**2
     1/(G*(P2*AAXR*RKT)**2)*(WU2**2/C2-TE))-1.)
      V2=SQRT ((TT2-T2)*C2)
      VA2=SQRT(V2**2-VU2**2)
  615 WA2=VA2
      W2=SQRT (WA2**2+WU2**2)
      ALPH2=ATAN (VU2/VA2)
      BETA2=ATAN (WU2/WA2)
      RETURN
      END
```

```
      SUBROUTINE PERFRM  (G,R,CP,C1,C2,EX2,GAM,TTPL,PTPL,PHUB,PTIP,PHD,
     1RPM,FLOWT,DYNA,DP,P2,T1IS,T1,T2IS,PR,ETA,XKIS,COEFL,COEFM,COEFP,
     2COEFS,REACMN,REACHB ,REACTP ,ZETAR,ALPH1,ALPH2,BETA1,BETA2,DBETA,
     3HP,U2,W1,W2,EX1,TT2,T2,ETAT,U1)
      PR=PTPL/P2
      T2TH=TTPL*(PHD/PTPL)**EX2
      DHIS=CP*(TTPL-T2TH)
      ETA=DP/DHIS/FLOWT
      PT2=P2*(TT2/T2)**EX1
      TT2IS=TTPL*(PT2/PTPL)**EX2
      ETAT=DP/(CP*(TTPL-TT2IS))/FLOWT
      XKIS=DHIS*C1/U1**2
      DEL=PTPL/14.69
      THETA=SQRT (GAM* R*TTPL)/196.8107
      COEFL=FLOWT*THETA/DEL
      COEFM=DYNA/DEL
      HP=3600./2545.*DP
      COEFP=HP/(DEL*THETA)
      COEFS=RPM/THETA
      REACMN=1.0-CP*(TTPL-T1IS)/DHIS
      REACHB=((PHUB/PHD)**EX2-1.)/((PTPL/PHD)**EX2-1.)
      REACTP=((PTIP/PHD)**EX2-1.)/((PTPL/PHD)**EX2-1.)
      SQW2TH=C2*(T1-T2IS)+W1**2+(U2**2-U1**2)
      ZETAR=1.-W2**2/SQW2TH
      ALPH1=ALPH1*57.295779
      ALPH2=ALPH2*57.295779
      BETA1=BETA1*57.295779
```

```
      BETA2=BETA2*57.295779
      DBETA=BETA1-BETA2
      RETURN
      END



      SUBROUTINE OUTPTA (NRUN,AXCLR,RADCLR,FLOWT,N ,HP,XKIS,COEFL,COEFM,
     1COEFP,COEFS,V1,V2,W1,W2,U1,U2,T1,T2,T2IS,TT2,ALPH1,ALPH2,BETA1,
     2BETA2,DBETA,ETA,ETAT,ZETAR,ZETAS,     REACHR ,REACMN,REACTP ,
     3VM1,WM1,PHI,     XI,PRS,RPM,TTPL,PR)
      DIMENSION FLOWT(50),PR(50),HP(50),XKIS(50),COEFL(50),COEFM(50),
     1COEFP(50),COEFS(50),V1(50),V2(50),W1(50),W2(50),U1(50),U2(50),
     2T1(50),T2(50),T2IS(50),TT2(50),ALPH1(50),ALPH2(50),BETA1(50),
     3BETA2(50),DBETA(50),ETA(50),ETAT(50),ZETAR(50),ZETAS(50),ZETA(50),
     4REACHR (50),REACMN(50),REACTP (50),VM1(50),WM1(50),PHI(50),
     5          XI(50),PRS(50),RPM(50),TTPL(50)
      WRITE(6,805)
  805 FORMAT(1H1//24H TURBINE CIRCULAR ARC  T //10H STATOR  T //)
      WRITE(6,806)NRUN,AXCLR,RADCLR
  806 FORMAT(11H RUN NUMBER I3,8H SPACING F10.3,11H TIP CLEAR. F10.3//)
      WRITE(6,807)
  807 FORMAT (5X,6H POINT  6X,10H FLOW RATE  9X,4H RPM
     1 5X,15H PRESSURE RATIO   5X,11H HORSEPOWER  /)
      DO 808 I=1,N
  808 WRITE(6,809)I,FLOWT(I),RPM(I),PR(I),HP(I)
  809 FORMAT (I5,12X,4(F10.4,5X))
      WRITE(6,810)
  810 FORMAT(///20X,37H DIMENSIONLESS PERFORMANCE PARAMETERS //
     15X, 6H POINT 11X, 2H K 10X, 9H REFERRED  8X, 9H REFERRED
     27X,9H REFERRED  7X,9H REFERRED  6X,      /
     317X,11H ISENTROPIC  5X,10H FLOW RATE  8X, 7H TORQUE
     4 9X, 6H POWER 10X, 6H SPEED  9X,/)
      DO 811 I=1,N
  811 WRITE(6,812)     I,XKIS(I),COEFL(I),COEFM(I),COEFP(I),COEFS(I)
  812 FORMAT ( I5,12X,6(F10.4,6X))
      WRITE(6,813)NRUN
  813 FORMAT(1H1/////5X,16H GENERAL RESULTS //20X,20H VELOCITIES (FT/SEC
     1)//,20X,11H RUN NUMBER   I5/
     2//5X, 6H POINT 10X, 3H V1 12X, 3H V2 12X,3H W1 12X,3H W2
     312X,3H U1 12X,3H U2  /  )
      DO 814 I=1,N
  814 WRITE(6,815)   I,V1(I),V2(I),W1(I),W2(I),U1(I),U2(I)
```

```
815 FORMAT ( I5,12X, 6(F10.5,5X))
    WRITE(6,816)
816 FORMAT (       /20X,23H TEMPERATURES (DEG R )  //
   1 5X, 6H POINT    8X, 7H PLENUM  6X, 7H STATOR  9X, 6H ROTOR
   2 9X,11H ISENTROPIC   4X, 6H TOTAL  /19X, 6H TOTAL   7X,
   310H DISCHARGE  5X,10H DISCHARGE  5X, 8H FROM T1   7X,
   410H DISCHARGE / )
    DO 817 I = 1,N
817 WRITE(6,818)       I, TTPL(I), T1(I), T2(I), T2IS(I), TT2(I)
818 FORMAT ( I5,12X, 5(F10.5,5X))
    WRITE(6,819)NRUN
819 FORMAT(1H1/////20X,33H FLOW ANGLES (DEGREES FROM AXIAL)  //
   120X,11H RUN NUMBER    I5///
   2 5X, 6H POINT    7X, 8H ALPHA 1  8X, 8H ALPHA 2  7X, 7H BETA 1
   3 8X, 7H BETA 2   6X,12H DELTA BETA  / )
    DO 820 I=1,N
820 WRITE(6,821) I, ALPH1(I),ALPH2(I),BETA1(I),BETA2(I),DBETA(I)
821 FORMAT ( I5,12X, 5(F10.5,5X))
    WRITE(6,822)
822 FORMAT (       ///20X,24H EFFICIENCIES AND LOSSES     //
   12X,6H POINT 10X, 11H EFFICIENCY 14X, 11H EFFICIENCY 17X, 5H ZETA
   220X, 5H ZETA/ 17X, 13H TOTAL STATIC 13X, 12H TOTAL TOTAL 16X, 6H R
   3OTOR 18X, 7H STATOR/)
    DO 823 I=1,N
823 WRITE(6,824)   I,ETA(I),ETAT(I),ZETAR(I),ZETAS(I)
824 FORMAT (I5,12X,4(F10.5,15X))
    WRITE(6,825)NRUN
825 FORMAT  (1H1,36H MACH NUMBERS AND DEGREE OF REACTION   //
   120X,11H RUN NUMBER    I5///
   25X,6H POINT  8X,9H REACTION  6X,9H REACTION  7X,9H REACTION
   37X,9H ABSOLUTE  7X,9H RELATIVE  / 23X,4H HUB  9X,5H MEAN  11X,
   44H TIP  12X,7H MACH 1  9X,7H MACH 1   //)
    DO 826 I=1,N
826 WRITE(6,827) I,REACHB (I),REACMN(I),REACTP (I),VM1(I),WM1(I)
827 FORMAT  (I5,12X,5(F10.4,6X))
    WRITE(6,828)
828 FORMAT (//49H STATOR PRESSURE RATIO AND THROAT BLOCKAGE FACTOR//
   12X,6H POINT 11X,9H PRESSURE 17X,9H BLOCKAGE /
   221X,6H RATIO 19X,7H FACTOR /)
    DO 829 I=1,N
829 WRITE(6,830) I,PRS(I),XI(I)
830 FORMAT(I5,12X,2(F10.5,15X))
    RETURN
    END
```

```
      SUBROUTINE OUTPUT(NRUN,AXCLR,RADCLR,N,PR,XKIS,EFF,COEFL,COEFM,
     1                  COEFP,COEFS,REACHB ,REACTP ,PTPL)
      DIMENSION PR(50),XKIS(50),EFF(50),COEFL(50),COEFM(50),COEFP(50),
     1          COEFS(50),REACHB (50),REACTP (50),PTPL(50),NPTS(8),
     2          NPTSS(8),ICOEFS(50)
      READ(5,905)D,A,T,E
      READ(5,906)                                TTYPER,STATOR,METHOD
      READ(5,907)RMEAN
      READ(5,908)J
      READ(5,909)  (NPTS(K),NPTSS(K),K=1,8)
      DO 919 I=1,N
  919 EFF(I)=100.*EFF(I)
      DO 950 JJ=1,2
      IF (N+3*J-43) 920,920,921
  920 NPP=1
      NXX=N
      GO TO 922
  921 NPP=2
      NXX=43
  922 NP=1
      NX=1
      K=1
  923 WRITE(6,900)                          NP,NPP,       TTYPER,STATOR,RADCLR,
     1           AXCLR,NRUN,D,A,T,E,METHOD
      WRITE(6,901)RMEAN
      DO 940 I=NX,NXX
      ICOEFS(I)=COEFS(I)
      II=I
      WRITE(6,902)  I,PR(I),XKIS(I),EFF(I),COEFL(I),COEFM(I),COEFP(I),
     1           ICOEFS(I),REACHB (I),REACTP (I)
      IF (J-K) 940,924,924
  924 IF (I-NPTSS(K)) 940,925,940
  925 LL=NPTS(K)
      LLL=NPTSS(K)
      INTGER =LLL-LL+1
      AVG=INTGER
      AVGATM=0.0
      AVGPR=0.0
      DO 926 L=LL,LLL
      AVGATM=AVGATM+PTPL(L)/14.69 /AVG
  926 AVGPR=AVGPR+PR(L)/AVG
```

```
      LLL=LLL-1
      COMPAR =PR(LL)
      DO 931 L=LL,LLL
      IF (COMPAR -PR(L+1)) 930,931,931
  930 COMPAR =PR(L+1)
  931 CONTINUE
      DEVHI  =100.*(COMPAR -AVGPR)/AVGPR
      COMPAR =PR(LL)
      DO 934 L=LL,LLL
      IF (COMPAR -PR(L+1)) 934,934,933
  933 COMPAR =PR(L+1)
  934 CONTINUE
      DEVLOW=100.*(AVGPR-COMPAR )/AVGPR
      WRITE(6,903)  NPTS(K),NPTSS(K),AVGPR,DEVHI  ,DEVLOW,AVGATM
      IF (NPTSS(K+1)+3*(K+1)-43) 935,936,935
  935 IF (NP-2) 944,936,944
  936 K=K+1
  940 CONTINUE
  944 IF (N-II) 950,950,945
  945 K=K+1
      NP=2
      NX=II+1
      NXX=N
      WRITE(6,904)NP
      GO TO 923
  900 FORMAT(1H1,/ ,9X,7H REPORT,12X      ,77X,6H SHEET,1X,I1,3H OF,1X,I1
     1,//,33X,53H TURBO PROPULSION LABORATORY USNPGS, MONTEREY, CALIF. ,
     2///,21X,79H REDUCED PERFORMANCE DATA OF TURBINE FROM TESTS WITH TR
     3ANSONIC TURBINE TEST RIG // ,27H TURBINE TYPE CIRCULAR-ARC A2,8H S
     4TATOR 1X, A2,4X,25H RADIAL ROTOR TIP CLEAR.=,2X,F6.3,3H IN.  AXIA
     5L CLEAR. STATOR-ROTOR=,1X,F5.3,4H IN./ ,24X,13H TEST RUN NO.,1X,I2
     6,3X,13H DATE OF TEST1X,4A2,2X,22H DATA REDUCTION METHOD,2X,A2 // )
  901 FORMAT(7X,105H POINT  PRESSURE  ISENTROPIC  EFFICIENCY  REFERRED
     1   REFERRED  REFERRED  REFERRED  DEGREE OF  DEGREE OF / ,15X, 94H
     2RATIO     HEAD COEFF.  TOT-STATIC  FLOW RATE   TORQUE     POWER
     3 SPEED    REACTION   REACTION / ,24X, 4H (R=,   F5.3,7H IN.)  PER
     4CENT     LBM/SEC     FT-LB       HP          RPM       (HUB)      (TIP)
     5  //)
  902 FORMAT(9X,I2,5X,F6.4,5X,F6.4,8X,F5.2,6X,F6.4,5X,F6.3,4X,F6.3,4X,
     1I5,4X,F6.4,6X,F5.4 )
  903 FORMAT(/5X,12H FOR POINTS , I2,3H TO,1X,I2,21H AVG. PRESSURE RATIO
     1=,1X,F6.4,18H , MAX.DEVIATION +,   F5.3,7H PCT. -,   F5.3,10H PCT.
     2, PAVG./PATMO=,1X,F6.4 /)
  904 FORMAT(/45X,16H CONTD. ON SHEET,1X,I1,/)
  905 FORMAT(10X,4A2)
```

```
906 FORMAT(15X,3A2)
907 FORMAT(F5.3)
908 FORMAT(I1)
909 FORMAT(8(2I5))
950 CONTINUE
    RETURN
    END
```

TURBINE CIRCULAR ARC I
STATOR I

RUN NUMBER 32 SPACING 0.250 TIP CLEAR. 0.009

POINT	FLOW RATE	RPM	PRESSURE RATIO	HORSEPOWER
1	1.4920	11320.0000	2.0276	40.7987
2	1.4894	12000.0000	2.0258	41.8028
3	1.4833	12980.0000	2.0305	42.8282
4	1.4760	14010.0000	2.0265	42.5820
5	1.4745	15030.0000	2.0318	43.7748
6	1.4724	15900.0000	2.0265	44.0891
7	1.4714	17000.0000	2.0247	43.1480
8	1.4685	17930.0000	2.0300	42.6642
9	1.4710	19080.0000	2.0212	40.8000

DIMENSIONLESS PERFORMANCE PARAMETERS

POINT	K ISENTROPIC	REFERRED FLOW RATE	REFERRED TORQUE	REFERRED POWER	REFERRED SPEED
1	7.4668	1.3702	16.2194	32.6023	10559.4414
2	6.6408	1.3662	15.6545	33.3479	11190.6172
3	5.6990	1.3614	14.8276	34.1468	12097.7617
4	4.8795	1.3597	13.7092	34.0765	13057.7539
5	4.2537	1.3564	13.1181	34.9811	14008.4258
6	3.7862	1.3537	12.4858	35.2321	14823.4297
7	3.3047	1.3517	11.4254	34.4895	15857.8203
8	2.9807	1.3509	10.7266	34.1515	16725.3359
9	2.6162	1.3509	9.6259	32.6218	17803.0430

GENERAL RESULTS

VELOCITIES (FT/SEC)
RUN NUMBER 32

POINT	V1	V2	W1	W2	U1	U2
1	1077.36328	242.01395	678.67090	575.14404	418.85059	423.98730
2	1058.00562	232.69995	636.31982	581.46729	444.01099	449.45630
3	1058.29004	216.44083	602.89697	564.04712	480.27197	486.16211
4	979.92944	216.12202	497.84912	601.83301	518.38306	524.74048
5	961.74756	212.15552	448.06494	615.91431	556.12402	562.94434
6	906.65039	211.66402	376.85962	658.28198	588.31470	595.52979
7	875.18652	210.88635	321.41577	655.48096	629.01587	636.72998
8	848.35034	214.36365	282.91382	667.54639	663.42676	671.56299
9	848.87915	243.27753	256.61719	631.34473	705.97778	714.63574

TEMPERATURES (DEG R)

POINT	PLENUM TOTAL	STATOR DISCHARGE	ROTOR DISCHARGE	ISENTROPIC FROM T1	TOTAL DISCHARGE
1	596.05835	499.47339	510.63477	499.51709	515.50854
2	596.39209	503.24683	509.20996	499.80786	513.71582
3	597.05884	503.86353	508.10937	498.53223	512.00757
4	597.05884	517.15356	508.19019	509.37891	512.07690
5	597.05884	520.09131	505.86572	507.71973	509.61108
6	596.72559	528.32422	504.79419	514.27661	508.52222
7	596.05835	532.32202	505.97852	512.45142	509.67920
8	596.05835	536.17090	506.65405	513.59888	510.47778
9	595.72485	535.76270	509.09790	509.25195	514.02271

FLOW ANGLES (DEGREES FROM AXIAL)

RUN NUMBER 32

POINT	ALPHA 1	ALPHA 2	BETA 1	BETA 2	DELTA BETA
1	75.96136	-26.77655	67.35133	-67.93442	135.28575
2	75.99814	-23.06314	66.27835	-68.39478	134.67313
3	76.19102	-9.55927	65.23016	-67.76537	132.99553
4	74.95389	-10.19390	59.27167	-69.30226	128.57393
5	75.04497	-4.18564	56.36424	-69.90741	126.27165
6	74.12514	-7.72282	48.84682	-71.42027	120.26709
7	73.98924	4.32282	41.32071	-71.28787	112.60858
8	73.59174	10.26967	32.10794	-71.58015	103.68810
9	74.17421	29.51349	25.56148	-70.40727	95.96875

EFFICIENCIES AND LOSSES

POINT	EFFICIENCY TOTAL STATIC	EFFICIENCY TOTAL TOTAL	ZETA ROTOR	ZETA STATOR
1	0.73897	0.77189	0.28770	0.11427
2	0.75891	0.79019	0.25048	0.11783
3	0.77754	0.80508	0.26566	0.10535
4	0.77887	0.80644	-0.04106	0.21401
5	0.79883	0.82607	-0.06240	0.21131
6	0.80887	0.83649	-0.35679	0.28544
7	0.79391	0.82079	-0.22107	0.29110
8	0.78394	0.81124	-0.23044	0.31767
9	0.75301	0.78720	-0.00466	0.27875

MACH NUMBERS AND DEGREE OF REACTION

RUN NUMBER 32

POINT	REACTION HUB	REACTION MEAN	REACTION TIP	ABSOLUTE MACH 1	RELATIVE MACH 1
1	-0.1127	-0.0004	0.1398	0.9834	0.6195
2	-0.1063	0.0308	0.1519	0.9621	0.5787
3	-0.0775	0.0477	0.1773	0.9618	0.5479
4	-0.0487	0.0683	0.2008	0.8791	0.4466
5	-0.0208	0.1085	0.2258	0.8603	0.4008
6	0.0066	0.1222	0.2475	0.8047	0.3345
7	0.0344	0.1737	0.2694	0.7738	0.2842
8	0.0617	0.1960	0.2896	0.7474	0.2493
9	0.0993	0.2338	0.3164	0.7482	0.2262

STATOR PRESSURE RATIO AND THROAT BLOCKAGE FACTOR

POINT	PRESSURE RATIO	BLOCKAGE FACTOR
1	0.49304	0.91360
2	0.50562	0.91097
3	0.51117	0.90776
4	0.52033	0.90663
5	0.53545	0.90455
6	0.54228	0.90302
7	0.56424	0.90384
8	0.57263	0.90468
9	0.59092	0.90864

REPORT

TURBO PROPULSION LABORATORY USNPGS, MONTEREY, CALIF.

REDUCED PERFORMANCE DATA OF TURBINE FROM TESTS WITH TRANSONIC TURBINE TEST RIG

TURBINE TYPE CIRCULAR-ARC I STATOR I RADIAL ROTOR TIP CLEAR.= .009 IN. AXIAL CLEAR. STATOR-ROTOR= 0.250 IN.
TEST RUN NO. 32 DATE OF TEST 5/21/68 DATA REDUCTION METHOD MF

POINT	PRESSURE RATIO	ISENTROPIC HEAD COEFF. (R=4.240 IN.)	EFFICIENCY TOT-STATIC PERCENT	REFERRED FLOW RATE LBM/SEC	REFERRED TORQUE FT-LB	REFERRED POWER HP	REFERRED SPEED RPM	DEGREE OF REACTION (HUB)	DEGREE OF REACTION (TIP)
1	2.0276	7.4668	73.90	1.3702	16.219	32.602	10559	-.1127	.1398
2	2.0258	6.6408	75.89	1.3662	15.655	33.348	11190	-.1063	.1519
3	2.0305	5.6990	77.75	1.3614	14.829	34.147	12097	-.0775	.1773
4	2.0265	4.8795	77.89	1.3597	13.709	34.077	13057	-.0487	.2008
5	2.0318	4.2537	79.88	1.3564	13.118	34.981	14008	-.0208	.2258
6	2.0265	3.7862	80.89	1.3537	12.486	35.232	14823	0.0066	.2475
7	2.0247	3.3047	79.39	1.3517	11.425	34.490	15857	0.0344	.2694
8	2.0300	2.9807	78.39	1.3509	10.727	34.151	16725	0.0617	.2896
9	2.0212	2.6162	75.30	1.3509	9.626	32.622	17803	0.0993	.3164

FOR POINTS 1 TO 9 AVG. PRESSURE RATIO= 2.0272 , MAX.DEVIATION +0.226 PCT. -0.295 PCT., PAVG./PATMO= 1.1669

629

TURBINE CIRCULAR ARC I
STATOR I

RUN NUMBER 33 SPACING 0.250 TIP CLEAR. 0.009

POINT	FLOW RATE	RPM	PRESSURE RATIO	HORSEPOWER
1	1.5694	12640.0000	2.5358	56.3838
2	1.5723	13070.0000	2.5416	57.0580
3	1.5762	14000.0000	2.5365	57.8311
4	1.5492	14980.0000	2.5154	59.0277
5	1.5524	15950.0000	2.5311	60.7246
6	1.5426	17080.0000	2.5276	61.2334
7	1.5427	17920.0000	2.5020	61.0611
8	1.5385	19470.0000	2.5104	61.5244

DIMENSIONLESS PERFORMANCE PARAMETERS

POINT	K ISENTROPIC	REFERRED FLOW RATE	REFERRED TORQUE	REFERRED POWER	REFERRED SPEED
1	7.8914	1.3668	18.7382	41.3960	11605.2930
2	7.4104	1.3703	18.3335	41.8407	11988.9023
3	6.4308	1.3720	17.3476	42.4586	12857.3984
4	5.5670	1.3481	16.5525	43.3718	13764.7695
5	5.0629	1.3721	16.0440	44.2123	14476.2227
6	4.4242	1.3621	15.0679	44.3898	15475.9180
7	3.9898	1.3630	14.3136	44.1904	16218.3320
8	3.3957	1.3622	13.2917	44.5508	17607.6523

GENERAL RESULTS

VELOCITIES (FT/SEC)
RUN NUMBER 33

POINT	V1	V2	W1	W2	U1	U2
1	1289.63599	279.42017	840.54761	631.35254	467.69165	473.42725
2	1287.03613	271.74951	823.09814	620.65771	483.60205	489.53320
3	1230.52710	266.79199	738.53198	638.63477	518.01294	524.36572
4	1228.33325	252.13721	698.32300	631.50928	554.27393	561.07153
5	1268.18994	268.32153	703.86011	593.65674	590.16504	597.40259
6	1236.12891	273.90576	635.50928	604.89526	631.97583	639.72656
7	1236.00073	295.99170	605.22388	581.53101	663.05664	671.18848
8	1172.39966	300.95093	497.01172	625.65991	720.40820	729.24316

TEMPERATURES (DEG R)

POINT	PLENUM TOTAL	STATOR DISCHARGE	ROTOR DISCHARGE	ISENTROPIC FROM T1	TOTAL DISCHARGE
1	615.26172	476.86694	502.93848	469.48779	509.43530
2	616.41113	478.57373	503.37500	469.94067	509.52002
3	614.93311	488.93408	500.93286	480.53003	506.85571
4	614.27563	488.72534	496.74976	470.54199	502.03979
5	629.63452	495.80444	508.41797	476.42822	514.40894
6	631.74341	504.59448	508.57446	483.62720	514.81738
7	633.20117	506.07861	509.32104	480.98828	516.61133
8	634.17212	519.79565	508.84302	488.60034	516.37964

FLOW ANGLES (DEGREES FROM AXIAL)

RUN NUMBER 33

POINT	ALPHA 1	ALPHA 2	BETA 1	BETA 2	DELTA BETA
1	76.99704	-21.36789	69.80518	-65.65991	135.46509
2	76.98311	-15.63952	69.37848	-65.06241	134.44089
3	76.02126	-12.74319	66.26637	-65.95438	132.22075
4	77.30249	-4.14075	67.25517	-66.53308	133.78825
5	77.46133	13.79737	66.97333	-63.96379	130.93712
6	77.19234	19.74188	64.45714	-64.77330	129.23044
7	77.63324	30.21010	64.06329	-63.90504	127.96834
8	77.08606	31.74139	58.18478	-65.85362	124.03841

EFFICIENCIES AND LOSSES

POINT	EFFICIENCY TOTAL STATIC	EFFICIENCY TOTAL TOTAL	ZETA ROTOR	ZETA STATOR
1	0.73678	0.76941	0.50211	-0.01596
2	0.74121	0.77207	0.51053	-0.01697
3	0.75266	0.78305	0.37546	0.06909
4	0.78863	0.81750	0.44126	-0.01185
5	0.78527	0.81694	0.52172	-0.05299
6	0.79523	0.82876	0.45036	-0.00895
7	0.79878	0.83886	0.50170	-0.05458
8	0.80323	0.84482	0.38327	0.00992

MACH NUMBERS AND DEGREE OF REACTION

RUN NUMBER 33

POINT	REACTION HUB	REACTION MEAN	REACTION TIP	ABSOLUTE MACH 1	RELATIVE MACH 1
1	-0.0716	0.0516	0.1698	1.2048	0.7852
2	-0.0642	0.0602	0.1780	1.2002	0.7676
3	-0.0418	0.0574	0.2012	1.1353	0.6814
4	-0.0301	0.1281	0.2191	1.1335	0.6444
5	-0.0096	0.1338	0.2355	1.1619	0.6449
6	0.0226	0.1429	0.2630	1.1226	0.5771
7	0.0425	0.1741	0.2779	1.1208	0.5483
8	0.0843	0.2123	0.3087	1.0491	0.4447

STATOR PRESSURE RATIO AND THROAT BLOCKAGE FACTOR

POINT	PRESSURE RATIO	BLOCKAGE FACTOR
1	0.41648	0.91140
2	0.41934	0.91372
3	0.41892	0.91483
4	0.45397	0.89892
5	0.45424	0.91488
6	0.45899	0.90823
7	0.47753	0.90885
8	0.49469	0.90830

REPORT

TURBO PROPULSION LABORATORY USNPGS, MONTEREY, CALIF.

REDUCED PERFORMANCE DATA OF TURBINE FROM TESTS WITH TRANSONIC TURBINE TEST RIG

TURBINE TYPE CIRCULAR-ARC I STATOR I RADIAL ROTOR TIP CLEAR.= .009 IN. AXIAL CLEAR. STATOR-ROTOR= 0.250 IN.
TEST RUN NO. 33 DATE OF TEST 5/22/68 DATA REDUCTION METHOD ME

POINT	PRESSURE RATIO	ISENTROPIC HEAD COEFF. (R=4.240 IN.)	EFFICIENCY TOT-STATIC PERCENT	REFERRED FLOW RATE LBM/SEC	REFERRED TORQUE FT-LB	REFERRED POWER HP	REFERRED SPEED RPM	DEGREE OF REACTION (HUB)	DEGREE OF REACTION (TIP)
1	2.5358	7.8914	73.68	1.3668	18.738	41.396	11605	-.0716	.1698
2	2.5416	7.4104	74.12	1.3703	18.334	41.841	11988	-.0642	.1780
3	2.5365	6.4308	75.27	1.3720	17.348	42.459	12857	-.0418	.2012
4	2.5154	5.5670	78.86	1.3481	16.553	43.372	13764	-.0301	.2191
5	2.5311	5.0629	78.53	1.3721	16.044	44.212	14476	-.0096	.2355
6	2.5276	4.4242	79.52	1.3621	15.068	44.390	15475	0.0226	.2630
7	2.5020	3.9898	79.88	1.3630	14.314	44.190	16218	0.0425	.2779
8	2.5104	3.3957	80.32	1.3622	13.292	44.551	17607	0.0843	.3087

FOR POINTS 1 TO 8 AVG. PRESSURE RATIO= 2.5250 , MAX.DEVIATION +0.656 PCT. -0.912 PCT., PAVG./PATMO= 1.2499

TURBINE CIRCULAR ARC I
STATOR I

RUN NUMBER 34 SPACING 0.250 TIP CLEAR. 0.009

POINT	FLOW RATE	RPM	PRESSURE RATIO	HORSEPOWER
1	1.5638	13080.0000	2.5368	56.9356
2	1.5651	13080.0000	2.5000	56.9356
3	1.5755	13070.0000	2.5170	56.9750
4	1.5815	13050.0000	2.5377	56.7222
5	1.5974	13060.0000	2.5130	56.1028

DIMENSIONLESS PERFORMANCE PARAMETERS

POINT	K ISENTROPIC	REFERRED FLOW RATE	REFERRED TORQUE	REFERRED POWER	REFERRED SPEED
1	7.4897	1.3727	18.2834	41.4678	11914.5898
2	7.3174	1.3663	18.2689	41.6311	11971.0352
3	7.3174	1.3669	18.2567	41.7377	12009.7148
4	7.2855	1.3643	18.2374	41.9466	12022.5742
5	7.1124	1.3667	17.9957	41.6982	12172.3242

GENERAL RESULTS

VELOCITIES (FT/SEC)
RUN NUMBER 34

POINT	V1	V2	W1	W2	U1	U2
1	1318.88477	267.69214	853.66870	596.26221	483.97217	489.90747
2	1279.49170	269.61963	814.51025	626.52783	483.97217	489.90747
3	1257.67358	275.64624	794.72070	641.65601	483.60205	489.53320
4	1210.93018	291.96460	752.07837	678.17187	482.86230	488.78369
5	1153.45264	304.01587	697.10840	704.95728	483.23193	489.15845

TEMPERATURES (DEG R)

POINT	PLENUM TOTAL	STATOR DISCHARGE	ROTOR DISCHARGE	ISENTROPIC FROM T1	TOTAL DISCHARGE
1	625.07959	480.33618	511.87354	473.18994	517.83643
2	619.19824	482.97217	505.99438	472.22339	512.04346
3	614.27563	482.65601	501.43115	473.24316	507.75366
4	605.03418	483.01636	492.29102	475.66357	499.38428
5	597.05884	486.34937	485.91309	477.04297	493.60400

FLOW ANGLES (DEGREES FROM AXIAL)

RUN NUMBER 34

POINT	ALPHA 1	ALPHA 2	BETA 1	BETA 2	DELTA BETA
1	77.21069	-9.62638	70.00117	-63.72823	133.72940
2	77.24178	-17.58957	69.70180	-65.78139	135.48319
3	76.74695	-20.86003	68.72781	-66.33249	135.06030
4	75.83826	-28.40329	66.80083	-67.74727	134.54810
5	75.24397	-33.75546	65.07465	-68.98868	134.06332

EFFICIENCIES AND LOSSES

POINT	EFFICIENCY TOTAL STATIC	EFFICIENCY TOTAL TOTAL	ZETA ROTOR	ZETA STATOR
1	0.73465	0.76386	0.56665	-0.04325
2	0.75133	0.78259	0.50833	-0.03380
3	0.74804	0.78065	0.45138	0.01050
4	0.74744	0.78452	0.30288	0.09065
5	0.74858	0.79010	0.17661	0.14345

MACH NUMBERS AND DEGREE OF REACTION

RUN NUMBER 34

POINT	REACTION HUB	REACTION MEAN	REACTION TIP	ABSOLUTE MACH 1	RELATIVE MACH 1
1	-0.0655	0.0496	0.1770	1.2276	0.7946
2	-0.0730	0.0761	0.1765	1.1877	0.7561
3	-0.0681	0.0659	0.1791	1.1678	0.7380
4	-0.0595	0.0507	0.1823	1.1240	0.6981
5	-0.0648	0.0648	0.1815	1.0670	0.6449

STATOR PRESSURE RATIO AND THROAT BLOCKAGE FACTOR

POINT	PRESSURE RATIO	BLOCKAGE FACTOR
1	0.41544	0.91529
2	0.43279	0.91100
3	0.42565	0.91146
4	0.41579	0.90968
5	0.42578	0.91131

REPORT

TURBO PROPULSION LABORATORY USNPGS, MONTEREY, CALIF.

REDUCED PERFORMANCE DATA OF TURBINE FROM TESTS WITH TRANSONIC TURBINE TEST RIG

TURBINE TYPE CIRCULAR-ARC I STATOR I RADIAL ROTOR TIP CLEAR.= .009 IN. AXIAL CLEAR. STATOR-ROTOR= 0.250 IN.
TEST RUN NO. 34 DATE OF TEST 5/23/68 DATA REDUCTION METHOD ME

POINT	PRESSURE RATIO	ISENTROPIC HEAD COEFF. (R=4.240 IN.)	EFFICIENCY TOT-STATIC PERCENT	REFERRED FLOW RATE LBM/SEC	REFERRED TORQUE FT-LB	REFERRED POWER HP	REFERRED SPEED RPM	DEGREE OF REACTION (HUB)	DEGREE OF REACTION (TIP)
1	2.5368	7.4897	73.46	1.3727	18.283	41.468	11914	-.0655	.1770
2	2.5000	7.3174	75.13	1.3663	18.269	41.631	11971	-.0730	.1765
3	2.5170	7.3174	74.80	1.3669	18.257	41.738	12009	-.0681	.1791
4	2.5377	7.2855	74.74	1.3643	18.237	41.947	12082	-.0595	.1823
5	2.5130	7.1124	74.86	1.3667	17.996	41.698	12172	-.0648	.1815

FOR POINTS 1 TO 5 AVG. PRESSURE RATIO= 2.5209 , MAX.DEVIATION +0.669 PCT. -0.830 PCT., PAVG./PATMO= 1.2525

APPENDIX II

EVALUATION OF THE FORCE ACTING ON THE STATOR ASSEMBLY BY THE STATOR DISCHARGE PRESSURE

The pressure at the stator discharge P_1 varies between the pressure P_{h1} at the hub and the pressure P_{t1} at the tip. This pressure is not necessarily a linear function of radius r. In the present study the pressure P_1 will be assumed to vary parabolically from P_{h1} at R_{h1} to P_{t1} at R_{t1} such that at the mean radius R_{m1} the pressure is $(1 + \epsilon) P_{m1}$, where $P_{m1} = (P_{h1} + P_{t1})/2$. The value of the factor ϵ will be determined by comparing momentum results with those from the continuity equation.

Let

$$P_1 = P_{h1} + \frac{P_{t1}-P_{h1}}{R_{t1}-R_{h1}}(r-R_{h1}) + \Delta P = P_{h1} + \delta(r-R_{h1}) + \Delta P \quad (64)$$

where

$$\delta = \frac{P_{t1} - P_{h1}}{R_{t1} - R_{h1}} \quad (65)$$

and

$$\Delta P = A_o + A_1 r + A_2 r^2 \quad (66)$$

The constant factors A_o, A_1, and A_2 are obtained from the conditions $\Delta P = 0$ at $r = R_{h1}$, $\Delta P = 0$ at $r = R_{t1}$, and $\Delta P = P_{m1}$ at $r = R_{m1} = (R_{t1} + R_{h1})/2$. Thus

$$0 = A_o + A_1 R_{h1} + A_2 R_{h1}^2$$

$$0 = A_o + A_1 R_{t1} + A_2 R_{t1}^2$$

$$\epsilon P_{m1} = A_o + A_1 R_{m1} + A_2 R_{m1}^2$$

The above simultaneous equations are solved by Cramer's Rule, with

$$C = \begin{vmatrix} 1 & R_{h1} & R_{h1}^2 \\ 1 & R_{t1} & R_{t1}^2 \\ 1 & R_{m1} & R_{m1}^2 \end{vmatrix} = (R_{t1} - R_{h1})[R_{m1}^2 - R_{m1}(R_{t1} + R_{h1}) + R_{h1}R_{t1}]$$

with $R_{m1} = (R_{h1} + R_{t1})/2$

$$C = (R_{t1} - R_{h1})[\tfrac{1}{4}(R_{h1} + R_{t1})^2 - \tfrac{1}{2}(R_{h1} + R_{t1})^2 + R_{h1}R_{t1}]$$

$$C = -\tfrac{1}{4}(R_{t1} - R_{h1})^3 \qquad (67)$$

Thus

$$A_o = 1/C \begin{vmatrix} 0 & R_{h1} & R_{h1}^2 \\ 0 & R_{t1} & R_{t1}^2 \\ \epsilon P_{m1} & R_{m1} & R_{m1}^2 \end{vmatrix} = \frac{\epsilon P_{m1}\left[R_{t1}^2 R_{h1} - R_{h1}^2 R_{t1}\right]}{C}$$

with Eq. (67)

$$A_o = -4\epsilon P_{m1} \frac{R_h R_{t1}}{(R_{t1} - R_{h1})^2} \qquad (68)$$

with Eq. (67), in like manner

$$A_1 = \frac{4\epsilon P_{m1}(R_{t1} + R_{h1})}{(R_{t1} - R_{h1})^2} \qquad (69)$$

$$A_2 = - \frac{4 \epsilon P_{m1}}{(R_{t1} - R_{h1})^2} \tag{70}$$

Substituting Eqs. (68), (69), and (70) into Eq. (66)

$$\Delta P = \frac{4 \epsilon P_{m1}}{(R_{t1} - R_{h1})^2} [- R_{h1} R_{t1} + (R_{t1} - R_{h1})\, r - r^2] \tag{71}$$

The force on the stator assembly due to the stator discharge pressure is

$$F_{sD} = 2\pi \int_{R_{h1}}^{R_{t1}} P_1 r \, dr \tag{72}$$

with Eqs. (64) and (71)

$$F_{sD} = 2\pi \int_{R_{h1}}^{R_{t1}} [(P_{h1} - \delta R_{h1}) r + \delta r^2 + \Delta P r] \, dr$$

$$= \pi (P_{h1} - \delta R_{h1})(R_{t1}^2 - R_{h1}^2) + \frac{2\pi}{3} \delta [R_{t1}^3 - R_{h1}^3] + 2\pi \int_{R_{h1}}^{R_{t1}} \Delta P \, r \, dr$$

with Eq. (65)

$$F_{sD} = \pi (P_{h1} - R_{h1} \frac{P_{t1} - P_{h1}}{R_{t1} - R_{h1}})(R_{t1}^2 - R_{h1}^2) + \frac{2\pi}{3} \frac{P_{t1} - P_{h1}}{R_{t1} - R_{h1}} (R_{t1}^3 - R_{h1}^3)$$

$$+ \frac{2\pi 4 \epsilon P_{m1}}{(R_{t1} - R_{h1})^2} \left[- R_{h1} R_{t1} \frac{(R_{t1}^2 - R_{h1}^2)}{2} + (R_{h1} + R_{t1}) \frac{(R_{t1}^3 + R_{h1}^3)}{3} - \frac{R_{t1}^4 - R_{h1}^4}{4} \right]$$

Simplifying

$$F_{sD} = \frac{\pi}{3}P_{h1}[R_{t1}^2 + R_{h1}R_{t1} - 2R_{h1}^2] + \frac{\pi}{3}P_{t1}[2R_{t1}^2 - R_{h1}R_{t1} - R_{h1}^2]$$

$$+ 2/3\,\pi \frac{\epsilon P_{m1}}{(R_{t1} - R_{h1})^2}[(R_{t1}^2 - R_{h1}^2)(R_{t1} - R_{h1})^2]$$

With $P_{m1} = (P_{h1} + P_{t1})/2$, the final expression for the force F_{sD} acting on the stator assembly by the pressure at the stator exit is

$$F_{sD} = 2\pi \int_{R_{h1}}^{R_{t1}} P_1 r\,dr = \frac{\pi}{3}P_{h1}[(1+\epsilon)R_{t1}^2 + R_{h1}R_{t1} - (2+\epsilon)R_{h1}^2] \tag{73}$$

$$+ \frac{\pi}{3}P_{t1}[(2+\epsilon)R_{t1}^2 - R_{h1}R_{t1} - (1+\epsilon)R_{h1}^2]$$

INITIAL DISTRIBUTION LIST

		Copies
1.	Defense Documentation Center Cameron Station Alexandria, Virginia 22314	20
2.	Library Naval Postgraduate School Monterey, California 93940	2
3.	Commander, Naval Air Systems Command Navy Department Washington, D.C. 20360	1
4.	Commandant of the Marine Corps (Code A03C) Headquarters, U.S. Marine Corps Washington, D.C. 20380	1
5.	Commander, Naval Ship Systems Command Navy Department Washington, D.C. 20360	1
6.	Professor M. H. Vavra Department of Aeronautics Naval Postgraduate School Monterey, California 93940	3
7.	Chairman, Department of Aeronautics Naval Postgraduate School Monterey, California 93940	1
8.	Professor A. E. Fuhs Department of Aeronautics Naval Postgraduate School Monterey, California 93940	1
9.	Professor R. D. Zucker Department of Aeronautics Naval Postgraduate School Monterey, California 93940	1
10.	Dr. E. S. Lamar (Code 03C) Chief Scientist, Research and Technology Naval Air Systems Command Navy Department Washington, D.C. 20390	1
11.	Commander Naval Ordnance Systems Command Navy Department Washington, D.C. 20390	1

12.	Dr. O. H. Johnson Naval Air Systems Command (Code 330 B) Navy Department Washington, D.C. 20360	1
13.	Head, Department of Engineering Naval Academy Annapolis, Maryland 21402	1
14.	Superintendent Naval Academy Annapolis, Maryland 21402	1
15.	Mr. I. Silver, Code 330 Propulsion Administrator Research and Technology Naval Air Systems Command Navy Department Washington, D.C. 20390	1
16.	Office of Naval Research Air Programs Office Navy Department Washington, D.C. 20360	1
17.	Capt. A. Bodnaruk, USN Naval Ship Systems Command (Code 6140) Navy Department Washington, D. C. 20360	1
18.	Office of Naval Research (Power Branch) Attn: Mr. J. K. Patton, Jr. Navy Department Washington, D. C. 20360	1
19.	Dr. F. I. Tanczos Technical Director, Research and Technology Naval Air Systems Command Navy Department Washington, D. C. 20390	1
20.	Captain Martin J. Lenzini 100 Lakewood Place Highland Park, Illinois 60035	2

DOCUMENT CONTROL DATA - R & D

Security classification of title, body of abstract and indexing annotation must be entered when the overall report is classified)

1 ORIGINATING ACTIVITY (Corporate author)
Naval Postgraduate School
Monterey, California 93940

2a. REPORT SECURITY CLASSIFICATION
UNCLASSIFIED

2b. GROUP

3 REPORT TITLE
CALIBRATION OF TURBINE TEST RIG WITH IMPULSE TURBINE AT HIGH PRESSURE RATIOS

4 DESCRIPTIVE NOTES (Type of report and inclusive dates)
Thesis

5 AUTHOR(S) (First name, middle initial, last name)
Martin J. Lenzini, Captain, U. S. Marine Corps

6. REPORT DATE
June 1968

7a. TOTAL NO. OF PAGES
144

7b. NO. OF REFS
9

8a. CONTRACT OR GRANT NO.

b. PROJECT NO.

c.

d. Unlimited dist

9a. ORIGINATOR'S REPORT NUMBER(S)

9b. OTHER REPORT NO(S) (Any other numbers that may be assigned this report)

10. DISTRIBUTION STATEMENT
This document is subject to special export controls and each transmittal to foreign governments or foreign nationals may be made only with prior approval of Naval Postgraduate School.

11. SUPPLEMENTARY NOTES

12. SPONSORING MILITARY ACTIVITY
Naval Postgraduate School
Monterey, California 93940

13 ABSTRACT

The Transonic Turbine Test Rig of the Turbo-Propulsion Laboratory, Department of Aeronautics, of the Naval Postgraduate School was designed to investigate the performance of turbines with transonic or supersonic rotor inlet velocities. The test rig has provisions for testing single stage axial turbines at high pressure ratios and at variable axial and radial clearances. The present study describes the calibration of the turbine test rig with an impulse turbine at high pressure ratios. The turbine stage consists of a double circular-arc rotor with sharp leading edges and a stator with converging nozzle type blading. The results of the flow rate calibration and labyrinth seal leakage tests are described. The instrumentation necessary to separate rotor and stator losses is also discussed.

14 KEY WORDS	LINK A		LINK B		LINK C	
	ROLE	WT	ROLE	WT	ROLE	WT
Impulse Turbine						
Transonic Turbine						
Transonic Turbine Test Rig						



thesL527
Calibration of turbine test rig with imp
3 2768 002 12055 2
DUDLEY KNOX LIBRARY C.1